ABSTRACT

CHOWDHURY, ISHIKA NAWRIN. Hazard-Consistent Ground Motions for Geotechnical Earthquake Engineering Analysis (Under the direction of Dr. Ashly Cabas Mijares).

Earthquake ground motions serve as the link between evaluations of seismic hazards and assessments of civil infrastructure performance. However, the selection of hazard-consistent ground motions continues to prove challenging with limited guidelines focused on geotechnical engineering applications. This study investigates if current practices for ground motion selection provide hazard consistent ground motions for geotechnical earthquake engineering analysis. This study focuses on two sources of uncertainty in ground motion selection: the effect of target spectrum definitions and the effect of ground motion duration.

Current practices for ground motion selection are compared in terms of target spectrum definitions and different ground motion databases; and their impacts on the variability in estimated site response parameters are investigated. The study sites are selected to represent idealized site conditions in two locations with distinct tectonic settings. One-dimensional nonlinear site response analysis are performed. When directly incorporated into target spectrum definitions, different types of seismic sources and the corresponding databases have a significant impact on the estimated site response as captured by spectral amplification factors and non-spectral intensity measures, particularly in subduction zone regions. The variability in spectral amplification factors is found to be higher near the site period. Conditional spectra is identified as a suitable target spectrum for sites having hazard contribution from multiple seismic sources; while it showed limited utility at stable continental region. The variability in site response estimates from different ground motion selection techniques is dependent on the site characteristics. Estimated responses at stiffer sites are more greatly influenced by ground motion

selection techniques, whereas the onset of nonlinear soil behavior at softer sites can suppress such variability.

This study also investigates the effect of ground motion duration on seismic slope displacement analysis and site response analysis. To isolate the effect of duration from frequency content and amplitude, in this work, ground motion pairs are selected such that they have similar spectral shapes and the same peak ground acceleration (PGA), but different significant duration. These criteria result in a long duration suite and an equivalent short duration suite of ground motions, which are then used in a nonlinear finite element analysis to assess their effect on slope displacement. The long duration motions are found to cause larger permanent displacements compared to their short duration counterparts, especially at higher ground shaking intensity levels. Comparisons with simplified analyses show that the simplified methods can underestimate the permanent displacement of design level long duration motions as they often use equivalent linear analysis.

The long and short duration suite of motions having ground motion pairs of different intensity levels are used to investigate the effect of duration on site response analysis also. One-dimensional, total stress, fully nonlinear site response analyses are conducted at two study sites with different local subsurface conditions. Several damage indices including amplification factors, maximum shear strain and spectral displacement are computed to determine whether the ground motion duration has a significant effect. It is observed that long-duration ground motions used as input in nonlinear site response analysis can result in larger damage indices for the estimated ground motion at the ground surface. The difference in maximum strain between the long and short duration motions is also more prominent for the stiff site after it reaches the threshold of intensity for nonlinear soil behavior. The results of this study provide evidence of

the need to consider ground motion duration along with the other ground motion characteristics (amplitude and spectral shape) and to conduct nonlinear analysis for properly assessing the damage potential of design level long-duration motions.

Hazard-Consistent Ground Motions for Geotechnical Earthquake Engineering Analysis

by
Ishika Nawrin Chowdhury

A dissertation submitted to the Graduate Faculty of
North Carolina State University
in partial fulfillment of the
requirements for the degree of
Doctor of Philosophy

Civil Engineering

Raleigh, North Carolina
2022

APPROVED BY:

_____	_____
Dr. Ashly Cabas Mijares Committee Chair	Dr. Mohammed Gabr
_____	_____
Dr. Brina Montoya	Dr. Mervyn Kowalsky

DEDICATION

To my mother who inspires me to be a strong woman like her with a kind soul. To my father whose thirst for knowledge has always inspired me to carry on with my own quest for knowledge that is beneficial to humankind.

BIOGRAPHY

Ishika received her B.Sc. and M.Sc. degrees in Civil Engineering from Bangladesh University of Engineering and Technology (BUET). Later, she joined as a Lecturer in BUET. She worked on several projects funded by national and international organizations. She co-organized training courses and seminars with a focus on disaster risk reduction for Bangladesh. She also worked as a consultant on various civil engineering projects and conducted site explorations, dynamic field tests, and prepared technical reports. During her Master's degree she worked as a visiting researcher at University of Trieste in Italy and performed neo-deterministic studies for seismic hazard assessment of Bangladesh. As a PhD student at North Carolina State University (NCSU), she has received the Provost Doctoral Fellowship and Thomas G. Coffey Graduate Fellowship. She has also served as the Vice-President of Earthquake Engineering Research Institute (EERI) Graduate Student Chapter at NCSU.

ACKNOWLEDGMENTS

My earnest gratitude to my advisor Dr. Ashly Cabas for her continuous guidance, unlimited time and endless encouragement throughout the course of this doctoral study. She went above and beyond to support me on not only the academic tasks but also my personal life whenever I needed her help. I could not have asked for a better mentor and I am honored to have her as my PhD advisor.

My sincere thanks to my committee members Dr. Brina Montoya, Dr. Mo Gabr, and Dr. Mervyn Kowalsky for their guidance and valuable comments. I feel fortunate to be a part of NCSU where I got knowledgeable and kind professors, supportive staff members, and incredible fellow graduate students.

I express my gratitude to Dr. James Kaklamanos for being an integral part of my doctoral journey and providing me with continuous guidance. I also sincerely thank Dr. Nick Gregor and Dr. Albert Kottke for their continuous support towards my research.

I would like to extend my gratitude to the U.S. Geological Survey for funding my research project. My sincere thank goes to all my peers who have helped me and motivated me during this journey. Finally, this long journey was not possible without the endless love and support from my parents, husband, family members, and friends.

TABLE OF CONTENTS

LIST OF TABLES

LIST OF FIGURES

CHAPTER 1: INTRODUCTION

1.1 Background

Earthquake ground motions serve as the link between evaluations of seismic hazards and assessments of civil infrastructure performance. In addition to their frequent usage in dynamic analyses of critical infrastructure, ground motions also provide critical inputs for geotechnical engineering analyses such as site response analyses, liquefaction and seismic slope stability assessments. Thus, to predict an unbiased seismic response, using appropriate input ground motions that represent the seismic hazard at the site of interest is unequivocally important. However, the selection of hazard-consistent ground motions continues to prove challenging for both geotechnical and structural engineering applications.

The selection of input ground motions varies with the application, as evidenced by the multiple protocols that populate the literature concerning ground motion selection for: (a) building seismic design (e.g., Chapter 16 of the ASCE/SEI 7-16 Standard; ASCE 2016), (b) performing response-history analyses of low- to medium-rise buildings (NEHRP Consultants Joint Venture 2011), (c) nonlinear response history analyses of buildings within the performance-based design framework (Kwong and Chopra 2015), and (d) nuclear power plants (McGuire et al. 2001). However, none of these guidelines has a particular focus on ground motions required for geotechnical engineering analyses (e.g., site response analysis, liquefaction assessment, or seismic slope stability analyses). A notable exception is the Pacific Earthquake and Research Center (PEER) report (Stewart et al. 2014), which does provide guidance on the selection of input motions for one-dimensional ground response analyses. The majority of ground motion selection methods are based on defining a target response spectrum predicted from probabilistic seismic hazard analysis (PSHA), scenario based

seismic hazard analysis or seismic code requirements. A target spectrum is defined in terms of 5%-damped spectral acceleration (Sa), with Sa representing the maximum response of an elastic single-degree-of freedom system at a given oscillating period. After defining this target spectrum for the reference site condition, ground motion time series that are compatible with the target are selected for further dynamic analyses. The selection of ground motions involves two steps: i) initial screening based on tectonic regime, source characteristics of the controlling earthquake (magnitude M_w, distance R, fault type) and site conditions (time-averaged shear wave velocity in the top 30 m, V_{s30}); ii) final selection based on spectral shape (i.e., the shape of the response spectrum) and potential modification of the ground motion record (e.g., via linear scaling or spectral matching) (Stewart et al. 2014, Haselton et al. 2017). There are multiple sources of uncertainty involved in each step within the ground motion selection process. Thus, variability in the estimated seismic response is expected from our choice among the different available options. Moreover, ground motion intensity measures (IMs) that are critical in structural engineering analyses may not always provide the most sufficient and efficient characterization of the seismic demand for geotechnical engineering analyses. For example, spectral acceleration is often used as an IM in assessing seismic demand of infrastructure. In geotechnical earthquake engineering analyses, the seismic response of a site often depends on cumulative effects, especially in the context of liquefaction and seismic slope stability analyses. For such evaluations, IMs such as peak ground acceleration (PGA), Arias intensity (I_a), cumulative absolute velocity (CAV), and significant duration (D_{s5-75} or D_{s5-95}) can also be crucial.

This study will focus on two fundamental sources of uncertainty in hazard consistent ground motion selection for geotechnical engineering analysis: target spectrum definitions for different seismotectonic and geologic settings and the effects of ground motion duration.

a) Definition of Target Spectrum

Past studies have attempted to assess the variability associated with the input motion selection in geotechnical engineering analysis (e.g., Bazzurro and Cornell 2004, Rathje et al. 2010) focusing on record-to-record variability or suite-to-suite variability. To this date, however, the uncertainties associated with different target spectra used in geotechnical engineering applications have received limited attention (e.g., Bradley 2010, Hashash et al. 2015, Peterman and Rathje 2017). The most commonly used target spectra in earthquake engineering practice include: the uniform hazard spectrum (UHS) derived from PSHA results, scenario based spectrum such as the conditional mean spectrum (CMS) or conditional spectra (CS, Baker 2011), and the risk-targeted maximum considered earthquake (MCE_R) spectrum from the ASCE 7-16 design standard. While the design code allows the use of any of these target spectra, the definition of a target spectrum is often generalized and guidelines for evaluating them in different seismotectonic and geologic settings are not available. Thus, the implications of different choices in target spectrum definitions and their outcomes on the estimated dynamic responses of soils for geotechnical engineering applications are not clearly understood yet. Moreover, most of the aforementioned studies had focused on shallow crustal earthquakes. The paucity of recorded strong ground motions in the Subduction zones like Pacific Northwest for design conditions (i.e., large magnitude and short distances) and in stable continental regions, such as Central and Eastern United States (CEUS), also constitutes a major hurdle when selecting hazard-consistent ground motions for design. As

the NGA-SUB and NGA-East databases become available, they provide a unique opportunity to compare hazard consistent ground motion selection protocols for different seismotectonic settings.

b) Effects of Duration

Current practice of ground motion selection relies on spectral shape as the primary indicator for assessing the compatibility of candidate motions to the selected target spectrum. Past studies (e.g., Shome et al. 1998, Baker and Cornell 2006) have shown that the spectral shape can be a good predictor of the damage potential of a ground motion. Spectral shape can implicitly represent the amplitude and frequency content of a ground motion; however, they often fail to correlate strongly with the duration of a motion (Chandramohan et al. 2016). In geotechnical earthquake engineering analyses, the seismic response of a soil deposit often depends on cumulative effects, especially for liquefaction and seismic slope stability analysis. For such analyses, it is still not clearly understood if the current practice for ground motion selection can provide an unbiased estimate of dynamic response of soil. Research efforts to investigate the influence of duration on structural collapse (e.g., Hancock and Bommer 2007, Raghunandan and Liel 2013, Chandramohan et al 2016, Zengin et al 2020) have resulted in contradicting findings depending on the type of structure analyzed, whether the modeling approach accounts for the accumulation of damage, the capacity of isolating duration effects from those corresponding to frequency content and amplitude of the ground motion, and the consideration of cumulative parameters to measure damage. Raghunandan and Liel (2013) showed that ground motion duration influences cumulative damage indices (e,g., collapse capacity) although it does not affect peak deformations of a reinforced concrete moment frame building. More recently, Chandramohan et al. (2016) showed that long-duration ground motions have a significant effect on structural collapse capacity (29% lower estimated median)

compared to short-duration motions for a five-story steel moment frame building. However, the only geotechnical engineering analysis where duration effects have received some attention is liquefaction analysis. This is evidenced in simplified assessments of liquefaction triggering where duration and energy effects are explicitly considered (e.g., Green and Terri 2005), and in duration-dependent liquefaction-induced lateral spreading empirical models (e.g., Rauch and Martin 2000). The effects of ground motion duration in other geotechnical engineering applications such as seismic slope displacement analysis and site response analysis have not been rigorously quantified yet and hence, not incorporated in the current state-of-practice guidelines (e.g., ASCE/SEI 7-16, USBR 2015).

1.2 Objectives

The overarching goal of this study is to investigate if current practices for ground motion selection provide hazard consistent ground motions for geotechnical earthquake engineering analyses at different seismotectonic settings. This study focuses on two sources of uncertainty in ground motion selection: the effect of target spectrum definitions and the effect of ground motion duration. In pursuit of the aforementioned goal, the specific objectives of this study include:

(1) To investigate the effect of ground motion selection techniques on seismic site response analyses at different seismotectonic settings. Current practices for ground motion selection are compared in terms of target spectrum definitions and different ground motion databases; and their impacts on the variability in estimated site response parameters are investigated.

(2) To investigate the effect of ground motion duration on seismic slope displacement analysis. A long duration suite and an equivalent short duration suite of earthquake ground motions are selected and used as input to a finite element analysis of an idealized slope.

(3) To investigate the effect of ground motion duration on seismic site response analyses. A long duration suite and an equivalent short duration suite of ground motions are used to conduct one-dimensional, total stress, fully nonlinear site response analysis at two study sites with different local subsurface conditions.

The results of the proposed study will advance our understanding of how ground motion selection techniques influence the dynamic response of soil in geotechnical earthquake engineering analyses. Moreover, the findings from this study will provide recommendations for hazard consistent ground motion selection at different seismotectonic and geologic settings. Ultimately, the findings from this study will contribute to the long-term goal of improving the accuracy of seismic hazard assessments and reduce its adverse effects on civil infrastructure and community resilience.

1.3 Dissertation Organization

This dissertation consists of five chapters. In Chapter 2, the study sites selected to represent idealized site conditions in Seattle and Boston are described, which are exposed to distinct tectonic settings. Then current practices for ground motion selection are compared, namely the uniform hazard spectrum (UHS) and the conditional spectrum (CS). One-dimensional site response analysis are performed at the study sites and the variability in estimated results is evaluated for different ground motion selection techniques, in terms of spectral amplification factors and two

non-spectral acceleration (non-SA) intensity measures (IMs): significant duration and Arias intensity. The effect of soil non-linearity and the effect of considering non-SA Ims (via the Generalized Conditional IM approach, GCIM, Bradley 2010) in ground motion selection are then discussed. Recommendations are provided about the most appropriate target spectra for different seismotectonic settings.

In Chapter 3, to isolate the effect of duration from other characteristics of a ground motion, ground motion pairs with similar spectral shape and with the same amplitude in terms of peak ground acceleration (PGA), but different significant duration are used. The selection and modification of ground motions used in the analysis are described, followed by an explanation of the modeling choices made in the construction of the finite element model of an idealized slope with hypothetical properties, and in the implementation of simplified seismic slope stability approaches. Resulting trends in slope displacements for the long- and short-duration ground motion suites are compared and discussed, and final recommendations for the consideration of duration effects in seismic slope stability analysis are provided.

In Chapter 4, the long and equivalent short duration motion suites created in Chapter 3 are used to determine the effect of ground motion duration on site response analysis. Two geological conditions at the study location in Seattle, Washington are evaluated, namely a soft site (representative of a sedimentary basin) and a stiff site (representative of a glacial till and rock site). Fully nonlinear site response analysis is conducted, which is imperative for capturing the strength and stiffness degradation of soil under cyclic load from earthquake. Finally, the results from site response analysis are compared for the long and short duration suites in terms of several intensity

measures: response spectral amplification factors, maximum shear strain and spectral displacement. Recommendations are provided about the conditions at which the consideration of duration effects in seismic site response analysis are important.

Finally, Chapter 5 summarizes the main findings of this study, contributions to the state of the art, limitations and future works.

References

American Society of Civil Engineers (ASCE) (2016). *Minimum Design Loads for Buildings and Other Structures (Standards ASCE/SEI 7-16)*. American Society of Civil Engineers, Reston, Virginia.

Baker, J. W. (2011). Conditional mean spectrum: Tool for ground motion selection. *Journal of Structural Engineering*, 137(3), 322–331.

Baker, J. W., and Cornell, C. A. (2006). Spectral shape, epsilon, and record selection. *Earthquake Engineering and Structural Dynamics*, 35, 1077–1095.

Bazzurro, P., and Cornell, C. A. (2004). Ground-motion amplification in nonlinear soil sites with uncertain properties. *Bulletin of the Seismological Society of America*, 94, 2090–2109.

Bradley, B. A. (2010). A generalized conditional intensity measure approach and holistic ground motion selection. *Earthquake Engineering and Structural Dynamics*, 39, 1321–1342.

Chandramohan, R., Baker, J. W., and Deierlein, G. G. (2016). Quantifying the influence of ground motion duration on structural collapse capacity using spectrally equivalent records. *Earthquake Spectra*, 32(2), 927–950.

Green, R. A., and Terri, G. A. (2005). Number of equivalent cycles concept for liquefaction evaluations – revisited. *J Geotech Geoenviron Eng*, 131(4), 477–88.

Hancock, J., and Bommer, J. J. (2007). Using spectral matched records to explore the influence of strong motion duration on inelastic structural response. *Soil Dynamics and Earthquake Engineering*, 27, 291–299.

Haselton, C. B., Baker, J. W., Stewart, J. P., Whittaker, A. S., Luco, N., Fry, A., Hamburger, R. O., Zimmerman, R. B., Hooper, J. D., Charney, F. A., and Pekelnicky, R. G. (2017). Response history analysis for the design of new buildings in the NEHRP provisions and ASCE/SEI 7 Standard: Part I - overview and specification of ground motions. *Earthquake Spectra*, 33(2), 373–395.

Hashash, Y. M. A., Abrahamson, N. A., Olson, S. M., Hague, S., and Kim, B. (2015). Conditional mean spectra in site-specific seismic hazard evaluation for a major river crossing in the central United States. *Earthquake Spectra*, 31(1), 47–69.

Kwong, N. S., and Chopra, A. K. (2015). Selection and scaling of ground motions for nonlinear response history analysis of buildings in performance-based earthquake engineering. *PEER*

Report 2015/11, Pacific Earthquake Engineering Research Center, University of California, Berkeley, Calif., 223 pp.

McGuire, R. K., Silva, W. J., and Constantino, C. J. (2001). Technical basis for revision of regulatory guidance on design ground motions: Hazard- and risk-consistent ground motion spectra guidelines. *NUREG/CR-6728*, Prepared for the U.S. Nuclear Regulatory Commission, Washington, D.C.

NEHRP [National Earthquake Hazards Reduction Program] Consultants Joint Venture (2011). Selecting and scaling earthquake ground motions for performing response-history analyses. *NIST GCR 11-917-15, Technical Report*, National Institute of Standards and Technology, Washington, D.C.

Rathje, E. M., Kottke, A. R., and Trent, W. L. (2010). Influence of input motion and site property variabilities on seismic site response analysis. *J. Geotech. Geoenviron. Engin.*, 136(4), 607–619.

Peterman, B. R., and Rathje, E. M. (2017). Evaluation of ground motion selection techniques for seismic rigid sliding block analyses. *Journal of Geotechnical and Geoenvironmental Engineering*, 143(4), DOI: 10.1061/(ASCE)GT.1943-5606.0001626.

Raghunandan, M., and Liel, A. B. (2013). Effect of ground motion duration on earthquake-induced structural collapse. *Structural Safety*, 41, 119–133.

Rauch, A. F., and Martin, J. R. (2000). EPOLLS model for predicting average displacements on lateral spreads, *J. Geotech. Eng.*, 126, 360–371.

Shome, N., Cornell, C. A., Bazzurro, P., and Carballo, J. E. (1998). Earthquakes, records, and nonlinear responses. *Earthquake Spectra*, 14(3), 469–500.

Stewart, J. P., Afshari, K., and Hashash, Y. M. A. (2014). Guidelines for performing hazard consistent one-dimensional ground response analysis for ground motion prediction. *PEER Report 2014/16*, Pacific Earthquake Engineering Research Center, University of California, Berkeley, Calif., 152 pp.

USBR (2015). Reclamation design standard No. 13: Embankment dams, chapter 13: Seismic analysis and design. U. S. Bureau of Reclamation.

Zengin, E., Abrahamson, N. A., and Kunnath, S. (2020). Isolating the effect of ground-motion duration on structural damage and collapse of steel frame buildings. *Earthquake Spectra*, 36(2), 718-740.

CHAPTER 2: EFFECT OF GROUND MOTION SELECTION TECHNIQUES ON SITE RESPONSE ANALYSIS AT DIFFERENT SEISMOTECTONIC SETTINGS

Some of the contents of this chapter are published in:

Kaklamanos, J., Chowdhury, I. N., Cabas, A., Kottke, A., and Greggor, N. (2021). Sensitivity of site response analyses to input motion selection protocols, American Society of Civil Engineers (ASCE) Geotechnical Engineering for Extreme Events (GeoExtreme) 2021, 7–10 November, Savannah, GA.

Abstract

This study investigates the effect of current practices for ground motion selection on the results from site response analyses. The selected study sites (i.e., Seattle and Boston) represented different tectonic and geologic settings, and the selected input motion suites represented variations in the target spectrum definition, spectral period of interest, seismic source scenario, and ground motion database. When directly incorporated into target spectrum definitions, different types of seismic sources and the corresponding databases have a significant impact on the estimated site response as captured by spectral amplification factors and non-spectral intensity measures: significant duration and Arias intensity, particularly in subduction zone regions. The variability in spectral amplification factors is found to be higher near the site period. Conditional spectra is identified as a suitable target spectrum for sites having hazard contribution from multiple seismic sources; while it showed limited utility at stable continental region. The variability in site response estimates from different ground motion selection techniques is dependent on the site characteristics. Estimated responses at stiffer sites are more greatly influenced by ground motion selection techniques, whereas the onset of nonlinear soil behavior at softer sites can suppress such variability.

2.1 Introduction

Earthquake ground motions are greatly influenced by near-surface geologic materials as seismic waves propagate to the ground surface. Site response analyses (SRA) are used to estimate site-specific ground motions. In addition to their critical role in nonergodic probabilistic seismic hazard analyses (PSHA) and dynamic analyses of critical infrastructure (e.g., bridges, earth dams, and nuclear power plants), SRA also provide critical inputs for liquefaction and seismic slope stability assessments. Despite their broad applications in engineering practice, SRA is burdened with significant uncertainties associated with: (i) the properties of the soil profile, (ii) the selected constitutive models to represent dynamic soil behavior, (iii) the input ground motions assumed to be representative of the excitation at the base of the modeled soil column, and (iv) other modeling choices (such as one-, two- or three-dimensional wave propagation, linear, equivalent-linear or nonlinear analysis, and the elastic halfspace assumption).

The variability in SRA due to uncertainties in soil properties (e.g., the V_s profile, and/or modulus reduction and damping curves), model-to-model variability (e.g., equivalent-linear or nonlinear), and input ground motion selection has been previously investigated (e.g., Bazzurro and Cornell 2004, Li and Assimaki 2011, Rathje et al. 2010, Kwok et al. 2008). The most important source of variability affecting site amplifications is the input ground motion selection. Even though the effects of record-to-record variability (Bazzurro and Cornell 2004) and suite-to-suite variability (Rathje et al. 2010) on site response have been evaluated, the variability from different ground motion selection techniques has received rather limited attention.

In engineering practice, design ground motions are selected based on a target performance associated with an annual probability of exceeding a ground-motion intensity measure or hazard level. In recent years, the effects of different ground motion selection techniques on the seismic performance of a slope (Peterman and Rathje 2017), on liquefaction and lateral spreading (Hashash et al. 2015), and on the structural performance of buildings (Uribe et al. 2019) have been examined considering only shallow crustal earthquakes. However, selecting appropriate design level ground motions can be particularly challenging at sites where hazard contributions come from multiple seismic sources, or at sites located in stable continental regions (e.g., Central and Eastern United States, CEUS), where there is a paucity of recorded design level ground motions. Hence, the objective of this study is to investigate the effects of ground motion selection techniques on site response estimates; particularly focusing on the contribution of ground motion suites developed using multiple definitions of target spectra for different tectonic settings and corresponding databases.

In this study, we first describe our study sites selected to represent idealized site conditions in Seattle and Boston, which are exposed to distinct tectonic settings. Then we compare current practices for ground motion selection, namely the uniform hazard spectrum (UHS) and the conditional spectrum (CS, Baker 2011). One-dimensional SRA are performed at the study sites and variabilities in estimated results are evaluated for different ground motion selection techniques, in terms of spectral amplification factors and two non-spectral acceleration (non-SA) intensity measures (IMs): significant duration and Arias intensity. The effect of soil non-linearity and the effect of considering non-SA IMs (via the Generalized Conditional IM approach, GCIM, Bradley 2010) in ground motion selection are then discussed.

2.2 Study sites

2.2.1 Site profiles

Study sites located in Seattle, Washington from Western Unites States (WUS) and in Boston, Massachusetts from Central and Eastern United States (CEUS) are selected due to their exposure to different tectonic settings and geologic conditions. Seattle is located in a region of active tectonic activity that includes earthquakes associated with crustal faults and with the Cascadia subduction zone located off the Pacific Northwest coast. In contrast, Boston is located in a stable continental region with lower relative seismic activity. A geotechnical profile (Figure 2.1) is developed for each location to be representative of typical conditions in the center of Seattle and Boston, although there are significant variations in subsurface conditions throughout each city (Woodhouse and Barosh 2011/2012, Galster and Laprade 1991). We focus upon softer sites in each city where site response is expected to be more substantial, engineering ground motions are more challenging to predict, and critical infrastructure (e.g., ports, oil and gas storage facilities, and airports) is located.

The Seattle site consists of artificial fill over a thick layer of deltaic sand and estuarine silt, overlying a dense layer of reworked glacial deposits to a depth of 56.5 m, which represents dense preglacial deposits. The bottom of the soil profile is consistent with the lowest downhole seismometer at the Seattle Liquefaction Array (Shannon and Wilson, 2018); the data in this report were also used as the basis for the assumed V_S profile, which was developed from suspension P-S logging. Numerous seismic studies in the Seattle area (e.g., Williams et al., 1999) have concluded that most of the observed ground-motion amplifications are attributed to the upper layers (which consist of younger alluvium, i.e., post-glacial Holocene deposits), and are governed by the impedance contrast between the younger and older alluvium. The time-averaged shear wave

velocity in the top 30 m (V_{S30}) for the profile is 135 m/s, making this a Class E site according to National Earthquake Hazards Reduction Program (NEHRP) guidelines.

The Boston site consists of artificial fill, organic silt, glacial outwash (sand), and a thick layer of Boston Blue Clay overlying dense glacial till and bedrock at a depth of 51 m. The subsurface profile is consistent with data from the Northeastern University downhole array (Yegian, 2004). The V_S profile is based on the assumed generic profile of Baise et al. (2016), which was derived from multiple spectral analysis of surface waves (SASW) measurements throughout the Boston basin (Thompson et al. 2014). Baise et al. (2016) found that the impedance contrast at the Boston Blue Clay significantly influences amplifications in the Boston basin. The V_{S30} for the profile is 207 m/s, making this a NEHRP Class D site.

2.2.2 Probabilistic seismic hazard analysis (PSHA)

PSHA is conducted for the selected study sites, using the computer program HAZ46 (Abrahamson and Gregor 2018) to estimate the design-level ground motions at reference rock conditions. The assumed reference rock conditions for Seattle (V_{S30} 760 m/s, soft rock) and Boston (V_{S30} 2830 m/s, hard rock) are prevalent throughout the WUS and CEUS regions, respectively. Different seismic source characterization (SSC) and ground motion characterization (GMC) models are used for each site. For Seattle, we use the SSC model of the U.S. Geological Survey 2014 national seismic hazard maps (Petersen et al. 2014). For the crustal GMC model, four equally weighted NGA-West2 ground motion prediction equations (GMPEs) are used: Abrahamson et al. (2014), Boore et al. (2014), Campbell and Bozorgnia (2014), and Chiou and Youngs (2014). The Abrahamson et al. (2016) model is used for the subduction GMC model, which includes GMPEs

for both interface and intraslab events. The EPRI (2012) SSC model is implemented for the study site in Boston. The suite of GMPEs used for Boston are based on the set of 11 models developed by Silva et al. (2002), with assigned weights consistent with those of EPRI (2004).

2.2.3 Definition of target spectra

The uniform hazard spectrum (UHS) and the conditional spectrum (CS) are evaluated herein as alternative definitions of target spectra. The UHS envelopes spectral accelerations at different periods corresponding to the same hazard level or probability of exceedance. We use a 2500-year return period representative of design levels for critical infrastructure. It is recommended to select ground motions from events having compatible magnitude, source-to-site distance, source mechanism and site conditions (often parameterized by V_{s30}) as those controlling the target spectrum (Stewart et al. 2014). Deaggregation is useful in this regard, as it separates the contributions of multiple rupture scenarios to the hazard and hence, allows us to identify the predominant sources. Figure 2.2 presents deaggregation results for Seattle and Boston at spectral periods (T) of 0.01 s and 1.0 s. Figure 2.2a shows the contributions to the seismic hazard in Seattle (at a T=0.01 s) from three types of seismic sources, shallow crustal, subduction intraslab and subduction interface that have distinct magnitude and distance ranges. At shorter periods, the highest contribution to the hazard comes from the nearby shallow crustal and deep intraslab seismic sources. On the other hand, at longer periods (i.e., T=1 s; Figure 2.2b), the relative importance of the crustal and distant large magnitude interface sources increases, while the contribution from the intraslab sources decreases. In Boston, higher contributions to the seismic hazard correspond to nearby areal sources at shorter periods, as seen in Figure 2.2c. However, at longer periods, the deaggregation does not show any predominant contribution to the hazard from

a particular seismic source (Figure 2.2d). As shown by the deaggregation, identifying events with compatible magnitude-distance (M-R) combinations becomes unclear when the UHS is used as the target spectrum. Because UHS envelopes the contributions to the hazard from different seismic sources. Moreover, the high spectral values from the UHS across all periods of engineering interest are unlikely to be associated with any single recorded ground motion. Therefore, the spectral shapes of recorded ground motions will not match the UHS at all periods. Despite these limitations, the UHS is still widely used as target spectrum for ground motion selection. Figure 2.3a depicts the UHS for the site located in Seattle, along with the selected ground motions to be described shortly.

As an alternative to the UHS, the conditional mean spectrum, CMS (Baker and Cornell 2006, Baker 2011) can provide a spectral shape that is more representative of a response spectrum corresponding to a recorded ground motion. The CMS approach is gaining popularity with structural engineers but has not been commonly used in geotechnical engineering applications. In recent years, the CMS has been used to assess the seismic performance of a slope (Peterman and Rathje 2017) and in evaluating liquefaction and lateral spreading (Hashash et al. 2015). The CMS has the same spectral acceleration as the UHS at the conditioning period, which is often chosen based on the fundamental period of the structure. The spectral accelerations at all other periods of the CMS are conditional on the spectral acceleration at the conditioning period and the corresponding epsilon value. Epsilon is the number of standard deviations by which the target spectral acceleration differs from the median values at the conditioning period. The calculation of the CMS provides only mean spectral values without consideration of spectral variability in the recorded ground motions. The consideration of the mean and the variance in spectral values can

be accomplished by defining the conditional spectra, CS (Jayaram et al. 2011, Lin et al. 2013), which is the target spectrum adopted herein.

For the CS computation, usually the fundamental period of the structure is chosen as the conditioning period. Current practices in geotechnical applications mostly relies on short periods such as peak ground acceleration (PGA). However, for long-period structures like high-rise buildings or embankments, and for softer site profiles like the ones chosen in this study a longer conditioning period can be of interest too. Moreover, the hazard at short and long period is often dominated by different seismic sources. The choice of conditioning periods might introduce variability in site response estimates. To capture this variability, CS is computed for a short conditioning period (i.e., 0.01 s) and a long conditioning period (1.0 s) in this study. Recently Dhulipala et al. 2020 has shown that while spectral accelerations at short periods are usually an adequate intensity measure to predict site amplifications across the period range, for softer sites it is a better practice to ensure the amplification and spectral acceleration share the same oscillator period.

The selection of a representative M-R scenario is critical for the CS computation. Previous studies have defined the CS based on mean M-R values from deaggregation results (e.g., Baker 2011, Stewart et al. 2014), and on earthquake scenarios with the highest contributions to the hazard (e.g., Hashash et al. 2015, Peterman and Rathje 2017). Due to the diverse tectonic setting in Seattle, the mean M-R combination is not representative of the seismic hazard (Chowdhury et al. 2019). Hence, three different dominant M-R scenarios are selected corresponding to the three main seismic sources: (1) M 7.0, R 5 km for shallow crustal earthquakes; (2) M 7.0, R 50 km for

subduction intraslab earthquakes; and (3) M 9.0, R 100 km for subduction interface earthquakes. For these three scenarios, GMPEs corresponding to each type of seismic source are used in the computation of the CS. The Baker and Jayaram (2008) inter-period correlation model, which was developed using the NGA West 1 database (Chiou et al., 2008) with shallow crustal events, is used to compute the CS for all tectonic regimes considered in this study. Jayaram et al. (2011) showed that this model is reasonably applicable to subduction zones, while Carlton and Abrahamson (2014) concluded that any variation in correlation coefficients comes from differences in spectral shape rather than the tectonic regime. Figure 2.3b shows the CS conditioned at 0.01 s spectral period (referred as CS 0.01s from herein) for Seattle crustal scenario.

The seismicity of Boston at short periods is dominated by nearby areal seismic sources (Figure 2.2c). The modal scenario with magnitude of 5.5 and distance 30 km is selected for the computation of CS 0.01s. At a long spectral period of 1.0s (Figure 2.2d), the seismicity of Boston is diffuse like many other parts of CEUS. In such a case, averaging of probabilistic seismic hazard does not necessarily yield a plausible scenario earthquake. Because the mean (M 6.22, R 149.21 km) is dragged away from moderate near-source earthquakes towards the more distant larger magnitude earthquakes. In such instance, consideration of multiple scenarios (both local and distant sources that contribute significantly to the probabilistic hazard) is an approach that can be more consistent with physical reality (Harmsen and Frankel 2001). Hence both a nearby (M 5.5, R 30 km) and a distant scenario (M 6.5, R 100 km) are explored for computation of CS 1.0s.

2.3 Input motion selection

Amongst the two approaches available to achieve compatibility of recorded ground motions to a target spectrum i.e., scaling and spectral matching, the latter is not recommended as part of hazard-consistent SRA preferred practices (Stewart et al. 2014) because it changes the frequency content of the ground motion. Hence, only the scaling approach is implemented for ground motion selection in this study. Most of the tools available for ground motion selection and scaling select ground motions based on their fit to a single target spectrum. However, the CS approach does not provide a single target spectrum to match the ground motions to, because it considers the variability in the target spectra along with the mean spectrum. We use the algorithm of Baker and Lee (2017), which is an improvement of the Jayaram et al. (2011) selection algorithm, to select ground motions matching the CS. This algorithm samples data from a multivariate normal distribution with the target conditional mean (unconditional means can also be prescribed) and the corresponding covariance matrix to simulate realizations of response spectra. Then, ground motions that best match each of the statistically simulated spectra are selected from the specified database using the Kolmogorov-Smirnov goodness of fit test (KS test). This algorithm is used to select ground motions matching the CS and UHS in this study. When selecting motions to fit the UHS, the variance is set as zero, so that the motions are matched directly to the target spectrum across the period range of 0.01s and 5s.

2.3.1 Ground motion databases

The NGA-West2 database (Ancheta et al. 2014), which contains 21,359 records, is used to select shallow crustal earthquake motions for the study site in Seattle. The preliminary ground motion suite (Mazzoni et al. 2021) from the NGA-SUB database (Bozorgnia and Stewart 2020) is used to

select subduction zone events. The preliminary ground motion suite is released to the public in November 2019 and consisted of 500 motions mainly from earthquakes with moment magnitude (M) larger than 6.0 and PGA values greater than 0.01 g. For the subduction intraslab and interface earthquake scenario used in this study, relevant ground motions from the NGA-SUB database were used. The study site in Boston requires ground motions from a stable continental tectonic regime, so the NGA-East database (Goulet et al. 2014) with 9,382 records is used. However, ground motions recorded at hard-rock sites with V_{S30} = 2830 m/s (i.e., the reference site condition for Boston) are not available. While screening the database, compatible input motions are identified by starting with narrow ranges for key causal parameters (i.e., magnitude, distance, and V_{S30}) and then gradually relaxing those criteria starting with V_{S30}, and then distance and magnitude. This process allows us to find a sufficient number of ground motions with a good match to the target spectral shape as prescribed by Stewart et al. (2014). The scaling factor was restricted up to 5 to avoid unrealistic changes to other ground motion intensity measures such as Arias intensity.

Eleven ground-motion records (each having two orthogonal horizontal components) are selected for each suite in this study. The median ground-motion response spectra of two horizontal components of a recorded ground motion when rotated over all horizontal orientations (i.e., RotD50 spectra; Boore 2010), are used in this study to assess the agreement of selected ground motions to the assumed target spectra. The details corresponding to the selected ground motion suites are provided in Appendix I of this dissertation.

2.3.2 Implications of the tectonic settings

The selection of input motions matching target spectra defined in terms of UHS for our study site located in Seattle poses yet another challenge: the representation of different tectonic regimes contributing to the seismic hazard. On the other hand, the CS provides an opportunity to consider each dominant scenario separately (i.e., crustal, intraslab, and interface events). For comparison purposes, we have selected three suites of ground motions matching the UHS using the corresponding databases for each tectonic regime. In total, nine suites of eleven ground motions each are selected for the study site in Seattle, while four suites are selected for the Boston site. Table 2.1 presents a description of each suite including the corresponding target spectrum, conditioning period (for the CS suites), earthquake scenario considered, and database used. The details of the selected ground motions in each suite are listed in Appendix I. Example target spectra, along with the selected and scaled ground motion spectra, are shown in Figure 2.3 for the UHS and CS defined for the Seattle site. This figure evidence how the selected motions are compatible to both the conditional mean and variability as defined by the CS (Figure 2.3b), but that the agreement to the UHS does not consider such variability (Figure 2.3a).

Figure 2.4 displays the magnitude-distance distributions associated with the selected records from different databases (i.e., NGA-West2, NGA-SUB, and NGA-East). For the Seattle site, selected motions from subduction database includes larger-magnitude and longer-distance earthquakes when compared to the shallow crustal earthquake database (Figure 2.4a). As expected for stable continental regions, the NGA-East database used for input motion selection at the Boston site provides small-to moderate-magnitude earthquakes matching the hazard at the site (Figure 2.4b).

2.4 Site response analysis

The site response analysis is started with validating the selected site profiles shown earlier in Figure 2.1. The one-dimensional (1D) theoretical linear transfer functions (TTFs) and empirical transfer functions (ETFs) are plotted in Figure 2.5. The ETF corresponding to the Boston site was computed using data from the 2011 M 5.8 Mineral, Virginia, earthquake recorded at the Northeastern University Downhole Array. The ETFs for the Seattle site were computed using data from five earthquakes recorded at the Seattle Liquefaction Array. There appears to be agreement between the TTFs and ETFs, especially in terms of the periods and amplitudes of the fundamental and first higher modes (especially for Boston), which serves to validate the assumed V_S profiles (in Figure 2.1), and our 1D SRA results.

The ground motions at the surface of the sites are predicted with 1D total-stress nonlinear (NL) SRA in the time domain using the program DEEPSOIL (Hashash et al. 2018). For all layers, the Darendeli (2001) modulus-reduction and damping curves are used as the target relations for the NL analyses, and the Phillips and Hashash (2009) procedure is used to determine the hysteretic unload/reload parameters. The General Quadratic/Hyperbolic (GQ/H) constitutive model (Groholski et al. 2016), which incorporates shear strength corrections at large strains, is used to model dynamic soil behavior. The large shear strains incurred throughout the soil profile in Seattle necessitated the use of a NL constitutive model instead of an equivalent-linear (EQL) model (e.g., Kaklamanos and Bradley 2018); the differences are less substantial in Boston (where the levels of induced shear strain were smaller). Although both NL and EQL calculations were performed, we only focus on the NL results in this study.

SRA are conducted using the selected suites of motions for the study sites in Seattle and Boston (Table 2.1). As an example, Figure 2.6 shows the predicted NL site response results (amplification spectra and maximum shear strain [γ_{max}] profiles) for the CS suite with a conditioning period of 0.01 s for both sites. Both the sites show greater amplification of long period (low frequency) motions which is typical for soft sites (Seed et al. 1976). Nonetheless, the amplification spectra of Seattle illustrate significant deamplifications at short periods (high frequency). The maximum shear strain γ_{max} profile of Seattle (Figure 2.6c) can explain this behavior which exhibit the buildup of high strain level (with a median γ_{max} of approximately 3% at 5m depth) within the profile. Therefore, the effect of nonlinear soil behavior is high, and it has caused the deamplification of ground motion at periods shorter than 1 s (frequencies greater than 1 Hz). At periods longer than 1 s (frequencies less than 1 Hz), ground motion amplifications are observed as nonlinear deamplification soil behavior is not expected at such long periods. For the Boston site, the SRA resulted in significant ground-motion amplifications across all periods, as evidenced by the amplification spectra relative to the input motion. The greatest γ_{max} (median of approximately 0.02%) occurs between depths of 12 and 20 m (Figure 2.6d), which represents minimal nonlinearity.

We investigate how the variability in ground motion selection techniques propagates to the site response estimates. More specifically, first we observe the effect in site amplification factors and then in non-spectral intensity measures namely Arias intensity and significant duration. Additionally, we investigate if soil nonlinearity has any effect on the resulting variability in site response estimates. Next, non-spectral IMs are considered in ground motion selection and the outcomes are evaluated.

2.4.1 Variability in spectral amplification factors

Figure 2.7a-c shows the UHS, CS 0.01s and CS 1.0s defined for the Seattle study site, and the corresponding median acceleration 5% damped response spectra of selected ground motion suites matching the target spectra. Results for crustal, intraslab, and interface scenario are depicted separately. The spectral shape of the UHS (unlike the CS) does not vary, but the median of the selected ground motion suites corresponding to the different seismic source scenarios and ground-motion databases (as shown in Table 2.1) does. A reasonable match to the UHS is achieved when selecting ground motions from crustal earthquakes. However, ground motions from subduction zone earthquakes provide a poor match with the UHS at shorter periods (Figures 2.7b and 2.7c). Because ground motions from the distant interface earthquake scenario are usually expected to have less high-frequency content, which attenuates fast with distance. This phenomenon is represented well by the CS for interface scenario. On the other hand, the intraslab earthquake motions are usually poor in low-frequency content as depicted by the corresponding CS. As seen in Figure 2.7, CS often results in a better match with the spectral shape of selected ground motions over a wider range of periods compared to the UHS, and this can be attributed to the CS being more representative of recorded ground motions.

After conducting SRA using the selected suites of motions, the estimated median spectral accelerations at the ground surface (5% damped) and amplification factors ($AF = SA_{\text{surface}}/SA_{\text{input}}$) are illustrated in Figures 2.7d-i. UHS suites selected from crustal and subduction databases resulted in notable differences in predicted spectral accelerations and AFs. Ground motions from subduction events resulted in slightly higher predicted *AF* than those from crustal events at long periods. Differences in *AFs* are also significant when comparing CS suites defined for crustal,

interface, and intraslab scenario. One potential cause for these observations is the difference in frequency content and duration of ground motions recorded in subduction zones, which generally correspond to higher magnitude, distant earthquakes (Figure 2.4). The *AFs* from suites with different target spectrum definitions mostly converge for the crustal earthquake scenario (Figure 2.7g). However, for the subduction intraslab and interface scenarios, the differences in *AFs* as a function of the assumed target spectrum is more significant.

Figure 2.8a shows the target spectra and median of selected motions for each suite defined for Boston site. A good match between selected ground motions and target spectra is often only achieved for a narrow range of periods, and discrepancies are more significant at short periods (i.e., less than 0.5 s). One potential cause of this discrepancy is the paucity of strong ground-motion records in CEUS. Figure 2.8b provides a comparison of the corresponding spectral acceleration and *AFs* after SRA. The UHS and CS suites show significant variability in *AFs,* especially at short periods (i.e., less than 0.3 s).

To further quantify the effect of input motion selection techniques on SRA, the inter-suite (suites with different target spectra) standard deviation of median amplification factors (σ_{AF}) over the period is plotted in Figure 2.9. For the Seattle site, values of σ_{AF} are plotted separately for three different seismic scenarios (Figure 2.9a). The σ_{AF} are higher for the subduction scenarios compared to crustal scenario. Notably, σ_{AF} are markedly low at shorter periods specially for crustal and intraslab scenario. After a period of approximately 0.4 s, σ_{AF} gradually increases and reaches a peak after the site period (degraded site period of about 2s). At the study site in Boston, σ_{AF} are significant at short periods and reaches a peak around the site period of 0.75s (Figure 2.9b). For

both study sites, values of σ_{AF} show a sudden drop after reaching the peak value at the site period or degraded site period. Similar dispersion of σ_{AF} values across periods has been observed in previous studies (Li and Assimaki 2011, Rathje et al. 2010), where σ_{AF} was calculated as a function of other sources of variability in SRA (e.g., the V_s profile, modulus degradation and damping, MRD, curves, model-to-model variability, and suite-to-suite variability of input motions matched to a single target spectrum). Figure 2.9 shows that the inter-target spectrum variability in input motions also results in a similar trend for standard deviations of site amplification.

2.4.2 Effect of soil non-linearity

We observe that the variability in AFs from different target spectrum definitions is significantly lower at the Seattle study site at shorter periods (< 0.4s), compared the Boston study site (Figure 2.9). The likely reason could be the nonlinearity present in the soft soil layers at the Seattle site. As seen in Figure 2.6c, the values of maximum shear strain generated at the Seattle site in excess of 1% indicate significant nonlinear behavior (Kaklamanos et al 2013). The effects of nonlinearity are generally observed at short periods, especially lower than the site's fundamental period. At longer periods than the site period, the soil column responds as a rigid body because the wavelengths are longer than the soil column's thickness. Recordings from earthquakes like Mexico 1985, Loma Prieta 1989 (Darragh and Shakal 1991) to the more recent Anchorage, Alaska 2018 (Cramer and Jambo 2019) has shown the evidence of ground motion deamplification at high frequencies, due to soil nonlinearity. Thus, we hypothesize that nonlinear behavior experienced in soft soil layers at the Seattle site suppresses the variability from input motion selection at short periods. To test this hypothesis, we consider an additional idealized study site with stiffer soil

conditions (i.e., expected reduced nonlinear soil behavior for the same set of input motions), as illustrated in Figure 2.10a.

The additional study site in Seattle is derived using V_S data from Seattle rock sites in Wong et al. (2011), and consists of 9 m of shallow soil (glacial outwash / till with V_{S30} = 578 m/s, site class C) over reference rock (Site Class B/C, V_S = 760 m/s). The same suites of motions outlined in Table 2.1 are used to conduct 1D SRA at this stiff study site. Similar to many sites that consist of shallow soil deposits over bedrock, most of the nonlinear soil behavior occurs in the top layers of the profile (as shown in Figure 2.10b, the maximum shear strains approach 0.3% to 0.7% in the first 2 m of the profile, where $V_S \leq$ 215 m/s). However, the maximum peak shear strains do not exceed 0.02–0.03% for the remaining portion of the soil profile, which is an indicator of linear behavior. The previously selected suites of ground motions matching different target spectra (i.e., UHS, CS 0.01s, and CS 1.0s) for the Seattle crustal scenario (shown in Table 2.1) are used for site response analysis at the stiff study site. As the *AFs* in Figure 2.11a illustrate, the net result is a slight amplification of spectral acceleration, rather than the significant deamplification observed at the softer study site in Seattle. The standard deviation of AFs at the stiff site (Figure 2.11b) show higher values at shorter periods (i.e., less than 0.5 s), compared to the AFs at the soft Seattle study site. Values of σ_{AF} reach a peak at a degraded site period (0.2s for the stiff site) and then decrease, which constitutes a similar trend to the one observed in Figure 2.9a for the softer Seattle study site. Moreover, the σ_{AF} for the stiff study site approximates zero at long periods (> 1 s). 1-D site response analysis cannot capture site effects accurately at periods longer than the site period, which may explain the observed behavior. The higher variability in AFs at the stiff study site at shorter periods, compared to the low variability at the soft study site, confirms our hypothesis that the

variability in site response estimates from different target spectra definitions is influenced by nonlinear soil behavior. The variability in site response at stiff soil sites that exhibit less nonlinear soil behavior is more strongly influenced by input motion selection techniques than at soft soil sites, where the variability is dominated by nonlinearity.

2.4.3 Variability in non-spectral intensity measures

Current practice for ground motion selection relies on spectral acceleration as the primary intensity measure (IM), although consideration of other intensity metrics may better characterize the ground motion for a specific application. The severity of a ground motion depends on its amplitude, frequency content, and duration. Spectral accelerations can indirectly quantify the amplitude and frequency content of a ground motion; but often fail to correlate strongly with the duration of a motion. In geotechnical engineering analyses, the seismic response of geosystems often depends on cumulative effects, especially for liquefaction and seismic slope stability. For such analyses, IMs such as PGA, Arias intensity (Ia), cumulative absolute velocity (CAV), and significant duration ($D_{s5\text{-}95}$) can also be important. Linear scaling of input ground motions modifies the (elastic) acceleration response spectral ordinates linearly to match the hazard level considered. The selection of ground motions from events with magnitude, source to site distance, source mechanism and recorded at site conditions representative of the hazard level considered (Stewart et al 2014) has been recommended to indirectly consider other ground motion characteristics in addition to spectral acceleration. However, several ground motion IMs do not have a linear relationship with scaling. For example, Arias intensity is scaled by the square of scale factor and significant duration is not effected by scale factor. Therefore, if the target spectra are defined only in terms of spectral acceleration, linear scaling cannot ensure the match of other non-spectral IMs

to the hazard level considered (Bradley 2010). Moreover, SRA will also change the values of these input IMs, as local site conditions modifies the duration and frequency content of a ground motion along with the amplitude.

To capture the variability of other relevant ground motion characteristics, such as duration and cumulative effects, with ground motion selection techniques; we investigate the non-spectral IMs, 5-95% significant duration ($Ds_{5\text{-}95}$) and Arias intensity (Ia). Figure 2.12 displays the resulting medians of the non-spectral IMs for each suite (described in Table 2.1) after conducting SRA for the study sites in Seattle and Boston. Notable differences can be observed in the predictions from suites with different target spectra at both study sites. The subduction scenarios developed for the Seattle study site led to significantly higher values of $Ds_{5\text{-}95}$ and Ia than the crustal earthquake scenario (Figure 2.12a and 2.12b). The longer duration of the associated large-magnitude and distant subduction events (as seen in Figure 2.3a) have contributed to this. Values of Ia increase substantially due to large scaling factors, while values of $Ds_{5\text{-}95}$ are not affected by the linear scaling of ground motions.

At the Boston study site, resulting Ia values from SRA using the UHS suite are higher than their counterparts using the CS suites (Figure 2.12d). However, estimated $Ds_{5\text{-}95}$ from CS 1.0s suite are longer than those obtained from the UHS suite (Figure 2.12c). This observation stems from CS 1.0s suite having a controlling earthquake scenario with comparatively higher magnitude and longer distance. Significant duration has been observed to increase with earthquake magnitude and source-to-site distance (Abrahamson and Silva 1996, Kempton and Stewart 2006).

2.4.4 Effect of adding non-SA intensity measures

The variability in $Ds_{5\text{-}95}$ and Ia values (observed in Figure 2.12) for ground motion suites developed using different selection techniques can be particularly of significance for infrastructures or geosystems that experience stiffness degradation under cyclic loading. For example, sites having the potential for earthquake induced liquefaction triggering, lateral spreading and seismic instability like landslides. The UHS and CS do not consider non-SA IMs in ground motion selection. Therefore, it is imperative to evaluate the effect of adding non-spectral IMs in ground motion selection on the site response estimates.

To study the effect of considering non-SA IMs in ground motions selection, we use the Generalized Conditional Intensity Measure (GCIM) approach proposed by Bradley (2010). The site response estimates from GCIM suites are then compared with the CS suites. The GCIM approach is similar in development as CS except that it can consider any number of SA or non-SA IMs in ground motion selection. The conditional distribution of any ground motion IM (IMi) on the occurrence of a specific value of another ground motion IM (IMj) is determined. This requires the GMPEs for the IMs considered and the correlation coefficients between IMi and IMj (note that IMi can be more than one). The distributions are then used as 'targets' to select a consistent suite of ground motions following the selection algorithm by Bradley 2012. The GCIM computation in this study considers two non-SA IMs; namely$Ds_{5\text{-}95}$ and Ia along with spectral accelerations. The crustal earthquake scenario considered for the study site in Seattle is used for computing the GCIM distribution. The GCIM approach usually considers all rupture scenarios from the deaggregation. However, a simplified approach was implemented herein using the dominant rupture scenario from the deaggregation (M 7.0, R 5 km) to keep consistency with the CS computation method

implemented in this study. Peterman and Rathje (2010) showed that the GCIM distribution developed using all rupture scenarios and the simplified approach are similar. Thus, two target GCIM distributions are computed, conditioned on the 2% in 50 years spectral acceleration at 0.01s and 1.0s periods. GMPEs by Travasarou et al. (2003) and Abrahamson and Silva (1996) are used to calculate Ia and $Ds_{5\text{-}95}$, respectively. The correlation coefficients for Ia and $Ds_{5\text{-}95}$ are computed from Bradley (2011, 2015). Ground motions matching the GCIM distribution are selected using the selection algorithm by Bradley 2012 which uses the NGA-West1 database (Chiou et al. 2008) for shallow crustal earthquakes.

The target distributions for $Ds_{5\text{-}95}$ and Ia along with the empirical distributions of the selected suite of motions to fit GCIM (conditioned at SA 0.01s) are shown in Figure 2.13. The distributions of the CS suite are also shown for comparison purposes, although the CS implementation does not consider non-SA IMs during ground motion selection. The distribution of IMs from GCIM suite agrees well with the target distribution. The distribution of $Ds_{5\text{-}95}$ from the CS suite is slightly deviated from the targets but still fall within the KS bounds for $\alpha = 0.1$. However, the distribution of Ia from the CS suite falls outside the KS bounds. Figures 2.14a-b show the median amplification factors from GCIM suites after SRA at Seattle soft site and stiff site. Again, the median amplification factors from CS suites are also plotted for comparison. The main difference between the CS suite and GCIM suite here is the CS only considered spectral acceleration during ground motion selection, whereas the GCIM suite considered the $Ds_{5\text{-}95}$ and Ia along with the spectral accelerations. The variability of AFs from the consideration of non-SA IMs are not significant at the conditioning periods for both site conditions. However, slightly higher variability is observed at the longer and shorter periods for the soft site and the stiff site respectively, which agrees well

with the nonlinear characteristics of the sites (as described in earlier section). The standard deviation of amplification factors from these CS and GCIM suites are plotted in Figure 2.14(c-d). For all the suites, the σ_{AF} is higher at periods close to the site period for both the sites and for both the conditioning periods. The σ_{AF} values are comparable for both soft site and stiff site conditions, with the suites having longer conditioning period (1.0s) showing slightly higher peak values compared to shorter period (0.01s) suites.

After comparing the AFs, the non-SA IMs $Ds_{5\text{-}95}$ and Ia for the GCIM suites are also compared to the CS suites. Table 2.2 shows the median $Ds_{5\text{-}95}$ and Ia of ground motion suites after selection and scaling (input), and after the site response analyses (output) at both soft and stiff study sites in Seattle. The input $Ds_{5\text{-}95}$ values for GCIM and CS suites are similar. Even after site response analysis, the differences in output $Ds_{5\text{-}95}$ for these two target spectra definitions are negligible for the suites with short conditioning period (T=0.01s). However, higher differences can be observed for the suites with long conditioning period (T=1.0s), particularly at the soft site. Site response analysis at the stiff site in general did not change the $Ds_{5\text{-}95}$ values, i.e., there is hardly any difference between the input and output $Ds_{5\text{-}95}$ values. However, the soft site in Seattle has increased the output $Ds_{5\text{-}95}$ values substantially which can be attributed to the seismic waves being trapped in the softer soil layers for a prolonged period of time. Significant duration increases with decreasing stiffness of site profile as shown by Kempton and Stewart 2006. The soft site in Seattle has a lower Vs_{30} (135 m/s) than the stiff site (578 m/s) and conforms to this observation.

The input Ia from the CS suites are slightly higher than the corresponding GCIM suite. The soft site shows deamplification of Ia values whereas the stiff site shows amplification. At the soft site,

the deamplification of short period spectral acceleration (shown in Figure 2.6a) along with the increased duration of output motions (shown in Table 2.2) can be attributed to the decrease in output Ia. In contrary to that, the amplification of short period spectral acceleration (Figure 2.11a) along with no change in duration values (Table 2.2) has resulted in higher output Ia values at the stiff site. It is interesting to note that despite the differences in median Ia of selected and scaled input motions, the CS and GCIM suite has resulted in similar median Ia values at the soft site after site response analysis. On the other hand, the output Ia in the Seattle stiff site shows higher differences for GCIM and CS suites. Overall, the characteristics of the sites has significantly governed the differences between the site estimates from CS and GCIM suites. Higher difference in spectral amplification factors is observed near the site period. The estimates for non-SA IMs were also highly influenced by the site characteristics.

2.5 Discussion

2.5.1 Comparing different sources of variability at Seattle

Three different sources of uncertainty in ground motion selection considered in this study are compared in Figure 2.15 for Seattle soft site and stiff site. These three are: i) target spectrum definition varied for crustal scenario (UHS, CS 0.01s, GCIM 0.01s), ii) conditioning period varied for CS crustal scenario (CS 0.01s, CS 1.0s), and iii) seismic source type and database varied for CS 0.01s (crustal, intraslab and interface). The variability in AFs for all three sources are higher near the site period (or degraded site period) for each site. The variability from target spectrum definitions is suppressed at the shorter periods of soft site due to soil non-linearity (as described in previous sections). For the stiffer site, σ_{AF} from target spectrum definitions is evident for short periods but diminishes at longer periods. σ_{AF} from CS with short and long conditioning periods is

slightly higher for stiffer site. When the source type and database is varied for CS 0.01s, σ_{AF} reached a peak near the site period for both sites. However, the soft site showed higher variability compared to stiff site. Because the higher variation in targets at the long period were conveyed to site AF at the long site period for soft site.

2.5.2 CS exceeding UHS at Boston

Interestingly, the CS 0.01s and CS 1.0s (near) at Boston exceeds UHS at short periods despite the typical argument of UHS being the conservative spectrum. These two instances stem from two different conditions as described in the following paragraphs.

a) Negative epsilon value:

CS 0.01s exceeds UHS slightly at short periods (0.01-0.02s) due to the associated negative epsilon value (ε = -0.25). We observe similar exceedance of UHS by CS for other short conditioning periods (e.g., 0.2s, 0.5s) also. As an example, Figure 2.16a shows that the median response spectrum from GMPE is larger than the UHS when epsilon is negative (ε = -0.132). Hence the corresponding CS 0.2s also predicts larger response than UHS. Although we did not perform a deaggregation of epsilon in this study, the deaggregation maps for PGA available from USGS for Eastern North America (Harmsen 2001) shows that the region around Boston has negative modal epsilon values. The likely reason for this negative epsilon values are the special seismicity model and ground motion prediction equations used for CEUS. Such negative epsilon values are not usually observed in more seismically active WUS, hence has received rather limited attention. As shown by Burks and Baker (2011), in case of such negative epsilon occurrence, the use of CS will not be useful for practical engineering analysis.

b) Occurrence rate of historical earthquakes:

Figure 2.16b shows that the CS 1.0s (near) also exceeds UHS at shorter periods (0.01-1s) despite having a positive epsilon value ($\varepsilon = 0.44$). The median spectrum in this case falls below the UHS at the conditioning period of 1.0s but has larger response than UHS at shorter periods (0.01-0.3s). It can be due to the high frequencies of this nearby rupture scenario and the associated return period which may be longer than 2500 years. We have also plotted the UHS for 5000 years of return period for comparison and it is larger than the median spectrum. The overall low seismicity of this region may cause the low annual occurrence rate of this rupture scenario. However, the historical earthquakes evidenced near northeast of Boston (e.g., 1727 M 5.5 Newburyport, 1755 M 6.1 Cape Ann earthquake) emphasizes the importance of considering nearby rupture scenarios for engineering design.

CS is of interest as an alternative target spectrum, partially because it usually predicts an unconservative response spectrum compared to UHS. However, our results indicate that in a low to moderate seismic region like CEUS, the utility of this tool may be limited. Hence, we need to be cautious about the use of CS for such regions. In cases where CS exceeds UHS, the later might be the preferred target spectrum for engineering design. Nonetheless, the choice of a best suited target spectrum depends on the goal of the analysis. One might even decide to use the median spectrum associated with the causal magnitude and distance as a practical target spectrum for critical infrastructure, although that would mean applying an additional level of conservatism.

2.6 Conclusions

This study investigated the effect of different ground motion selection techniques on the results from site response analyses. The selected study sites (Seattle and Boston) represented different tectonic and geologic settings, and the selected input motion suites represented variations in the target spectrum definition, spectral period of interest, seismic source scenario, and ground motion database. The following conclusions were obtained from this study:

- In a site such as Seattle, where hazard contributions come from multiple types of seismic sources, the use of ground motions from different databases (with crustal or subduction events) to match the same target spectra (UHS) resulted in significantly different estimated site response. CS can be a plausible alternative in this case to overcome the limitations of the UHS, as it provides the opportunity to consider the crustal and subduction scenarios separately and to use ground-motion databases that are appropriate for each type of seismic source. However, our results indicate that in a low to moderate seismic region like CEUS, the utility of this tool may be limited as CS can exceed UHS. Hence, we need to be cautious about the use of CS for such regions. In cases where the CS exceeds the UHS, the latter is the preferred target spectrum for engineering design.
- The variability in site response estimates for different target spectra definitions is higher for subduction scenario compared to crustal scenario. The spectral amplification factors and non-SA IMs (significant duration and Arias intensity) are higher for subduction scenarios and ground motions from corresponding databases. Using shorter-duration ground motions (from shallow crustal events relative to subduction events) can result in the underprediction of surface ground-motion IMs at locations where the hazard can be dominated by long-duration ground motions, such as subduction zone environments.

Therefore, it is crucial for such sites to consider all possible earthquake sources and use the corresponding databases to select input motions for site response analyses.

- The variabilities in spectral amplification factors for different target spectra definitions reach a peak near the site period and usually decreases beyond that. Similar trend was observed in several previous studies (e.g., Kwok et al. 2008, Li and Assimaki 2011, Rathje et al. 2010) for other sources of variability in site response analysis (Vs profile, MRD curves, model-to-model variability, and suite-to-suite variability of input motions). For the sites having significant nonlinearity (e.g., Seattle soft and stiff site), period elongation effect is also observed in this study, i.e., the variabilities in amplification factor reach a peak at a degraded site period.
- Ground motion selection techniques results in higher variabilities in stiffer sites compared to softer sites. When nonlinearity is significant, the effects of site-response modeling assumptions and parameters may outweigh the effects of input motion selection techniques at short spectral periods. At longer spectral periods for soft sites, nonlinear soil behavior is less prevalent, and predicted surface ground motions are more greatly affected by the input motion selection technique.
- The effect of adding non-SA IMs in ground motion selection is greatly influenced by the site characteristics. The variabilities in spectral amplification factors for the CS and GCIM suites are negligible at the conditioning period. However, slightly higher variability can be observed at the periods near the site period. The estimated non-SA IMs are also influenced by the nonlinear characteristics of the site, which in several cases obscured the difference in ground motion selection techniques.

The results of this study advance our understanding of how input motion selection techniques influence the results from 1D site response analyses and which factors in the selection process contributes to higher variabilities. The effect of ground motion selection techniques in site response is dependent on the site characteristics. The site estimates can often be governed by the characteristics of the site (presence of non-linearity, amplification or deamplification) rather than the differences in ground motion selection. The selection of compatible records to hard-rock conditions representative of the bedrock in the CEUS continues to be challenge. Efforts toward expanding and improving ground motion databases in low-to-moderate seismicity regions and subduction zones and developing corresponding GMPEs for SA and non-SA IMs remain a priority for our scientific community.

References

Abrahamson, N. A., and Gregor., N. (2018). *HAZ46*, Seismic Hazard Analysis Software, https://github.com/abrahamson/HAZ (last accessed 1 November 2019).

Abrahamson, N. A., and Silva W. J. (1996). Empirical ground motion models. *Report to Brookhaven National Laboratory*.

Abrahamson, N. A., Silva, W. J., and Kamai, R. (2014). Summary of the ASK14 ground motion relation for active crustal regions, *Earthquake Spectra,* 30(3), 1025–1055.

Abrahamson, N., Gregor, N., and Addo, K. (2016). BC Hydro ground motion prediction equations for subduction earthquakes, *Earthquake Spectra*, 32(1), 23-44.

Allen, T. I., Wald, D. J., Hotovec, A. J., Lin, K., Earle, P. S., and Marano, K. D. (2008). An atlas of ShakeMaps for selected global earthquakes, *U. S. Geological Survey Open-File Report 2008-1236*, 41 pp.

American Society of Civil Engineers (ASCE) (2016). *Minimum Design Loads for Buildings and Other Structures (Standards ASCE/SEI 7-16)*. American Society of Civil Engineers, Reston, Virginia.

Ancheta, T. D., Darragh, R. B., Stewart, J. P., Seyhan, E., Silva, W. J., Chiou, B. S.-J., Wooddell, K. E., Graves, R. W., Kottke, A. R., Boore, D. M., Kishida, T., and Donahue, J. L. (2014). NGA-West2 Database, *Earthquake Spectra*, 30(3), pp. 989–1005.

Arias, A. (1970). A measure of earthquake intensity. In: Hansen RJ, editor. Cambridge, MA: MIT Press, p. 438–83.

Bahrampouri, M., Rodriguez-Marek, A., and Bommer, J. J. (2019). Mapping the uncertainty in modulus reduction and damping curves onto the uncertainty of site amplification functions. *Soil Dynamics and Earthquake Engineering*, 126, article 105091.

Baise, L. G., Kaklamanos, J., Berry, B. M., and Thompson, E. M. (2016). Soil amplification with a strong impedance contrast: Boston, Massachusetts, *Engineering Geology*, 202, 1–13.

Baker, J. W. (2011). Conditional mean spectrum: Tool for ground motion selection. *Journal of Structural Engineering*, 137(3), 322–331.

Baker, J. W., and Cornell, C. A. (2006). Spectral shape, epsilon, and record selection. *Earthquake Engineering and Structural Dynamics*, 35, 1077–1095.

Baker, J. W., and Jayaram, N. (2008). Correlation of spectral acceleration values from NGA ground motion models. *Earthquake Spectra*, 24, 299–317.

Baker, J. W., and Lee, C. (2017). An improved algorithm for selecting ground motions to match a conditional spectrum. *Journal of Earthquake Engineering,* 22(4), 708–723.

Bazzurro, P., and Cornell, C. A. (2004). Ground-motion amplification in nonlinear soil sites with uncertain properties. *Bulletin of the Seismological Society of America,* 94, 2090–2109.

Boore, D. M, Stewart, J. P., Seyhan, E., and Atkinson, G. M. (2014). NGA-West2 equations for predicting PGA, PGV, and 5% damped PSA for shallow crustal earthquakes. *Earthquake Spectra,* 30(3), 1057–1085.

Bommer, J., and Acevedo, A. (2004). The use of real earthquake accelerograms as input to dynamic analysis. *Journal of Earthquake Engineering,* 8, 43–91.

Bradley, B. A. (2010). A generalized conditional intensity measure approach and holistic ground motion selection. *Earthquake Engineering and Structural Dynamics,* 39, 1321–1342.

Building Seismic Safety Council (BSSC) (2015). *NEHRP Recommended Seismic Provisions for New Buildings and Other Structures (FEMA P-1050-1): Volume 1: Part 1 Provisions, Part 2 Commentary*, Federal Emergency Management Agency, Washington, D.C., 555 pp.

Cabas, A., and Rodriguez-Marek, A. (2017). V_S-κ_0 correction factors for input ground motions used in seismic site response analysis. *Earthquake Spectra,* 33(3), 917–941.

Campbell, K. W., and Bozorgnia, Y. (2014). NGA-West2 ground motion model for the average horizontal components of PGA, PGV, and 5% damped linear acceleration response spectra. *Earthquake Spectra,* 30(3), 1087–1115.

Carlton, B., and Abrahamson, N. (2014). Issues and approaches for implementing conditional mean spectra in practice. *Bulletin of the Seismological Society of America,* 104(1), 503–512.

Chiou, B. S.-J., Darragh, R., Gregor, N., and Silva, W. (2008). NGA Project Strong-Motion Database. *Earthquake Spectra,* 24, 23–44.

Chiou, B. S.-J., and Youngs, R. R. (2014). Update of the Chiou and Youngs NGA model for the average horizontal component of peak ground motion and response spectra. *Earthquake Spectra,* 30(3), 1117–1153.

Chowdhury, I. N., Cabas, A., Kaklamanos, J., Kottke, A., Gregor, N., and Lang, K. M. (2019). Ground motion selection using the conditional spectrum: Insights for different tectonic environments, pp. 1803–1811 in *Earthquake Geotechnical Engineering for Protection and Development of Environment and Constructions: Proceedings of the VII ICEGE Seventh*

International Conference on Earthquake Geotechnical Engineering, F. Silvestri and N. Moraci (eds.), CRC Press, 17–20 June 2019, Rome, Italy.

Darendeli, M. B. (2001). Development of a new family of normalized modulus reduction and material damping curves, Ph.D. Thesis, University of Texas at Austin, Austin, Texas, 396 pp.

EPRI (2004). CEUS Ground Motion Project Final Report, *EPRI Report No. 1009684*, Electric Power Research Institute, Palo Alto, Calif.

EPRI (2012). Central and Eastern United States Seismic Source Characterization for Nuclear Facilities. *EPRI Report No. 1021097*, Electric Power Research Institute, Palo Alto, Calif.

Galster, R. W., and Laprade, W. T. (1991). Geology of Seattle, Washington, United States of America, *Bulletin of Engineering Geology and the Environment,* 28(3), 235–302.

Goulet, C. A., Kishida, T., Ancheta, T. D., Cramer, C. H., Darragh, R. B., Silva, W. J., Hashash, Y. M. A., Harmon, J., Stewart, J. P., Wooddell, K. E., and Youngs, R. R. (2014). NGA-East Database, *PEER Report 2014/07*, Pacific Earthquake Engineering Research Center, University of California, Berkeley, California, 124 pp.

Groholski, D. R., Hashash, Y. M. A., Kim, B., Musgrove, M., Harmon, J., and Stewart, J. P. (2016). Simplified model for small-strain nonlinearity and strength in 1D seismic site response analysis, *Journal of Geotechnical and Geoenvironmental Engineering,* 142(9).

Haselton, C. B., Baker, J. W., Stewart, J. P., Whittaker, A. S., Luco, N., Fry, A., Hamburger, R. O., Zimmerman, R. B., Hooper, J. D., Charney, F. A., and Pekelnicky, R. G. (2017). Response history analysis for the design of new buildings in the NEHRP provisions and ASCE/SEI 7 Standard: Part I - overview and specification of ground motions. *Earthquake Spectra*, 33(2), 373–395.

Hashash, Y. M. A., Abrahamson, N. A., Olson, S. M., Hague, S., and Kim, B. (2015). Conditional mean spectra in site-specific seismic hazard evaluation for a major river crossing in the central United States. *Earthquake Spectra,* 31(1), 47–69.

Hashash, Y. M. A., Musgrove, M. I., Harmon, J. A., Ilhan, O., Groholski, D. R., Phillips, C. A., and Park, D. (2018). *DEEPSOIL 7.0, User Manual*, Univ. of Illinois at Urbana-Champaign, Champaign, Illinois, 169 pp.

Heo, Y. A., Kunnath, S. K., and Abrahamson, N. (2011). Amplitude-scaled versus spectrum matched ground motions for seismic performance assessment. *Journal of Structural Engineering,* 137(3), 278–288.

Jayaram, N., Lin, T., and Baker J. W. (2011). A computationally efficient ground-motion selection algorithm for matching a target response spectrum mean and variance. *Earthquake Spectra*, 27, 797–815.

Kaklamanos, J., and Bradley, B. A. (2018). Challenges in predicting seismic site response with 1D analyses: Conclusions from 114 KiK-net vertical seismometer arrays. *Bulletin of the Seismological Society of America*, 108(5A), 2816–2838.

Kaklamanos, J., Bradley, B. A., Thompson, E. M., and Baise, L. G. (2013). Critical parameters affecting bias and variability in site response analyses using KiK-net downhole array data. *Bulletin of the Seismological Society of America*, 103(3), 1733–1749.

Kaklamanos, J., Baise, L. G., Thompson, E. M., and Dorfmann, L. (2015). Comparison of 1D linear, equivalent-linear, and nonlinear site response models at six KiK-net validation sites. *Soil Dynamics and Earthquake Engineering*, 69, 207–219.

Kaklamanos, J., B. A. Bradley, A. N. Moolacattu, and B. M. Picard (2020). Physical hypotheses for adjusting coarse profiles and improving 1D site response estimation assessed at 10 KiK-net sites, *Bulletin of the Seismological Society of America*, 110(3): 1338–1358.

Kim, B., Hashash, Y. M., Stewart, J. P., Rathje, E. M., Harmon, J. A., Musgrove, M. I., and Silva, W. J. (2016). Relative differences between nonlinear and equivalent-linear 1-D site response analyses. *Earthquake Spectra*, 32(3), 1845–1865.

Kishida, T., Bozorgnia, Y., Abrahamson, N., Ahdi, S., Ancheta, T., Boore, D., Campbell, K., Chiou, B., Darragh, R., Gregor, N., Kamai, R., Kwak, D., Kwok, A., Lin, P., Magistrale, H., Midorikawa, S., Parker, G., Si, H., Silva, W., Stewart, J., Tsai, C., Wooddell, K., and Youngs, R. (2017). Development of the NGA-Subduction database, Paper No. 3452 in *16th World Conference on Earthquake Engineering*, 9-13 January 2017, Santiago, Chile.

Kottke, A. R., and Rathje, E. M. (2008). A semi-automated procedure for selecting and scaling recorded earthquake motions for dynamic analysis. *Earthquake Spectra*, 24(4), 911–932.

Kwok, A. O. L., Stewart, J. P., and Hashash, Y. M. A. (2008). Nonlinear ground response analysis of Turkey Flat shallow stiff soil site to strong ground motion. *Bulletin of the Seismological Society of America*, 98(1), 331–343.

Kwong, N. S., and Chopra, A. K. (2015). Selection and scaling of ground motions for nonlinear response history analysis of buildings in performance-based earthquake engineering, *PEER*

Report 2015/11, Pacific Earthquake Engineering Research Center, University of California, Berkeley, Calif., 223 pp.

Li, W., and Assimaki, D. (2010). Site and ground motion dependent parametric uncertainty of nonlinear site response analyses in earthquake simulations. *Bulletin of the Seismological Society of America*, 100(3), 954–968.

Lin, T., Harmsen, S. C., Baker, J. W., and Luco, N. (2013). Conditional spectrum computation incorporating multiple causal earthquakes and ground motion prediction models. *Bulletin of the Seismological Society of America,* 103(2A), 1103–1116.

Luco, N., and Bazzurro, P. (2007). Does amplitude scaling of ground motion records result in biased nonlinear structural drift responses? *Earthquake Engineering and Structural Dynamics,* 36(13), 1813–1835.

Mazzoni, S., Kishida, T., Contreras, V., Ahdi, S. K., Kwak, D. Y., Bozorgnia, Y., and Stewart J. P. (2021). NGA Subduction Database Preliminary Ground Motion Suite (Public Release), The B. John Garrick Institute for the Risk Sciences. https://www.risksciences.ucla.edu/nhr3/gmdata/preliminary-nga-subduction-records

McGuire R. K. (1995). Probabilistic seismic hazard analysis and design earthquakes: closing the loop. *Bulletin of the Seismological Society of America,* 85(5), 1275–1284.

McGuire, R. K., Silva, W. J., and Constantino, C. J., (2001). Technical basis for revision of regulatory guidance on design ground motions: Hazard- and risk-consistent ground motion spectra guidelines, *NUREG/CR-6728*, Prepared for the U.S. Nuclear Regulatory Commission, Washington, D.C.

Naeim, F. and Lew, M. (1995). On the use of design spectrum compatible time histories. *Earthquake Spectra*, 11(1), 111–127.

NEHRP [National Earthquake Hazards Reduction Program] Consultants Joint Venture (2011). Selecting and scaling earthquake ground motions for performing response-history analyses, *NIST GCR 11-917-15, Technical Report*, National Institute of Standards and Technology, Washington, D.C.

Okada, Y., Kasahara, K., Hori, S., Obara, K., Sekiguchi, S., Fujiwara, H., and Yamamoto, A. (2004). Recent progress of seismic observations networks in Japan – Hi-net, F-net, K-net and KiK-net. *Earth, Planets, and Space*, 56, xv–xxviii.

Peterman, B. R., and Rathje, E. M. (2017). Evaluation of ground motion selection techniques for seismic rigid sliding block analyses. *Journal of Geotechnical and Geoenvironmental Engineering,* 143(4).

Petersen, M. D., Moschetti, M. P., Powers, P. M., Mueller, C. S., Haller, K. M., Frankel, A. D., Zeng, Y., Rezaeian, S., Harmsen, S. C., Boyd, O. S., Field, N., Chen, R., Rukstales, K. S., Luco, N., Wheeler, R. L., Williams, R. A., and Olsen, A. H. (2014). Documentation for the 2014 update of the United States national seismic hazard maps. *U.S. Geological Survey Open-File Report 2014–1091*, 243 pp.

Phillips, C., and Hashash, Y. M. A. (2009). Damping formulation for nonlinear 1D site response analyses. *Soil Dynamics and Earthquake Engineering,* 29, 1143–1158.

Rathje, E. M., Kottke, A. R., and Trent, W. L. (2010). Influence of input motion and site property variabilities on seismic site response analysis. J. Geotech. Geoenviron. Eng, 136(4), 607–619.

Shahi, S. K., and Baker, J. W. (2014). NGA-West2 models for ground motion directionality. *Earthquake Spectra,* 30, 1285–1300.

Shannon and Wilson (2018). Geotechnical data report, Stanford center liquefaction monitoring array, Seattle, Washington, *Report No. 21-1-21441-001,* 333 pp.

Silva, W., Gregor, N., and Darragh, R. (2002). Development of regional hard rock attenuation relations for central and eastern North America. *Pacific Engineering and Analysis Technical Report,* El Cerrito, Calif., 57 pp.

Stewart, J. P., Afshari, K., and Hashash, Y. M. A. (2014). Guidelines for performing hazard consistent one-dimensional ground response analysis for ground motion prediction. *PEER Report 2014/16,* Pacific Earthquake Engineering Research Center, University of California, Berkeley, Calif., 152 pp.

Tarbali, K., and Bradley, B. A. (2016). The effect of causal parameter bounds in PSHA-based ground motion selection. *Earthquake Engineering and Structural Dynamics,* 45, 1515–1535.

Toro, G. R. (1995). Probabilistic models of site velocity profiles for generic and site-specific ground-motion amplification studies. *Technical Report No. 779574*, Brookhaven National Laboratory, Upton, N.Y., 147 pp.

Thompson, E. M., Carkin, B., Baise, L. G., and Kayen, R. E. (2014). Surface wave site characterization at 27 locations near Boston, Massachusetts, including 2 strong-motion stations. *U.S. Geological Survey Open-File Report 2014–1232*, 27 pp.

Watson-Lamprey, J., and Abrahamson, N. (2006). Selection of ground motion time series and limits on scaling. *Soil Dynamics and Earthquake Engineering,* 26, 477–482.

Williams, R. A., Stephenson, W. J., Frankel, A. D., and Odum, J. K. (1999). Surface seismic measurements of near-surface P- and S-wave seismic velocities at earthquake recording stations, Seattle, Washington. *Earthquake Spectra,* 15, 565–584.

Woodhouse, D., and Barosh, P. J., (2011/2012). Geotechnical factors in Boston. *Civil Engineering Practice* 26/27, 237–263.

Wong, I. G., Stokoe, K. H., Cox, B. R., Lin, Y.-C., and Menq, F.-Y. (2011). Shear-wave velocity profiling of strong motion sites that recorded the 2001 Nisqually, Washington, earthquake. *Earthquake Spectra,* 27(1), 183–212.

Yegian, M. K. (2004). Seismic recording station at Northeastern University, Boston, Massachusetts. *Proceedings of the COSMOS International Workshop on Strong Motion Instrumentation,* Consortium of Organizations for Strong Motion Observation Systems (COSMOS), 15 pp., 26-27 May 2004, Richmond, Calif.

TABLES

Table 2.1 Suites of ground motions for Seattle and Boston

Suite	Target Spectrum	Conditioning period (s)	Earthquake scenario	Moment magnitude (M_w)	Rupture distance (km)	Database
Seattle:						
UHS-crustal	UHS	-	all	-	-	NGA-West2
UHS-intraslab	UHS	-	all	-	-	NGA-SUB (intraslab)
UHS-interface	UHS	-	all	-	-	NGA-SUB (interface)
CS 0.01s-crustal	CS		crustal	7	5	NGA-West2
CS 0.01s-intraslab	CS	0.01	intraslab	7	50	NGA-SUB (intraslab)
CS 0.01s-interface	CS		interface	9	100	NGA-SUB (interface)
CS 1.0s-crustal	CS		crustal	7	5	NGA-West2
CS 1.0s-intraslab	CS	1	intraslab	7	50	NGA-SUB (intraslab)
CS 1.0s-interface	CS		interface	9	100	NGA-SUB (interface)
Boston:						
UHS	UHS	-	all	-	-	NGA-East
CS 0.01s	CS	0.01	mode	5.5	30	NGA-East
CS 1.0s-near	CS	1	mode	5.5	30	NGA-East
CS 1.0s-distant	CS	1	mode	6.5	100	NGA-East

Table 2.2 Median intensity measures of selected and scaled input ground motion suites and output motions from site response analyses at Seattle soft and stiff site for crustal scenario.

Suite	Significant duration, $Ds_{5\text{-}95}$ (s)			Arias intensity, Ia (m/s)		
	Input	Output at soft site	Output at stiff site	Input	Output at soft site	Output at stiff site
GCIM 0.01s	11.93	25.27	13.16	3.42	1.16	7.71
CS 0.01s	9.83	25.4	11.64	4.71	1.23	11.97
GCIM 1.0s	13.88	23.54	13.95	1.99	1.45	3.78
CS 1.0s	13.1	33.61	16.01	3.16	1.43	5.98

FIGURES

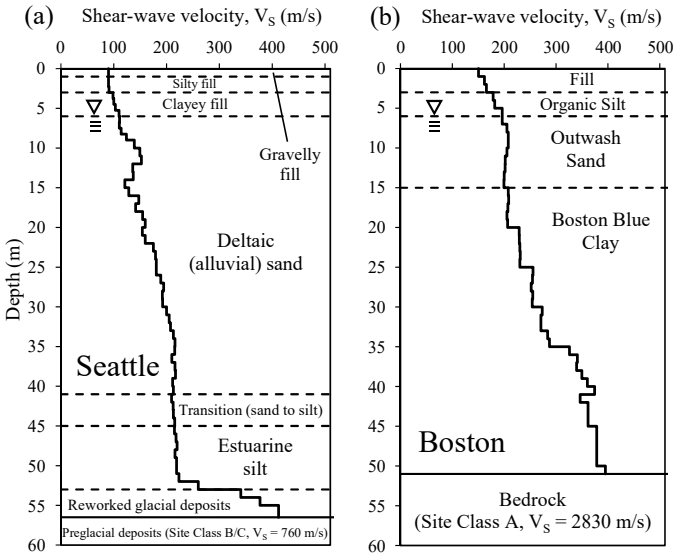

Figure 2.1 Shear-wave velocity profiles and geotechnical profiles used in the analyses for our study sites located in (a) Seattle and (b) Boston. The groundwater table is assumed to be at a depth of 5 m at each site.

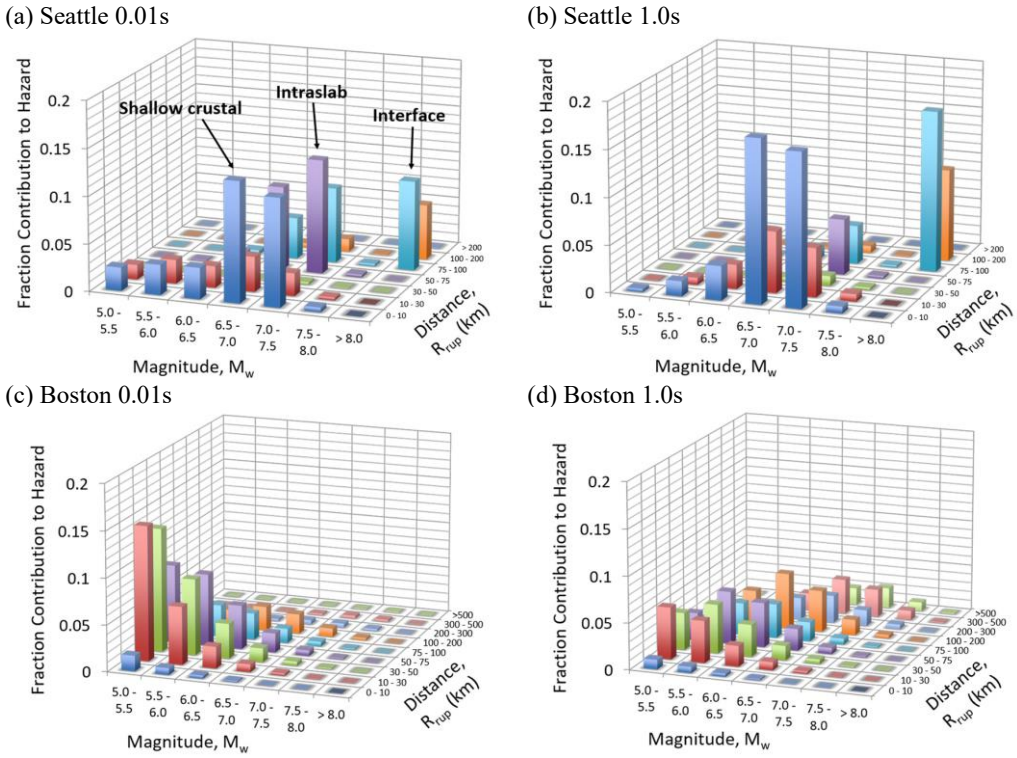

Figure 2.2 PSHA deaggregation results corresponding to the study site in Seattle at periods of (a) 0.01s and (b) 1.0s, and for the study site in Boston at periods of (c) 0.01s and (d) 1.0s.

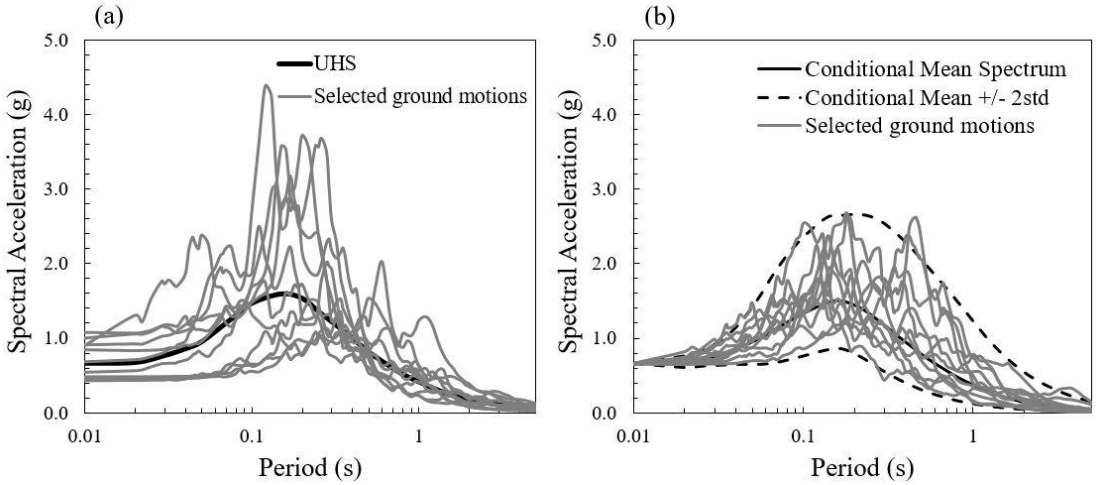

Figure 2.3 Target spectra and ground motion spectra of selected motions for (a) the UHS (2500-year return period), and (b) and the CS at 0.01 s defined for the study site located in Seattle.

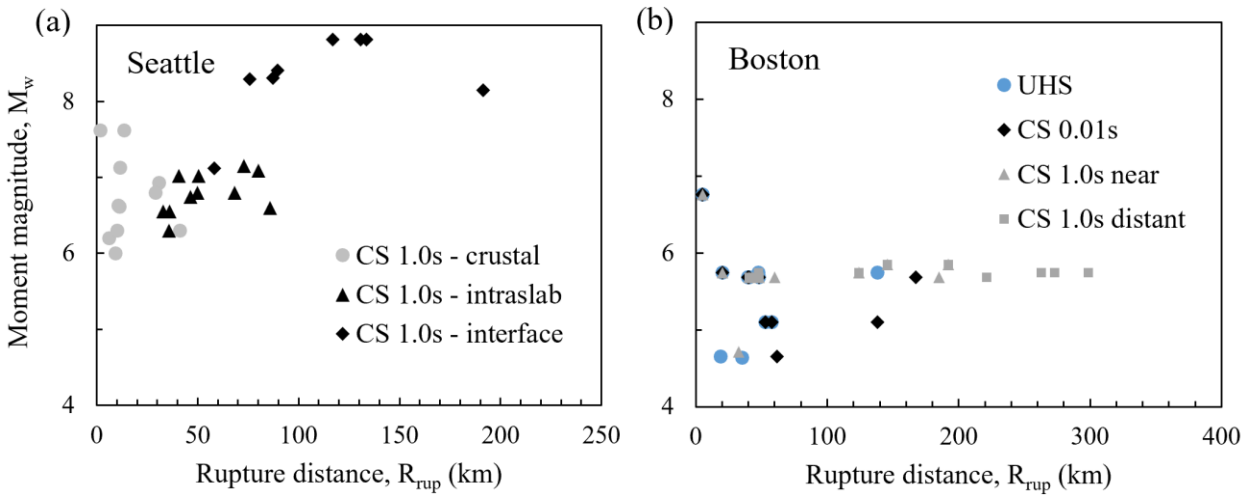

Figure 2.4 Magnitude-distance distributions of ground motions in selected suites for the study sites in (a) Seattle (i.e., CS 1.0 s for different tectonic regimes) and (b) Boston (i.e., UHS, CS 0.01s and CS 1.0s).

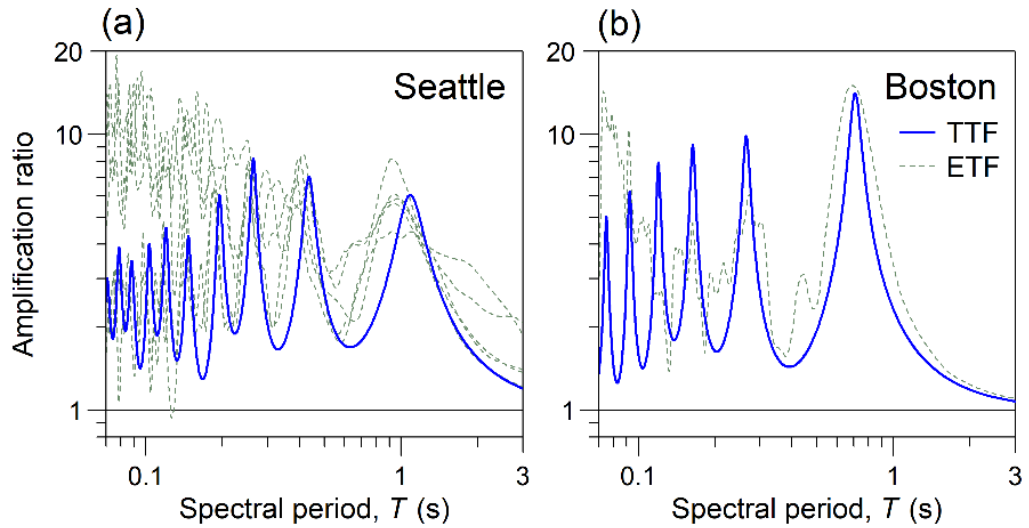

Figure 2.5 Comparisons of theoretical (1D linear) and empirical transfer functions for our study sites in (a) Seattle and (b) Boston. Data from five earthquakes recorded at the Seattle Liquefaction Array, and from 2011 Mineral Virginia earthquake recorded at the Northeastern University Downhole Array, were used to compute the ETFs for the Seattle and Boston sites, respectively.

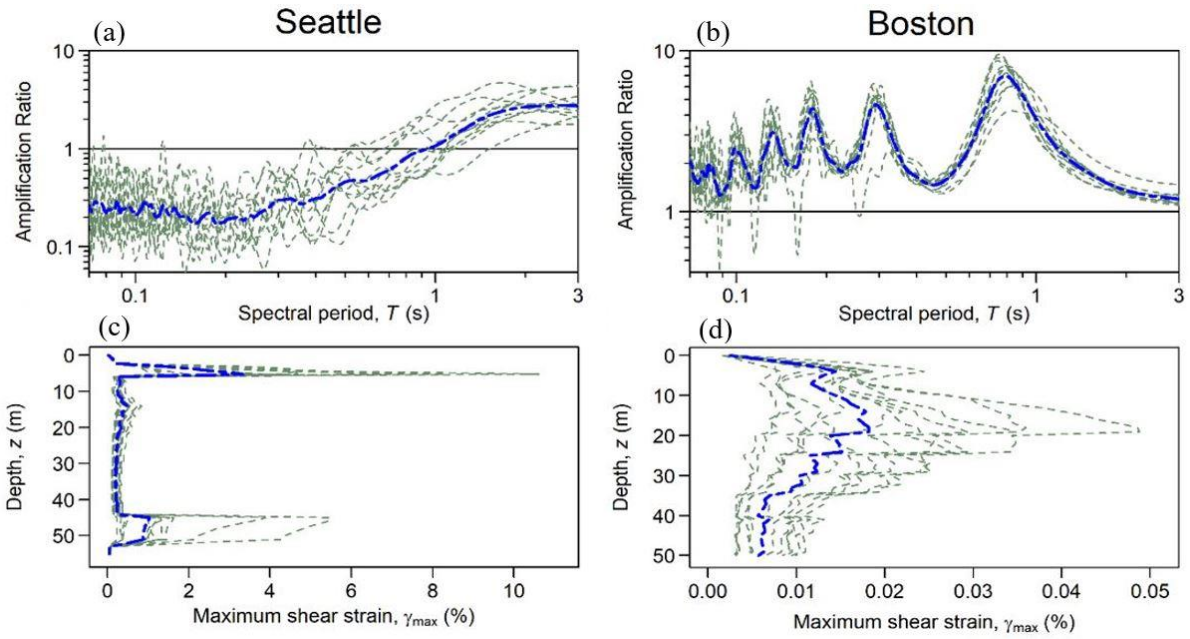

Figure 2.6 After NL site response analysis (a) amplification spectra of the CS 0.01s suite at Seattle site (crustal earthquake scenario), (b) amplification spectra of the CS 0.01s suite at Boston site (stable tectonic earthquake), and (c,d) the corresponding profiles of maximum shear strain with depth.

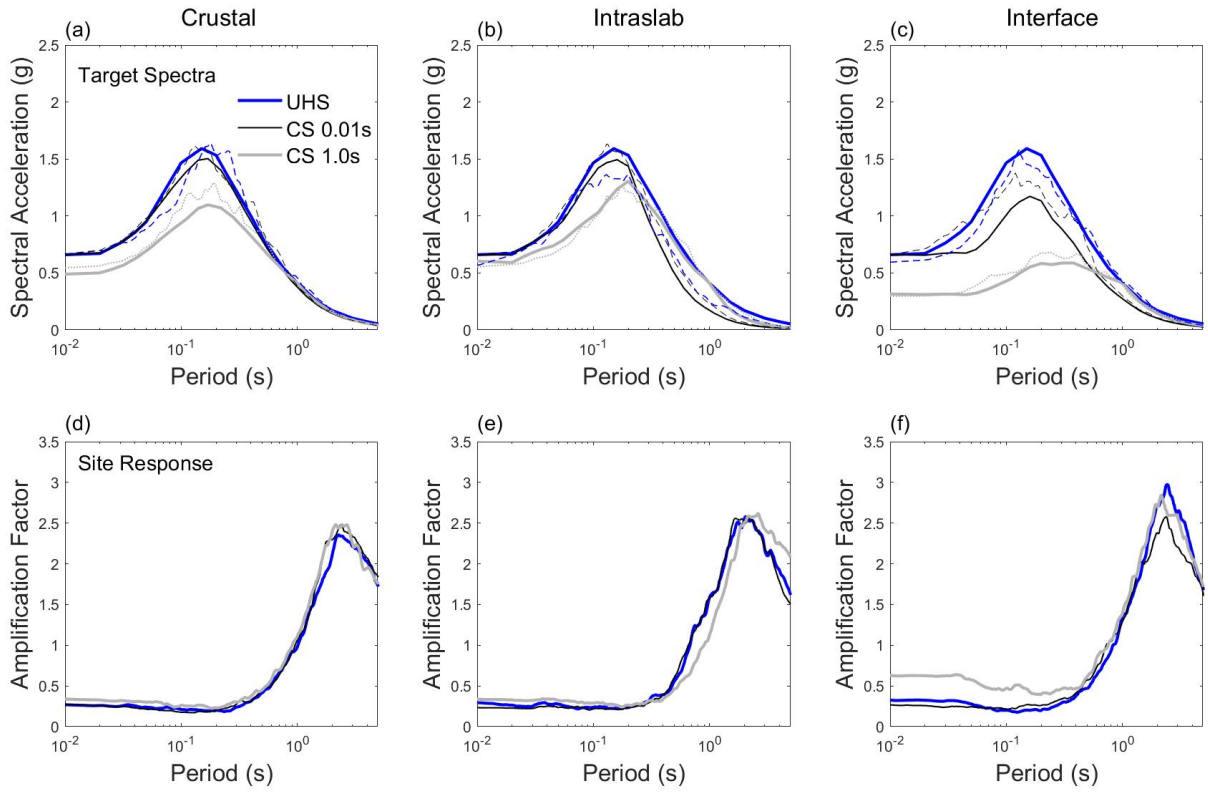

Figure 2.7 Comparisons of different target spectra (solid lines) and median acceleration response spectra (dashed lines) of selected ground motion suites for the (a) crustal earthquake scenario, (b) intraslab earthquake scenario, and (c) interface earthquake scenario in Seattle. Only the mean conditional spectra (and not the corresponding variability) are plotted for a clear comparison. Corresponding amplification factors from site response analyses, for (d) crustal, (e) intraslab, and (f) interface earthquake scenario are also shown.

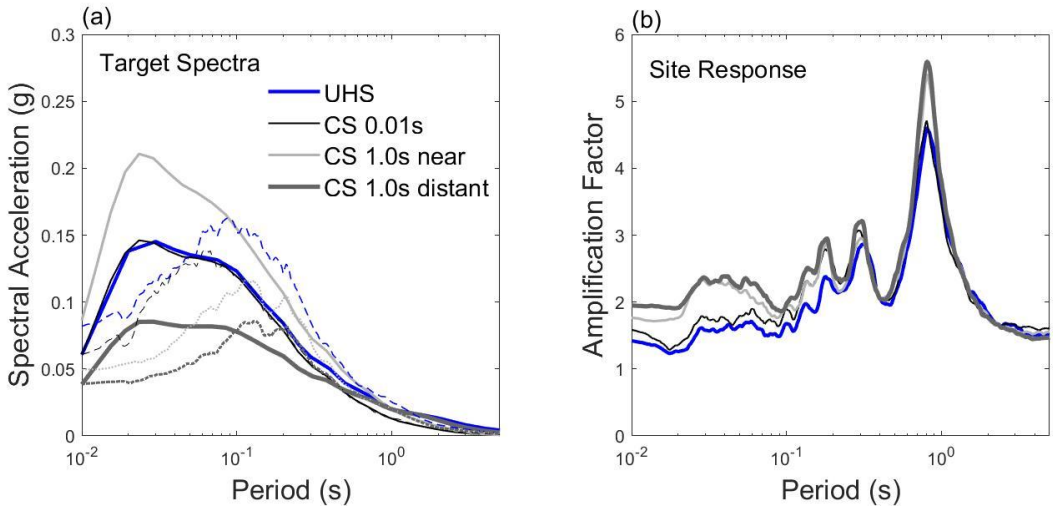

Figure 2.8 Comparisons of (a) different target spectra (solid lines) and median acceleration response spectra (dashed lines) of selected ground motion suites, and the (b) corresponding amplification factors from site response analyses at the Boston site.

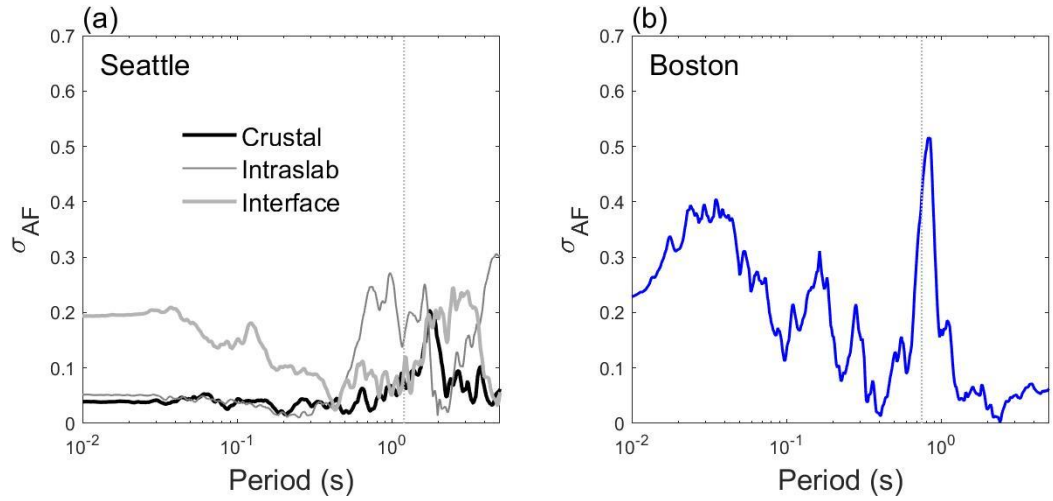

Figure 2.9 Comparison of inter-suite standard deviation of amplification factors for (a) Seattle and (b) Boston study sites. The site periods for each site (i.e., T_0= 1.2s, and 0.75s for Seattle and Boston respectively) are depicted with dashed vertical lines.

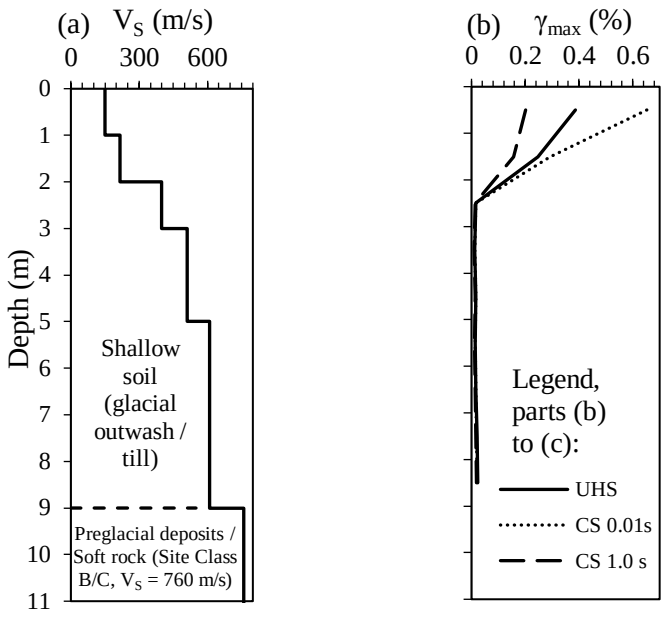

Figure 2.10 Comparisons of median predicted surface ground motions for a stiff site in Seattle, using ground motions from shallow crustal earthquakes: (a) V_S profile, and (b) predicted γ_{max} profiles corresponding to multiple definitions of the input motions (UHS, and CS conditioned at 0.01 s and 1 s). The groundwater table is assumed to be deep.

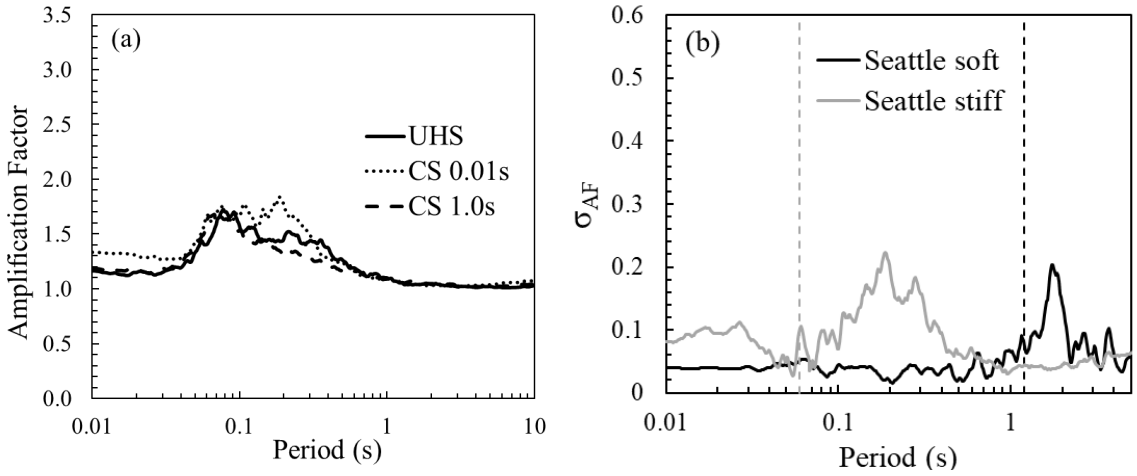

Figure 2.11 Comparisons of (a) the median predicted amplification factors corresponding to multiple suites of ground motions (UHS, CS 0.01s, and CS 1.0s) at the stiff study site in Seattle, using the crustal earthquake scenario, and (b) inter-suite standard deviation of amplification factors corresponding to the soft and stiff study sites in Seattle. The site periods for soft and stiff site (i.e., 1.2s and 0.06s respectively) are depicted with dashed vertical lines.

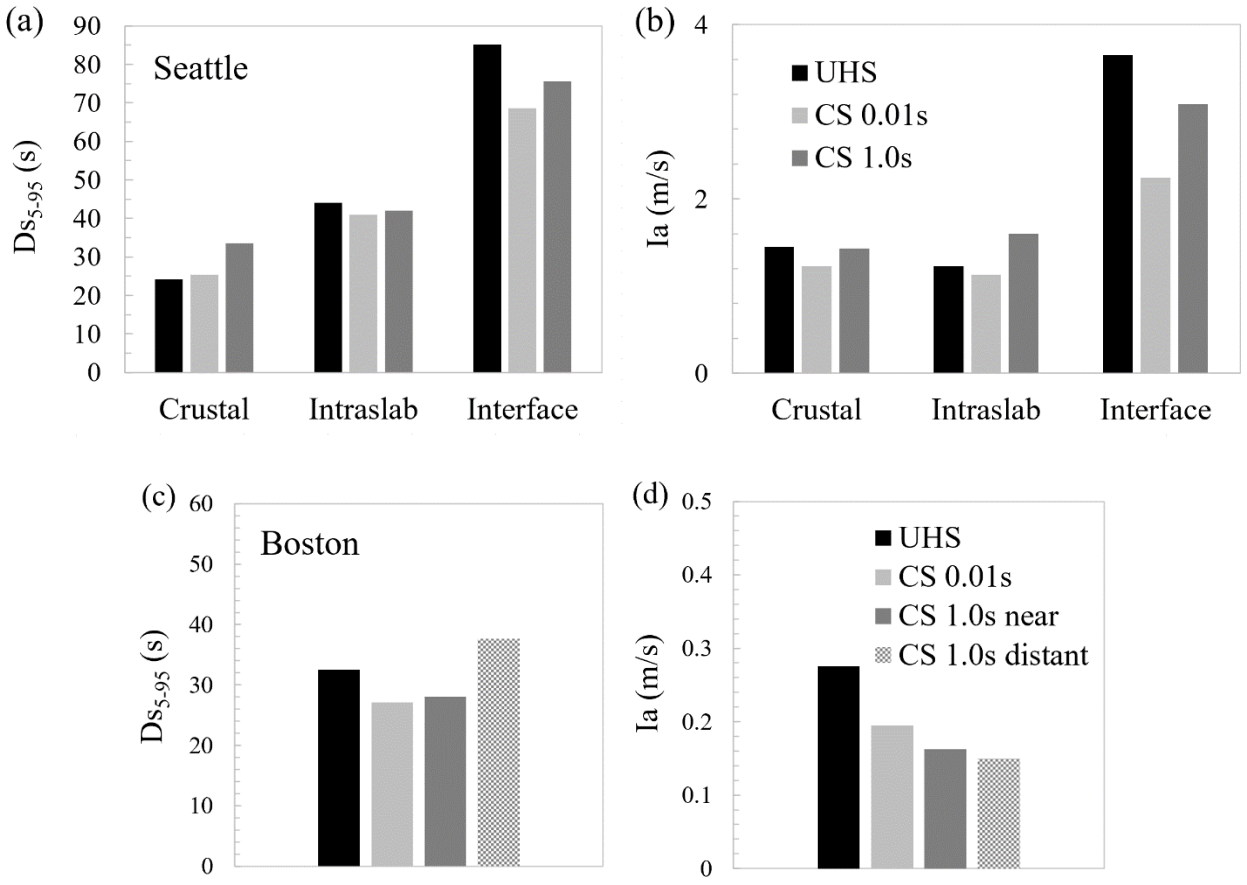

Figure 2.12 Median predicted 5-95% significant duration, Ds_{5-95} and Arias intensity, Ia from site response analysis corresponding to ground motion suites matching different target spectrum definitions for (a-b) the Seattle soft study site, and (c-d) the Boston study site.

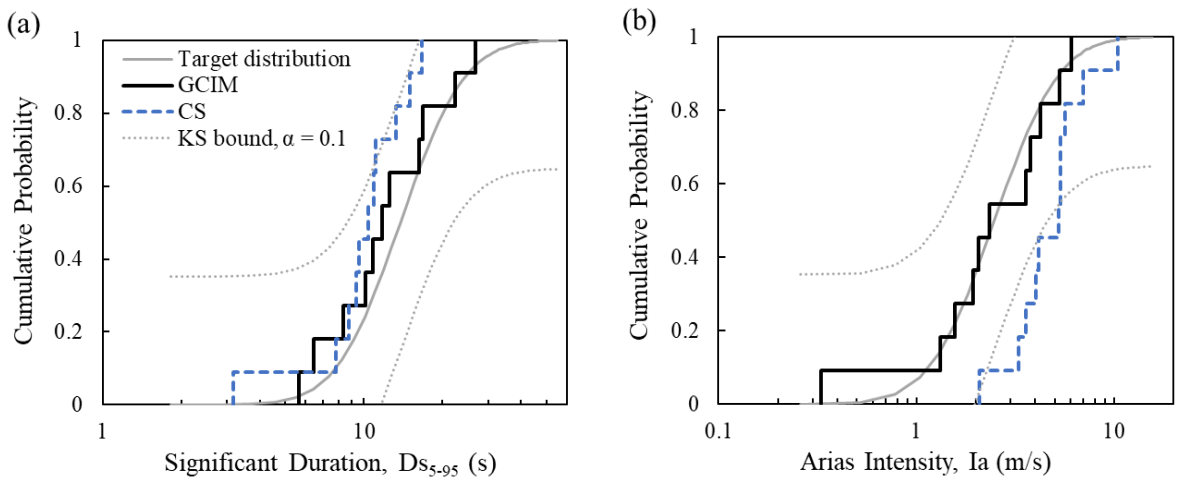

Figure 2.13 Target distribution of (a) 5-95% significant duration, Ds5-95, and (b) Arias intensity, Ia and the distribution of selected motions from CS and GCIM suites conditioned at Sa at 0.01s period.

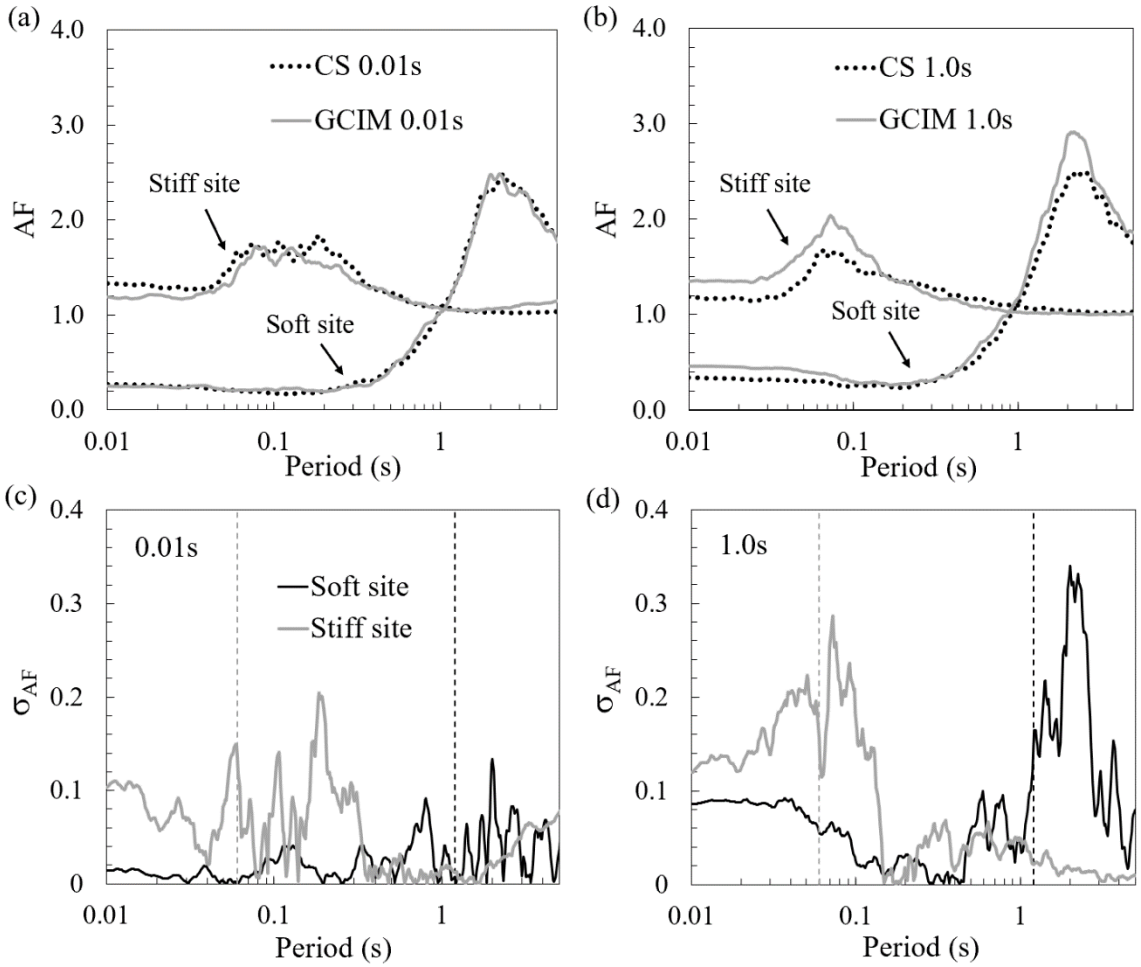

Figure 2.14 Effect of considering non-spectral IMs in ground motion selection at Seattle soft site and stiff site: (a-b) Amplification factors and, (c-d) inter-suite standard deviation of amplification factors, for CS and GCIM suites conditioned at Sa 0.01s and 1.0s. The site periods for soft and stiff site (i.e., 1.2s and 0.06s respectively) are depicted with dashed vertical lines.

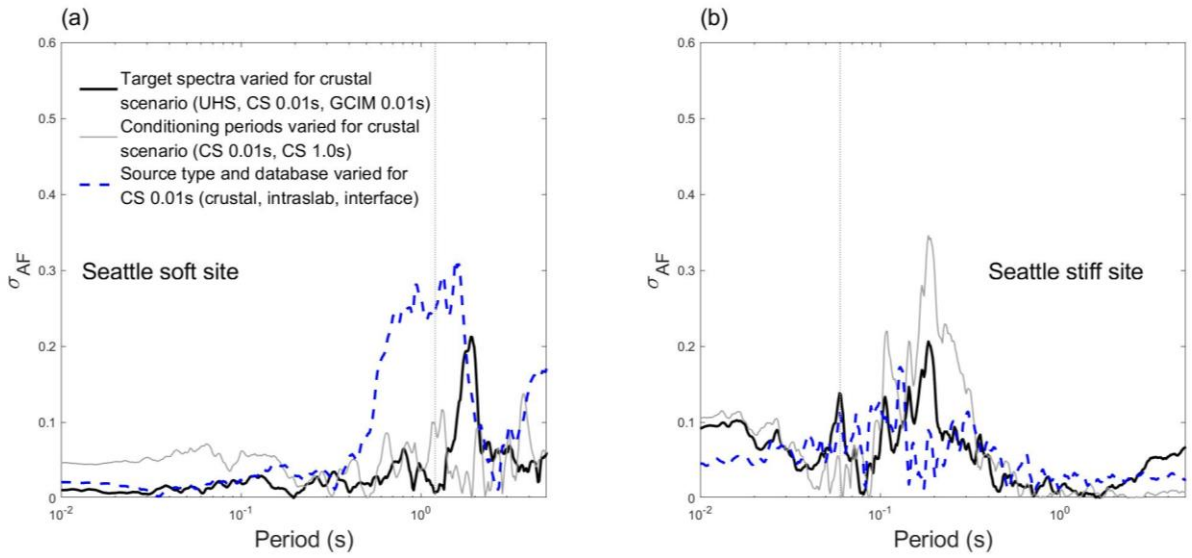

Figure 2.15 Effect of different sources of variability from ground motion selection on site amplification factors for the study sites in Seattle: (a) soft site and (b) stiff site, demonstrated with inter-target spectra standard deviation of amplification factors.

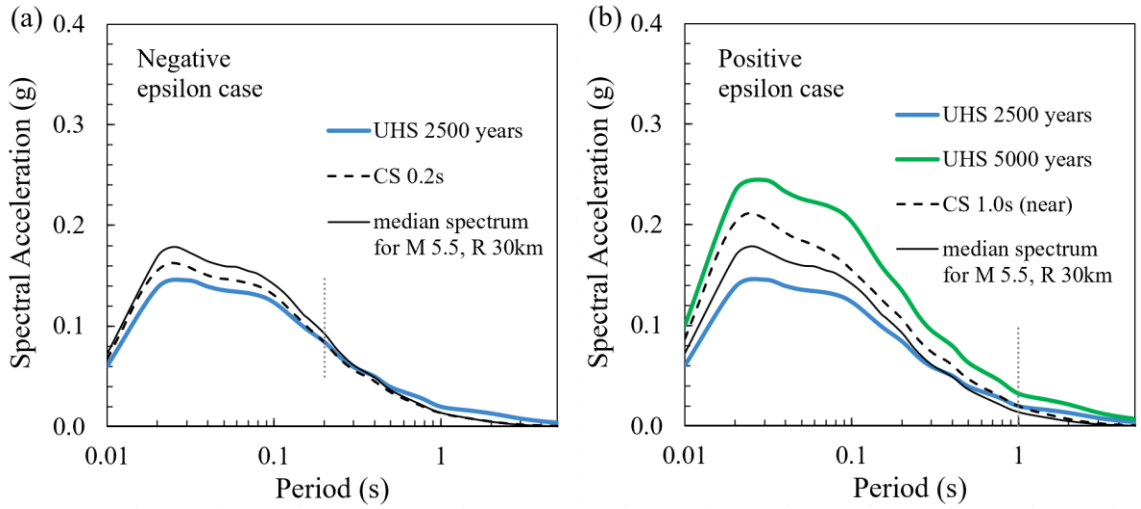

Figure 2.16 CS exceeding UHS at Boston for two cases: (a) CS 0.2s with negative epsilon (ε = -0.132), and (b) CS 1.0s (near) with positive epsilon (ε = 0.44); compared with the median response spectrum from GMPE for the selected M-R scenario and the UHS at two return periods (2500 years and 5000 years).

CHAPTER 3: THE EFFECT OF GROUND MOTION DURATION ON SEISMIC SLOPE DISPLACEMENT ANALYSIS

Abstract

Seismic slope displacement analyses are crucial for assessing the performance of earthen structures and natural slopes under earthquake loading. Input ground motions are often important components of such analyses and represent one of the main sources of variability. Most studies on seismic slope displacement analysis have been conducted using shallow crustal earthquake motions. However, ground motions from subduction zones are known to have comparatively longer duration. This study investigates the effect of ground motion duration on seismic slope displacement using short and long duration motions from subduction tectonic environments. The duration is isolated from other ground motion characteristics by selecting two ground motions with the same amplitude and similar spectral shape, but different significant duration. These short and long duration suites of motions are then used in a nonlinear finite element analysis to assess their effect on slope displacement. The finite element model can numerically simulate the strength and stiffness degradation of soils under cyclic loading from earthquake motion. The long duration motions are found to cause larger permanent displacements compared to their short duration counterparts, especially at higher ground shaking intensity levels. Comparisons with simplified analyses show that the simplified methods can underestimate the permanent displacement of design level long duration motions. A regression analysis is also conducted to identify efficient ground motion parameters for predicting permanent slope displacements of long-duration motions. The results of this study provide evidence of the need to consider ground motion duration along with the other ground motion characteristics (amplitude and spectral shape) to properly assess the damage potential of long-duration motions.

3.1 Introduction

The dynamic response of structural and geotechnical systems that degrade by accumulation of damage is a function of not only the amplitude and frequency content of the motion, but also its duration. Commonly used ground motion selection protocols for geotechnical and structural dynamic analyses (e.g., Baker and Jayaram 2008, Stewart et al. 2014, Haselton et al. 2017) only consider spectral shape, which can capture amplitude and frequency content characteristics of the motion, but not its duration. A notable exception is the ground motion selection algorithm based on the generalized conditional intensity measure approach (GCIM, Bradley 2010), which is not yet included in the design codes. The ASCE/SEI 7-16 design standard (ASCE, 2016) implicitly considers other relevant ground motion characteristics by recommending the selection of records whose causal parameters (e.g., magnitude and rupture distance) are similar to the site's hazard deaggregation results. Recent research efforts to investigate the influence of duration on structural collapse (e.g., Hancock and Bommer 2007, Raghunandan and Liel 2013, Chandramohan et al 2016, Zengin et al 2020) have resulted in contradicting findings depending on the type of structure analyzed, whether the modeling approach accounts for the accumulation of damage, the capacity of isolating duration effects from those corresponding to frequency content and amplitude of the ground motion, and the consideration of cumulative parameters to measure damage (instead of peak structural deformations).

Raghunandan and Liel (2013) showed that ground motion duration influences cumulative damage indices although it does not affect peak deformations of a reinforced concrete moment frame building. More recently, Chandramohan et al. (2016) showed that long-duration ground motions have a significant effect on structural collapse capacity (29% lower estimated median) compared

to short duration motions for a five-story steel moment frame building. In geotechnical earthquake engineering analyses, the seismic response of a soil deposit often depends on cumulative effects, especially for liquefaction and seismic slope stability analysis. For such analyses, it is still not clearly understood if the current practice for ground motion selection can provide an unbiased estimate of dynamic response of soil. A few studies on seismic slope displacement analysis (e.g., Bray et al. 1998, Stewart et al. 2003) have acknowledged the importance of considering ground motion duration. However, the effects of ground motion duration on geotechnical engineering analysis have not been rigorously quantified and, hence not yet incorporated in the current state-of-practice (e.g., ASCE 7-16, USBR 2015).

The objectives of this paper are to (1) quantify the effects of ground motion duration on seismic slope stability analysis, and (2) provide recommendations to minimize the potential associated bias in the resulting displacements. To isolate the effect of duration from frequency content and amplitude, in this work, ground motion pairs are selected such that they have similar spectral shapes and the same peak ground acceleration (PGA), but different significant duration. These criteria result in a long duration suite and an equivalent short duration suite of ground motions. To capture the effect of duration via numerical analysis, two additional components are necessary: (i) a fully nonlinear model that can numerically simulate the cyclic degradation of strength and stiffness of the soil, and ii) an index that can capture the cumulative damage (Chandramohan et al 2016). Hence, a nonlinear finite element analysis of slope under earthquake loading is adapted in this study. The effect of ground motion duration is studied on permanent slope displacements, which are expected to capture the cumulative effects of multiple cycles in a given ground motion.

This paper describes the selection and modification of ground motions used in the analysis, followed by an explanation of the modeling choices made in the construction of the finite element model of an idealized slope with hypothetical properties, and in the implementation of simplified seismic slope stability approaches. Resulting trends in slope displacements for the long- and short-duration ground motion suites are compared and discussed, and final recommendations for the consideration of duration effects in seismic slope stability analysis are provided.

3.2 Definitions of long- and short-duration ground motions

3.2.1 Assembling long and short duration dataset

Ground motions from the NGA-SUB database (Mazzoni et al. 2021) are used in this study. The NGA-SUB project (Bozorgnia and Stewart 2020) includes a global database that contains subduction zone earthquake records from Japan, Taiwan, Pacific North West, Alaska, Central America, Mexico, South America and New Zealand. The preliminary ground motion suite released to the public in November 2019 consisted of 500 motions mainly from earthquakes with moment magnitude (M) larger than 6.0 and PGA values greater than 0.01 g. We have further filtered out ground motions recorded at sites with a time-averaged shear wave velocity in the top 30 m (V_{s30}) lower than 360 m/s to minimize potential nonlinear site effects from soft soil conditions. Also, ground motions with the shortest usable period greater than 0.04s (25 Hz) were discarded. Lastly, because high intensity motions are desired in this study, records with PGA values lower than 0.1 g were discarded as well.

The duration of a ground motion is characterized in this study by means of 5-75% significant duration ($Ds_{5\text{-}75}$). It is defined as the time interval over which 5% to 75% of the integral $\int_0^{tmax} a(t)^2 dt$ is accumulated, where $a(t)$ is the acceleration of the ground motion at a specific

time t and $tmax$ is the time corresponding to the total length of the motion. A histogram is plotted in Figure 3.1 showing the $Ds_{5\text{-}75}$ values for each horizontal component from NGA-SUB preliminary released motions. A $Ds_{5\text{-}75}$ value of 25 s was chosen as the threshold between short- and long-duration ground motions subsets. A threshold of 25 s allows for a good number of motions to be available in the long duration subset and has been used in a previous study (Chandramohan et al. 2016) investigating the effect of duration in structural performance during earthquakes. However, using 25s as a threshold for both components of a ground motion pair would result in a small dataset, where some viable long-duration motions would be screened out. Hence, ground motion pairs with at least one of the two recorded horizontal components having a $Ds_{5\text{-}75}$ greater than 25 s were classified as long-duration motions. This criterion resulted in 30 pairs of ground motions in the long-duration dataset, which collectively have a geometric mean $Ds_{5\text{-}75}$ of 41.3 s. Likewise, a short-duration ground motion suite was identified as those with values of $Ds_{5\text{-}75}$, for both components, lower than 25 s. The PGA criterion was relaxed for the short-duration dataset to consider 0.05 g as the minimum allowable value. Thus, 142 pairs of ground motions were included in the short-duration dataset.

3.2.2 Selecting equivalent short duration ground motions

To isolate the effects of duration from those associated with frequency content and amplitude, 60 short-duration ground motions were further selected based on the similarity of their spectral shapes to those corresponding to each horizontal component of ground motion pairs in the long-duration dataset (with 30 ground motion pairs). The Baker and Lee (2017) algorithm for ground motion selection is used in this study. This algorithm was developed to select ground motions matching the conditional mean spectrum (Baker 2011), or the conditional spectrum (i.e., the conditional

mean spectrum and its variability). In this work, for each recorded component corresponding to a ground motion in the long-duration dataset, a spectrally equivalent short duration ground motion is to be selected that have the same PGA. Therefore, spectrally equivalent short duration horizontal components are scaled to the PGA of the corresponding long duration horizontal component. The scaling factor was limited to 4 to avoid unrealistic changes of other intensity measures such as the Arias intensity. The variance corresponding to the target spectrum used for the selection of ground motions is kept as zero, so that the spectral shape of candidate short duration ground motions is directly compared to their counterpart for the long duration motion. KS statistics were used to find the best match over a period range of 0.01s to 10s. Figure 3.2 shows an example of spectrally equivalent long and short duration ground motions having the same PGA. The $Ds_{5\text{-}75}$ distribution of the selected long- and short- duration datasets are shown in Figure 3.3. The geometric mean of the $Ds_{5\text{-}75}$ corresponding to the resulting equivalent short duration dataset is 11.2 s. The details corresponding to the ground motion pairs included in each dataset are provided in Appendix II of this dissertation.

3.3 Seismic slope displacement analysis

An idealized 2D slope model is analyzed in this study (Figure 3.4) using the finite element program PLAXIS (Plaxis 2020). The slope consists of a homogeneous sand layer and it has a height of 10 m and a slope gradient of 1:1.5 (33.69 degree). The idealized slope is underlain by 20 m of soil followed by bedrock. Following a sensitivity analysis, the left and right boundaries on both sides of the model are kept at a distance of 50 m and 100m, respectively, to minimize boundary effects on dynamic responses.

3.3.1 Constitutive model

To simulate the dynamic response of the slope model due to earthquake motion, the hardening soil with small strain (HSsmall) model was used in PLAXIS with the Mohr-Coulomb failure criterion. This model accounts for nonlinear soil behavior. Although we consider a homogeneous soil model, the stiffness of soil increases with depth and decreases with increasing strain levels induced by earthquake loading. In this study, the small strain damping properties are adapted from the Darendeli (2001) modulus reduction and damping model. When the shear modulus reduction curve reaches the plastic material domain, the degradation of the stiffness due to plastic straining is simulated with strain hardening. Table 3.1 lists the soil properties that are used in this study representing typical values for medium dense sand.

In addition to the hysteretic damping from the HSsmall model, Rayleigh damping is added to simulate viscous material damping. Rayleigh damping is a frequency dependent damping formulation in which a damping matrix, **C**, is composed of a portion of the mass matrix **M** and a portion of the stiffness matrix **K**:

$$[C] = \alpha[M] + \beta[K] \qquad (1)$$

Where α is the parameter that determines the influence of mass in the damping of the system. The higher α is, the more the lower frequencies are damped. β determines the influence of stiffness in the damping of the system. The higher β is, the more the higher frequencies are damped. To calculate the Rayleigh damping α and β parameters, two control frequencies are chosen in this study following Hudson et al (1994). The first frequency ($f_i = f_0$) is the fundamental frequency of the soil column. The second frequency $f_j = nf_0$, where n is the closest odd integer greater than f_p/f_0 where f_p is the predominant frequency of the input ground motion.

3.3.2 Boundary conditions and mesh size

A fifteen noded plain strain model was used to represent the 2D model. The input motion was applied at the bottom of the model as a prescribed displacement. A reduction factor of 0.5 was used to account for the free field effects of outcropping input motions when they are used as within motions. A compliant base boundary is used at the bottom of the model which simulates the continuation of waves into the deep soil with minimum reflection at the bottom boundary. For the lateral sides, free field boundary condition is used to simulate the propagation of waves into the far field.

To ensure that the wave transmission phenomenon through the numerical model is represented correctly, it is crucial to define a reasonable size of the mesh elements. According to Kuhlemeyer and Lysmer (1973), the element size should be less than or equal to one-eight of the wavelength (λ) associated with the maximum frequency component ($f_{\max}$) of the input wave. In other words, $f_{\max}$ is the highest frequency component in the input motions that contains appreciable energy. Given a $f_{\max}$:

$$Element\ size\ \leq \frac{Vs,min}{8f_{\max}} \qquad (2)$$

Where Vs,min is the minimum shear wave velocity of the soil model. In this study, we assume a minimum shear wave velocity ($Vs,\min$) of 233 m/s, and a $f_{\max}$ of 35 Hz. Using equation (2) the element size is 0.83 m. Therefore, an element size of 0.75 m was used to generate the mesh, which was further refined near the main slope, with element size as small as 0.2 m, to more accurately determine the permanent displacements on the slope.

3.3.3 Calculation phases in finite element analysis

The finite element modeling in this study consists of three phases:

1. Gravity loading: The first phase is the calculation of the initial stress field for the initial geometric configuration of the model. Due to the non-horizontal surface, gravity loading is adopted here, which generates the initial stress by applying the self-weight of soil. After the gravity loading, the ratio of horizontal effective stress over vertical effective stress (K_0) corresponds to 0.5.

2. Plastic phase: A plastic phase with no additional loading is added after the gravity loading phase to solve any existing out-of-balance forces. It is an elastic-plastic deformation analysis that brings the stress field into equilibrium condition.

3. Dynamic loading: The horizontal component of the earthquake ground motion (acceleration time history) is applied at the base of the model. A dynamic analysis is performed in time domain with the specified calculation duration.

3.4 Results of finite element analysis

3.4.1 Comparison of results from short and long duration suites

Each finite element analysis is performed using a single horizontal component of a ground motion. Hence, for the 30 pairs of long duration motions and the 30 pairs of equivalent short duration motions, a total of 120 numerical analyses are performed. The analyses are computationally expensive due to the fine mesh size required for dynamic analysis and the time domain approach used. After applying the earthquake load, the slope undergoes a displacement and shear strain concentration which are noticeable along the slope. Representative shear strain contours and horizontal displacement contours are shown in Figure 3.5. As seen in Figure 3.5a, the shear strain contours show the initiation of the failure surface at the toe of the slope. Figure 3.5b displays large

horizontal displacements observed on the slope. Similar patterns are observed for all the ground motions selected for this study. Comparing the displacement values at different points on the slope, the largest amount of displacement was observed to occur near the mid height of the slope (as also seen in Figure 3.5b. Hence, the horizontal displacement at the mid-point of the slope is recorded for each analysis and results are compared for long and short duration motions.

The permanent horizontal displacement from short and long duration motions are plotted against the 5-75% significant duration (Ds_{5-75}) in Figure 3.6a. On average, permanent displacement on the slope seems to increase with the longer significant duration of a ground motion. However, a least square linear regression shows that the increase is mild with a R^2 value of 0.09. It is to be noted that the short- and long-duration ground motion suites contain ground motions with different intensities. Figure 3.6b depicts permanent displacements and PGA values of the corresponding ground motion record used as excitation in the dynamic analysis. As expected, permanent displacements show a stronger trend of increase with increasing PGA values (with an R^2 of 0.36). The effect of duration is observed to be more prominent at higher intensity levels (PGA > 0.3g). Sorting the ground motions of different intensity levels into several PGA bins, the median displacements of all the motions in that PGA bins are recorded and presented in Figure 3.7a. At a very low PGA level, i.e., 0.1-0.2g, no difference is observed between the median from long and short duration motions. However, as the PGA levels increases, the long duration motions are found to cause significantly larger median displacement compared to short duration motions. The difference in median displacement is found to be 24% to 75%. Because the long and short duration motions are similar in spectral shape and were constrained to have the same PGA values, we hypothesize that the differences in permanent displacements are caused by the difference in their

significant durations. Ground motion duration plays an important role in resulting seismic slope displacements especially at higher intensity levels.

The predicted permanent displacement of slope is often used to evaluate probable damage or likelihood of landslide occurrence. Although it depends on several factors such as the problem under study, soil characteristics, type of structure on the slope etc., several studies have proposed some general guidelines for earthquake induced landslides as summarized in Jibson (2011). According to most of the studies (e.g., Jibson and Michael 2009, Bray et al. 2007), a displacement less than 1 cm can be considered negligible and incapable of causing significant damage. In our study, however, all the motions have caused a permanent displacement greater than 1 cm, owing to the comparatively higher intensity motions (PGA > 0.1 g) selected. Studies like Wieczorek et al. (1985) and Blake et al. (2002) have considered 5 cm as the critical displacement for landslide occurrence. According to California Geological Survey's (2008), displacements larger than 15 cm can cause strength loss of soil continuing to failure. For mapping landslides' hazards in Anchorage, Alaska, Jibson and Michael (2009) used the following permanent displacement ranges to relate those to the likelihood of landslide occurrence: 0–1 cm (low), 1–5 cm (moderate), 5–15 cm (high), >15 cm (very high). Considering these studies, we have adapted two threshold values for evaluating the permanent displacements calculated in our study: (1) a permanent displacement between 5 cm to 15 cm, and (2) a permanent displacement greater than 15 cm. The total number of motions in this study is divided into several bins with different PGA levels (e.g., PGA = 0.1-0.2 g) and the damage percentage is calculated as:

$$GM_{High}\ (\%) = \frac{Number\ of\ motions\ causing\ displacement\ between\ 5\ cm-15cm}{Total\ number\ of\ motions\ in\ that\ PGA\ bin} \quad (3)$$

$$GM_{Very\ High}\ (\%) = \frac{Number\ of\ motions\ causing\ displacement\ greater\ than\ 15\ cm}{Total\ number\ of\ motions\ in\ that\ PGA\ bin} \quad (4)$$

Where GM_{High} (%) refers to the percentage of ground motions that have a high (15–32 percent) likelihood of landslide occurrence, while $GM_{Very\ High}$ (%) refers to the percentage of ground motions that have a very high (>32 percent) likelihood of landslide occurrence.

Figure 3.7b and 3.7c presents a comparison of GM_{High} and $GM_{Very\ High}$ (from equations 3 and 4) for long duration and equivalent short duration motions obtained for selected PGA bins. As expected, the percentage of ground motions causing larger displacements (i.e., both GM_{High} and $GM_{Very\ High}$) increases for both long and short duration motions with the increase in PGA. GM_{High} percentage of long and short duration motions (Figure 3.7b) are small and shows no difference at low PGA levels (0.1-0.2 g). However, at a moderate PGA level (i.e., between 0.2-0.4 g), up to 30% more long duration motions have the potential to cause larger displacements in comparison to the equivalent short duration motions. At a higher PGA level (i.e., PGA greater than 0.4 g), almost all the long and short duration motions have the potential to cause a displacement greater than 5 cm. The comparison of long and short duration motions percentages for very high likelihood of landslide occurrence, $GM_{Very\ High}$ (Figure 3.7c) shows a similar trend as the ones observed for moderate damage at low intensity levels (i.e., PGA between 0.2 and 0.3 g). At a higher PGA values (> 0.3 g), a greater number of long duration motions (as high as 30% more) has the potential to cause larger displacements (>15cm) of the slope in comparison to the equivalent short duration motions.

3.4.2 Performance of other ground motion parameters

Although, $Ds_{5\text{-}75}$ is used in this study to classify long and short duration motions, there are several other duration metrics available, which we use to evaluate potential bias in our observations as a result of the parameterization of the ground motion duration:

(i) 5–95% significant duration ($Ds_{5\text{-}95}$): It is defined as the time interval over which 5% to 95% of the integral $\int_0^{tmax} a(t)^2 dt$ is accumulated (Trifunac and Brady 1975).

(ii) Arias Intensity (I_a): Proposed by Arias (1970), it is a hybrid metric of intensity and duration of a ground motion. I_a is defined as the energy released by the time series: $\frac{\pi}{2g}\int_0^{tmax} a(t)^2 dt$.

(iii) Cumulative absolute velocity (CAV): It is defined as $\int_0^{tmax} |a(t)| dt$ (Benjamin 1988). CAV is another hybrid metric of intensity and duration, that has a good correlation with damage.

A regression analysis is performed to assess the efficiency (i.e., the ability to predict an engineering demand parameter; Shome and Cornell, 1999) of the aforementioned duration metrics. The permanent displacement values obtained in this study and the duration metrics corresponding to the input motions are shown in Figure 3.8 along with a least square regression line. Efficiency is evaluated based on a measure of the associated aleatory variability (i.e., inherent randomness) in the engineering demand parameter, EDP, conditioned on a ground motion intensity measure, IM (i.e., EDP|IM) distribution (Shome and Cornell, 1999). In this case, we conduct a preliminary assessment of the efficiency of multiple duration metrics based on the R^2 values resulting from each regression.

Figure 3.8 shows the permanent displacements plotted vs 5-95% significant duration ($Ds_{5\text{-}95}$), Arias intensity (Ia), and cumulative absolute velocity (CAV) for long and short duration motions.

The least square linear regression line is also shown in the plot. The R^2 values calculated for the duration metrics considered are presented in Table 3.2. Ds_{5-75} (shown in Figure 3.6a) and Ds_{5-95} are observed to have a low correlation to the permanent displacement with R^2 values of 0.09 and 0.08 respectively. In contrast, the hybrid duration metrics Ia and CAV are found to have a stronger correlation to the permanent displacement (R^2 values of 0.55 and 0.47 respectively). Significant duration metrics are not affected by scaling of the ground motion, unlike Ia and CAV. If a ground motion is scaled by a factor of x (where x>1), the Arias intensity and CAV will increase by a factor of x^2 and x, respectively. As the short duration motions in our study are scaled to match the PGA of long duration motions, the Ia and CAV of the short duration motions are also changed. To evaluate whether scaling has introduced any bias in the R^2 statistics, another regression is done with the unscaled long duration motions only. It resulted in R^2 values of 0.54 and 0.52 for Ia and CAV respectively, which are close to the previously calculated values with both unscaled and scaled motions. Both Ia and CAV have a stronger correlation to the permanent displacement compared to Ds_{5-75} and $Ds_{5-95,}$ with Ia showing the strongest correlation. This is expected because they are hybrid IMs that also account for PGA, which was shown to significantly affect permanent displacements in Figure 3.6b and multiple previous studies (e.g., Yegian et al 1991).

Table 3.3 lists other ground motion parameters that have been examined in terms of their efficiency in predicting seismic slope displacement. Importantly, previous studies have only used shallow crustal earthquake databases. Ground motions from shallow crustal tectonic settings are known to produce shorter duration motions compared to their counterparts from subduction zones. Hence, to evaluate the performance of some of these parameters for long duration motions from

subduction zones, the relationships between selected IMs from Table 3.3 and estimated permanent displacements from our numerical analyses are compared.

PGA (Figure 3.6b), PGV and spectral acceleration at the degraded site period (1.5Ts) are considered here (Figure 3.9), where Ts is the fundamental period of the sliding mass (calculated as 4H/Vs). The value of Ts corresponding to the idealized slope considered in this study is 0.17 s. Hence, the degraded site period is 0.26 s. Additionally, spectral acceleration at a long period of 1.0 s is examined in this study as the long duration motions are expected to have higher long period content (Figure 3.9). The R^2 statistics for these ground motion parameters are summarized in Table 3.4. PGA, PGV and spectral acceleration (SA) at 1.0s period show similar robustness of the statistical regression to the estimated permanent displacements (i.e., R^2 values of 0.36, 0.38 and 0.34, respectively). However, SA at 0.26s (i.e., degraded site period) provides an improvement in the robustness of the regression (with $R^2 = 0.56$).

3.4.3 Comparison with simplified analysis of seismic slope stability

Although time domain analysis using the acceleration time history of a recorded earthquake provides us with a rigorous tool for seismic design, such analyses can be time consuming and computationally expensive, with the calibration of the model requiring particular attention and detailed evaluation. Hence, simplified methods of analysis are still often used for seismic design and seismic evaluations of slopes. In this section, we assess how sensitive commonly used simplified methods are with respect to capturing effects of ground motion duration on estimated slope displacement.

Most of the existing simplified methods are based on pseudo-static analysis (Terzhagi 1950). In earlier days, the limit equilibrium method was used to determine the factor of safety. Regardless of how straightforward this method was to use for the engineers, it did not provide any insight on the expected deformation of the slope. Later, to get an estimate of the deformation expected from an earthquake, the limit equilibrium method was combined with sliding block type of analysis (Newmark 1965). Newmark's method models a landslide as a rigid block that slides on an inclined plane. The slope displacement is calculated by integrating the part of the time series that exceeds the critical acceleration twice; once from acceleration to velocity, and then again from velocity to displacement. The critical acceleration value is the acceleration required to overcome the initial resistance and initiate sliding. The premise of Newmark's method is that acceleration values in a time series can exceed the critical acceleration multiple times, and the cumulative displacements can be added up to determine the total permanent displacement. Thus, slope displacement depends not only on the amplitude of the motion, but also on its frequency content and duration. Though Newmark's method enables a direct comparison of the effects of different ground motion characteristics, it has several limitations for slope displacement assessment. First, it considers the sliding mass as rigid block with no internal deformation, while in reality, the soil mass is deformable. Moreover, Newmark's method does not consider the dynamic response of earth structures. Hence, Maksidi and Seed (1978) proposed decoupled analysis, based on the work of Seed and Martin (1966). It performs the dynamic response computation considering a deformable mass and then uses Newmark's double integration method to determine the plastic displacement. This decoupled approach also has limitations, as it ignores the simultaneous occurrence of sliding while calculating the dynamic response. Thus, coupled analyses were introduced to account for the dynamic response and the plastic displacement, simultaneously. Several studies (e.g., Lin and

Whitman 1983, Rathje and Bray 1999) showed that the limitations of decoupled analyses can lead to conservative results compared to coupled sliding-block analysis. Therefore, coupled analyses are conducted in this study along with the Newmark's method to investigate their ability to predict permanent slope displacement for long-duration motions.

The USGS software program SLAMMER (Jibson et al. 2013) is used in this study to implement simplified methods to predict permanent slope displacements. These simplified methods are sensitive to the critical acceleration value, which can be determined through a pseudostatic analysis, in which a limit-equilibrium analysis is done iteratively using different values of the pseudostatic coefficient until the factor of safety is equal to one. To ensure a better comparison between the finite element method and simplified methods used in this work, the critical acceleration for the idealized slope is calculated using the finite element pseudostatic analysis. The finite element pseudostatic analysis is not as computationally intensive as the time domain method, but provides the benefit of a more accurately modeled initial stresses in the soil prior to the earthquake loading. The critical acceleration, a_c, for the idealized slope is 0.112g, which represent the acceleration value beyond which the slope is expected to initiate failure. Newmark's rigid-block analysis requires the time series and the critical acceleration value only. Nevertheless, the coupled analysis requires additional inputs that include the shear-wave velocities of the materials above and below the slip surface, the damping ratio, and the thickness of the potential landslide. Either linear-elastic or equivalent-linear soil models can be used for the coupled analysis. An equivalent-linear analysis is chosen to approximate the nonlinear behavior of soil. The damping and modulus reduction values are adapted from the Darendeli (2001) model that was used in the finite element analysis also.

The permanent displacement values obtained from the rigid block analysis and coupled analysis are compared with the finite element analysis results in terms of residuals. The residual is calculated as the displacement from finite element analysis (treated as the "observed" value) minus the displacement from simplified analysis (treated as the "predicted" value). Positive and negative residuals indicate that the simplified analysis is underestimating or overestimating the permanent displacement (as obtained from the finite element analysis), respectively. Figure 3.10 shows the residual values for rigid block analysis and coupled analysis with respect to the PGA of the long and short duration ground motions. The rigid block analysis (Figure 3.10a) underestimates the displacement at low PGA levels (up to 0.28 g). For moderate PGA values (from 0.28 g to 0.4g), the estimations from rigid block analysis show both underestimation and overestimation. However, at a high PGA levels (> 0.4 g), overestimation is apparent. These trends in residuals are similar for the long- and short-duration datasets. Therefore, we hypothesize that the rigid block analysis cannot capture effects of duration on permanent slope displacements. On the other hand, the coupled analysis (Figure 3.10b) provides fairly good estimations of permanent displacements until a PGA value of about 0.28 g, suggesting only a slight underestimation (1-5cm). At a higher PGA level (> 0.28 g), the coupled analysis shows residuals in general still gravitating around zero, but with a more significant variability (scatter). In general, the coupled analysis overestimates permanent displacements for short duration motions and underestimates permanent displacements for long duration motions. The poor performance of coupled analysis at a higher intensity levels can be due to the intrinsic limitations in modeling nonlinear soil behavior using an equivalent-linear method. When the nonlinear soil behavior starts governing at higher intensity levels, the equivalent-linear method fails to predict the actual response of the soil. The limitations of the equivalent-linear approach is well established by previous studies on site response analysis (e.g.,

Stewart et al. 2014, Kaklamanos et al. 2013, 2015, Kim and Hashash 2013). In summary, the simplified coupled analysis fails to predict the permanent displacement of slope for long duration motions at high intensity levels. A nonlinear finite element analysis should be the preferred approach for estimating slope displacement for design level ground motions.

3.5 Conclusion

While there have been numerous studies on seismic slope displacement for shallow crustal earthquakes with mostly short duration ground motions, the scarcity of high intensity subduction zone ground motions has so far limited our understanding of the effect of long duration motions on permanent slope displacements. This study investigated the effect of long duration motions on seismic slope stability analysis using the recently released subduction zone ground motions from the NGA-SUB database. A rigorous finite element analysis is used to more accurately assess the nonlinear soil behavior and strain accumulation due to multiple cycles in a long duration motion. An idealized slope consisting of medium dense sand with small strain shear modulus of 100 MPa is assumed. Two datasets consisting of 60 long-duration and 60 equivalent short duration ground motions were created. A comparison between the long duration suite of motions and the equivalent short duration suite of motions revealed that the duration of a motion affects the permanent displacement of the slope. The long duration suite resulted in up to 75% larger median permanent displacement compared to the median of its counterpart based on the short duration suite of motions. Moreover, a greater number of long duration motions (as high as 30% more) has the potential to cause slope displacements that indicate very high likelihood of landslide occurrence in comparison to the equivalent short duration motions. The effect of duration is more prominent at higher intensity levels of ground shaking. As the design level ground motions increase in

amplitude, it is crucial to consider the duration of a motion along with other characteristics (amplitude and spectral shape). Previously identified efficient ground motion parameters for predicting slope displacement; such as the Arias intensity, peak ground acceleration, spectral acceleration at a period 1.5 times the site period; are found to be good parameters for capturing the effects of long duration motions. Finally, a comparison with simplified slope displacement methods shows that the simplified coupled analysis can underestimate the displacements from long duration motions, especially at higher intensity levels. Therefore, for seismic slope displacement analysis, this study recommends the consideration of ground motion duration and a numerical method that can capture the cyclic degradation of strength and stiffness properties of soil.

References

American Society of Civil Engineers [ASCE] (2016). Minimum Design Loads for Buildings and Other Structures (Standards ASCE/SEI 7-16). American Society of Civil Engineers, Reston, Virginia.

Arias, A., (1970). A measure of earthquake intensity. In: Hansen, R.J. (Ed.), Seismic Design for Nuclear Power Plants. Massachusetts Institute of Technology Press, Cambridge, MA, pp. 438–483.

Baker, J. W., and Jayaram, N. (2008). Correlation of spectral acceleration values from NGA ground motion models, *Earthquake Spectra*, 24, 299–317.

Baker, J.W., and Lee, C. (2017). An Improved Algorithm for Selecting Ground Motions to Match a Conditional Spectrum. Journal of Earthquake Engineering, 22(4), 708–723.

Benjamin, J. R., (1988). A Criterion for Determining Exceedance of the Operating Basis Earthquake, EPRI Report NP-5930, Electric Power Research Institute, Palo Alto, CA.

Blake, T.F., Hollingsworth, R.A., and Stewart, J.P., (2002). Recommended procedures for implementation of DMG special publication 117-guidelines for analyzing and mitigating landslide hazards in California. Southern California Earthquake Center, Los Angeles, CA. 127 pp.

Bozorgnia, Y., and Stewart, J. (2020). Data Resources for NGA-Subduction Project. PEER 2020/02, Pacific Earthquake Engineering Research Center.

Bradley, B. A. (2010). A generalized conditional intensity measure approach and holistic ground-motion selection, *Earthquake Engineering and Structural Dynamics*, 39, 1321–1342.

Bray, J. D., Rathje, E. M., Augello, A. J., and Merry, S. M. (1998). Simplified seismic design procedure for geosynthetic-lined, solid-waste landfills, *Geosynthetics International*, 5, 203–235.

Bray, J.D., Travasarou, T., (2007). Simplified procedure for estimating earthquake-induced deviatoric slope displacements. Journal of Geotechnical and Geoenvironmental Engineering 133, 381–392.

California Geological Survey, (2008). Guidelines for Evaluating and Mitigating Seismic Hazards in California. California Geological Survey Special Publication 117A. 98 pp.

Chandramohan, R., Baker, J. W., and Deierlein, G. G. (2016a). Quantifying the influence of ground motion duration on structural collapse capacity using spectrally equivalent records, *Earthquake Spectra*, 32(2), 927–950.

Darendeli, M.B. (2001). Development of a new family of normalized modulus reduction and material damping curves, Ph.D. Thesis, University of Texas at Austin, Austin, Texas, 396 pp.

Jibson, R.W. (2011): Methods for assessing the stability of slopes during earthquakes—A retrospective: Engineering Geology, 122, 43-50.

Jibson, R.W., and Michael, J.A., (2009). Maps showing seismic landslide hazards in Anchorage, Alaska. U.S. Geological Survey Scientific Investigations Map 3077. 2 sheets (scale 1:25, 000), 11-p. pamphlet.

Jibson, R.W., Rathje, E.M., Jibson, M.W., and Lee, Y.W. (2013): *SLAMMER—Seismic LAndslide Movement Modeled using Earthquake Records* (ver.1.1, November 2014): U.S. Geological Survey Techniques and Methods, book 12, chap. B1.

Lin, J.S., Whitman, R.V., 1983. Earthquake induced displacements of sliding blocks. Journal of Geotechnical Engineering 112, 44–59.

Hancock J and Bommer JJ (2007) Using spectral matched records to explore the influence of strongmotion duration on inelastic structural response. Soil Dynamics and Earthquake Engineering 27: 291–299.

Haselton, C. B., Baker, J. W., Stewart, J. P., Whittaker, A. S., Luco, N., Fry, A., Hamburger, R. O., Zimmerman, R. B., Hooper, J. D., Charney, F. A., and Pekelnicky, R. G. (2017). Response history analysis for the design of new buildings in the NEHRP provisions and ASCE/SEI 7 Standard: Part I - overview and specification of ground motions, *Earthquake Spectra*, doi: 10.1193/032114EQS039M.

Hudson, M., I. M. Idriss, and M. Beikae (1994). QUAD4M – A Computer Program to Evaluate the Seismic Response of Soil Structures Using Finite Element Procedures and Incorporating a Compliant Base, Center for Geotechnical Modeling, Dept. of Civil Engineering, Univ. of California, Davis, California.

Kaklamanos, J., B. A. Bradley, E. M. Thompson, and L. G. Baise (2013). Critical parameters affecting bias and variability in site response analyses using KiK-net downhole array data, *Bull. Seism. Soc. Am.* 103, 1733–1749.

Kaklamanos, J., L. G. Baise, E. M. Thompson, and L. Dorfmann (2015). Comparison of 1D linear, equivalent-linear, and nonlinear site response models at six KiK-net validation sites, *Soil Dynam. Earthq. Eng.* 69, 207–219.

Kim, B., and Y. M. A. Hashash (2013). Site response analysis using downhole array recordings during the March 2011 Tohoku-Oki earthquake and the effect of long-duration ground motions, *Earthq. Spectra,* 29, S37–S54.

Kuhlemeyer R.L., and Lysmer J. (1973). Finite Element Method accuracy for wave propagation problems, *J. Soil Mech Found, ASCE*, 99(SM5): 421-427.

Raghunandan M., and Liel A.B. (2013). Effect of ground motion duration on earthquake-induced structural collapse. *Structural Safety* 2013; 41:119–133.

Makdisi, F.I., and Seed, H.B., 1978, Simplified procedure for estimating dam and embankment earthquake-induced deformations: ASCE Journal of the Geotechnical Engineering Division, v. 104, p. 849-867.

Mazzoni, S., Kishida, T., Contreras, V., Ahdi, S. K., Kwak, D. Y., Bozorgnia, Y., and Stewart J. P. (2021). NGA Subduction Database Preliminary Ground Motion Suite (Public Release), The B. John Garrick Institute for the Risk Sciences. https://www.risksciences.ucla.edu/nhr3/gmdata/preliminary-nga-subduction-records

Newmark, N.M., 1965, Effects of earthquakes on dams and embankments: Geotechnique, v. 15, p. 139-159.

Plaxis (2020). PLAXIS 2D reference manual, Delft, Netherlands.

Rathje, E.M., and Bray, J.D., (1999). An examination of simplified earthquake-induced displacement procedures for earth structures: Canadian Geotechnical Journal, v. 36, p. 72-87.

Seed, H.B., and Martin, G.R., (1966). The seismic coefficient in earth dam design: ASCE Journal of the Soil Mechanics and Foundations Division, v. 92, p. 25-58.

Stewart, J. P., Afshari, K., and Hashash, Y. M. A. (2014). Guidelines for performing hazard-consistent one-dimensional ground response analysis for ground motion prediction, *PEER Report 2014/16*, Pacific Earthquake Engineering Research Center, University of California, Berkeley, Calif., 152 pp.

Stewart, J. P., Blake, T. F., and Hollingsworth, R. A. (2003). A screen analysis procedure for seismic slope stability, *Earthquake Spectra,* 19(3), 697–712.

Terzhagi, K., 1950. Mechanism of landslides. In: Paige, S. (Ed.), Application of Geology to Engineering Practice (Berkey Volume). Geological Society of America, New York, NY, pp. 83–123.

Trifunac, M. D., and Brady, A. G., (1975). A study on the duration of strong earthquake ground motion, Bulletin of the Seismological Society of America 65, 581–626.

USBR (2015). Reclamation design standard No. 13: Embankment dams, chapter 13: Seismic analysis and design. U. S. Bureau of Reclamation.

Wieczorek, G.F., Wilson, R.C., and Harp, E.L., (1985). Map showing slope stability during earthquakes in San Mateo County, California. U.S. Geological Survey Miscellaneous Investigations Map I-1257-E, scale 1:62,500.

Zengin, E., Abrahamson, N. A., & Kunnath, S. (2020). Isolating the effect of ground-motion duration on structural damage and collapse of steel frame buildings. *Earthquake Spectra*, *36*(2), 718-740.

TABLES

Table 3.1 Soil parameters used in numerical analyses conducted in PLAXIS

γ_{dry}	Unit weight of soil [kN/m^3]	18
E_{50}^{ref}	Secant stiffness in standard drained triaxial test [kN/m^2]	30000
E_{oed}^{ref}	Tangent stiffness for primary oedometer loading [kN/m^2]	30000
E_{ur}^{ref}	Unloading / reloading stiffness (default E_{ur}^{ref} = 3E50ref) [kN/m^2]	90000
m	Power for stress-level dependency of stiffness	0.5
c'^{ref}	Effective cohesion [kN/m^2]	5
φ'	Effective friction angle	30
$\gamma_{0.7}$	Shear strain at which $Gs = 0.722\ G_0$	0.00012
G_0^{ref}	Reference shear modulus at very small strains ($\varepsilon < 10\text{-}6$) [MPa]	100

Table 3.2 R^2 statistics from regression analysis for all considered duration metrics

Duration metric	**R^2**
5-75% significant duration ($Ds_{5\text{-}75}$)	0.09
5-95% significant duration ($Ds_{5\text{-}95}$)	0.08
Arias intensity (Ia)	0.55
Cumulative absolute velocity (CAV)	0.47

Table 3.3 Efficient ground motion parameters from literature for slope displacement analysis

Study	**Parameters**
Makdisi and Seed (1978)	Moment magnitude (M_w)
Yegian et al. (1991)	PGA and the predominant period (Tp) of ground motion
Jibson (1993), Travasarou (2003)	Arias intensity (Ia)
Bray and Rathje (1998)	Mean period (Tm) of the ground motion and $Ds_{5\text{-}95}$
Travasarou and Bray (2003)	The spectral acceleration at the degraded site period (1.5Ts)
Athanasopoulos-Zekkos (2008)	Peak ground velocity (PGV)

Table 3.4 R^2 statistics from regression analysis for considered other ground motion parameters

Intensity measure	**R^2**
Peak ground acceleration (PGA)	0.36
Peak ground velocity (PGV)	0.38
Spectral acceleration at 1.0 s	0.34
Spectral acceleration at 1.5Ts	0.56

FIGURES

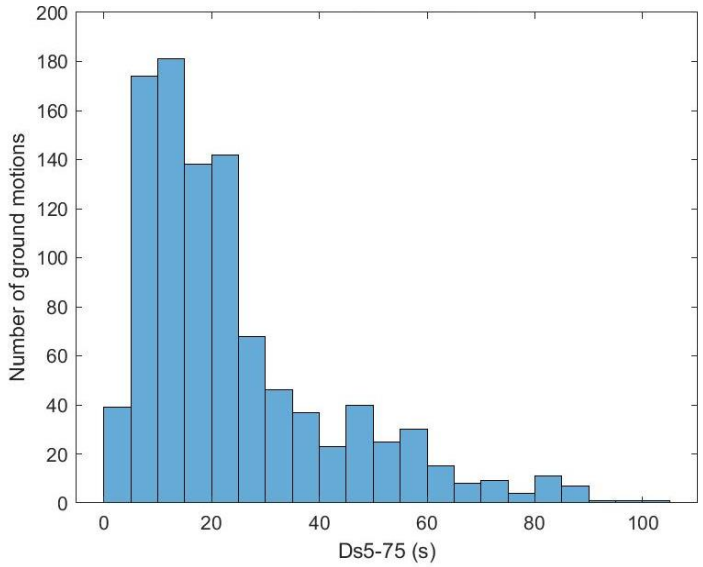

Figure 3.1 Distribution of $Ds_{5\text{-}75}$ for each horizontal component in NGA-SUB preliminary 500 pairs of ground motions released to the public in November 2019.

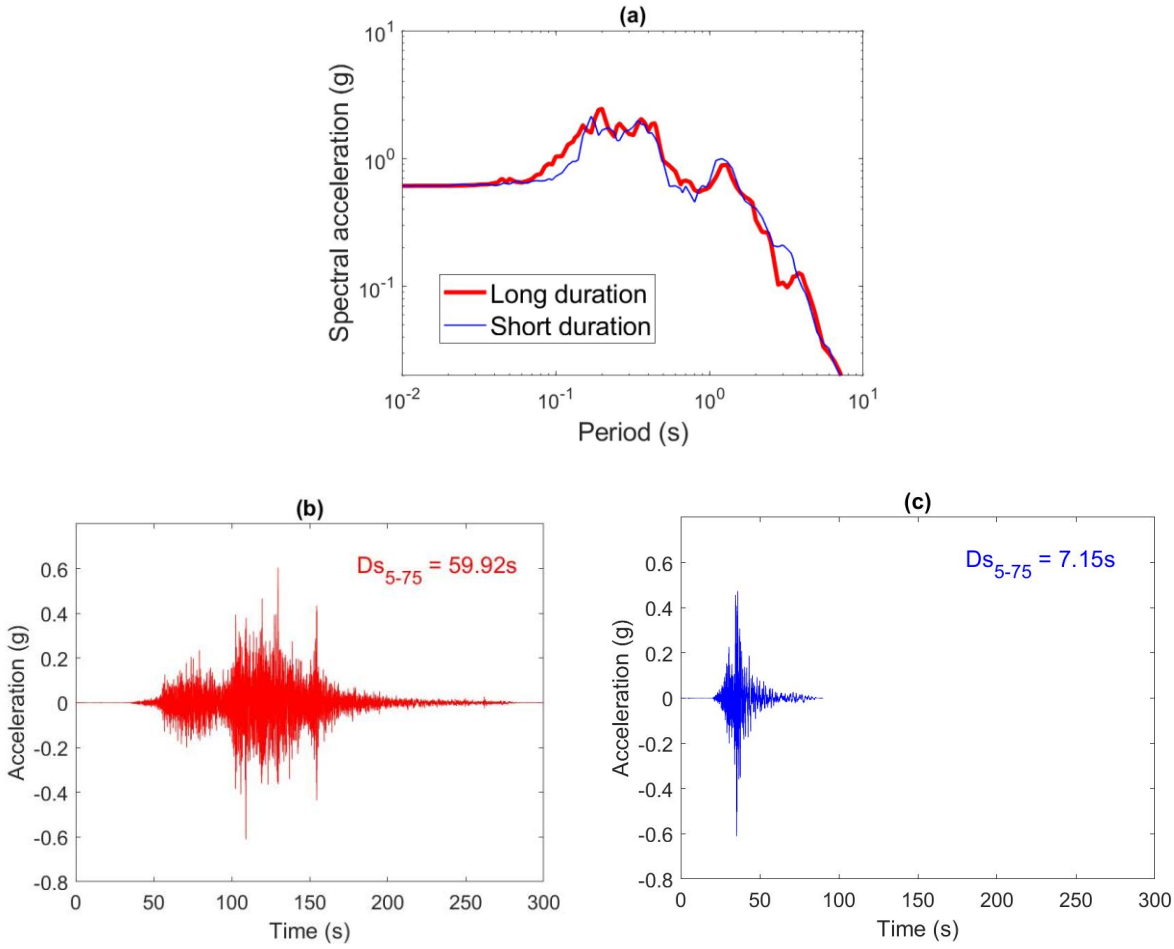

Figure 3.2 (a) Response spectra, and time series comparison of (b) a long duration motion ($Ds_{5\text{-}75}$ = 59.92 s) and (c) a short duration motion ($Ds_{5\text{-}75}$ =7.15 s) with similar spectral shape, scaled to the PGA of long duration motion (0.61g).

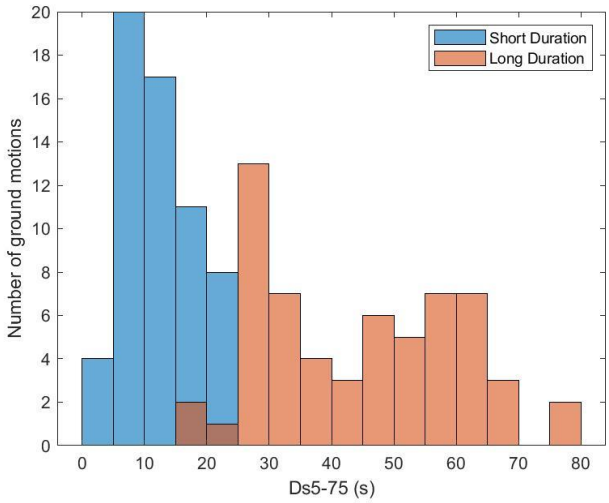

Figure 3.3 Distribution of $Ds_{5\text{-}75}$ (per horizontal component) for selected long and short duration datasets of ground motions, with a geometric mean of 41.3s and 11.2s respectively.

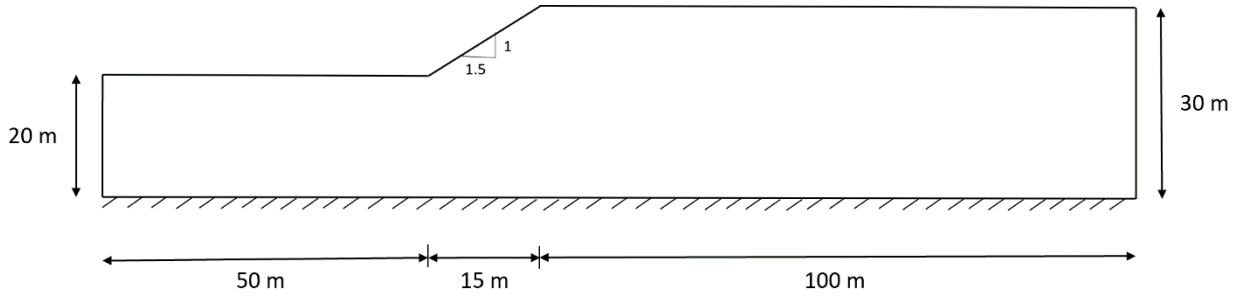

Figure 3.4 Schematic diagram of the idealized slope analyzed in this work. A homogeneous sand layer overlying bedrock is assumed.

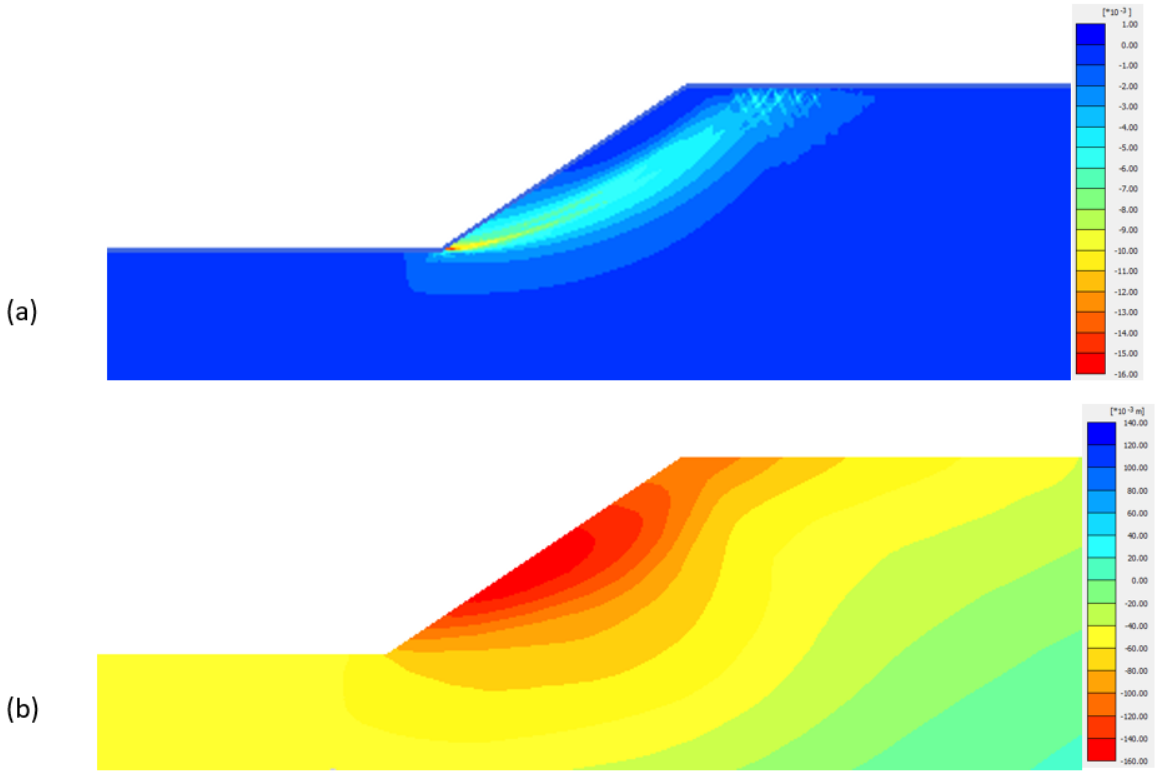

Figure 3.5 A representative contour of (a) shear strain, and (b) horizontal displacement.

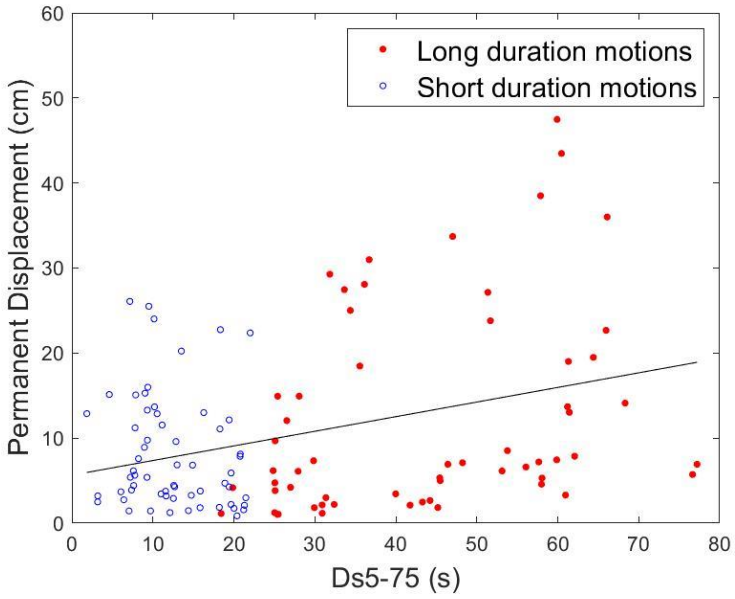

(a)

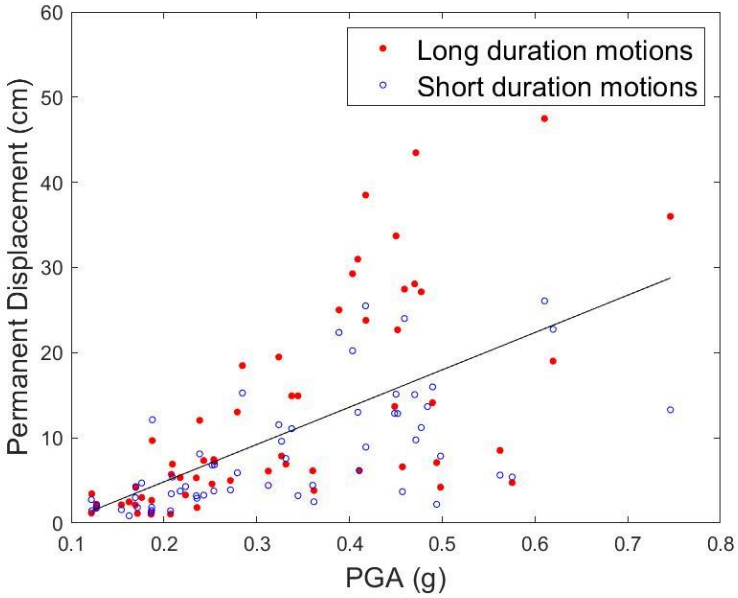

(b)

Figure 3.6 Permanent horizontal displacement at mid- height of the slope as a function of (a) 5-75% significant duration (Ds_{5-75}), and (b) Peak ground acceleration (PGA).

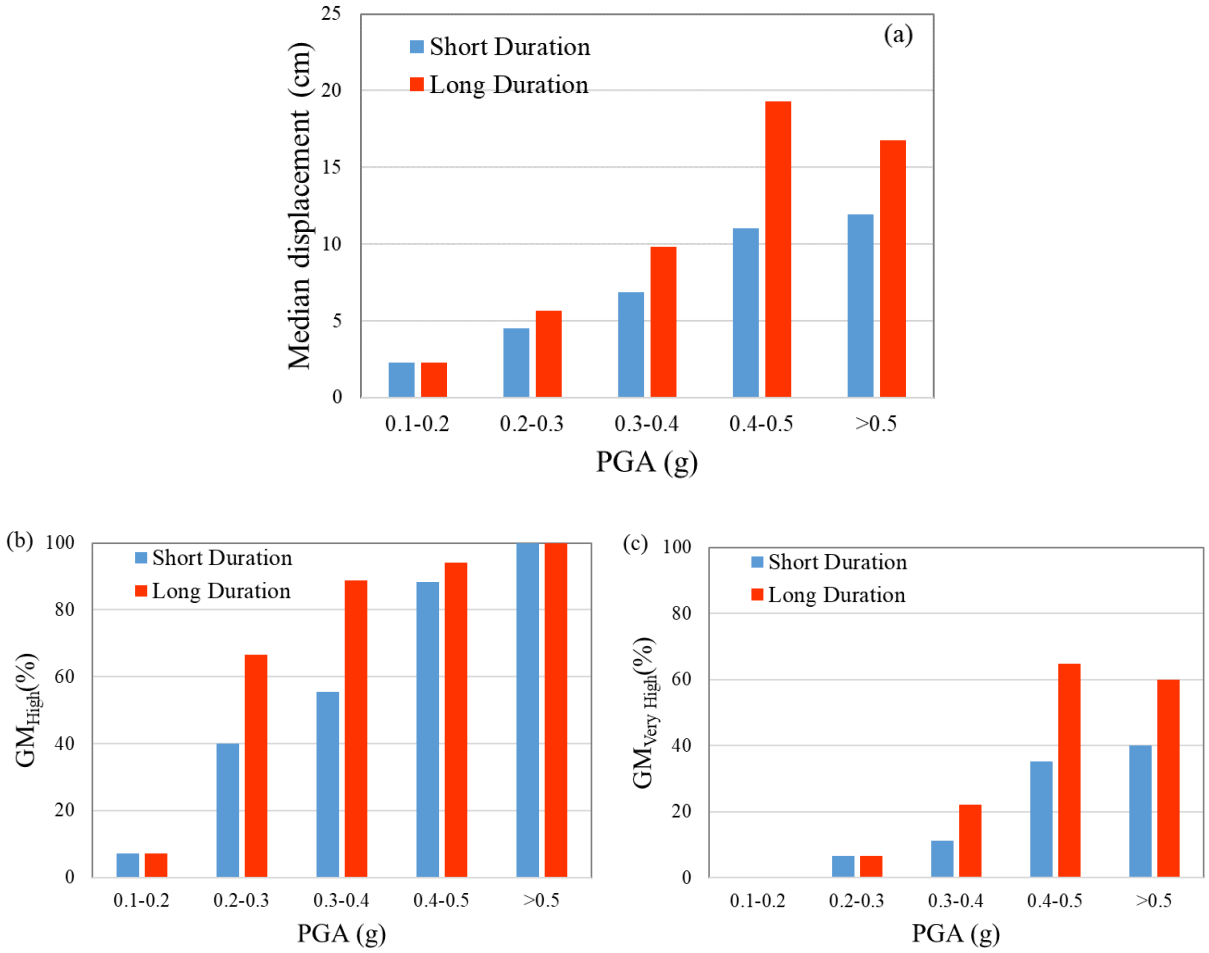

Figure 3.7 Comparison of (a) median permanent displacements, and (b) percentages of ground motions with high and (c) very high likelihood of landslide occurrence for long and short duration motions at several PGA bins.

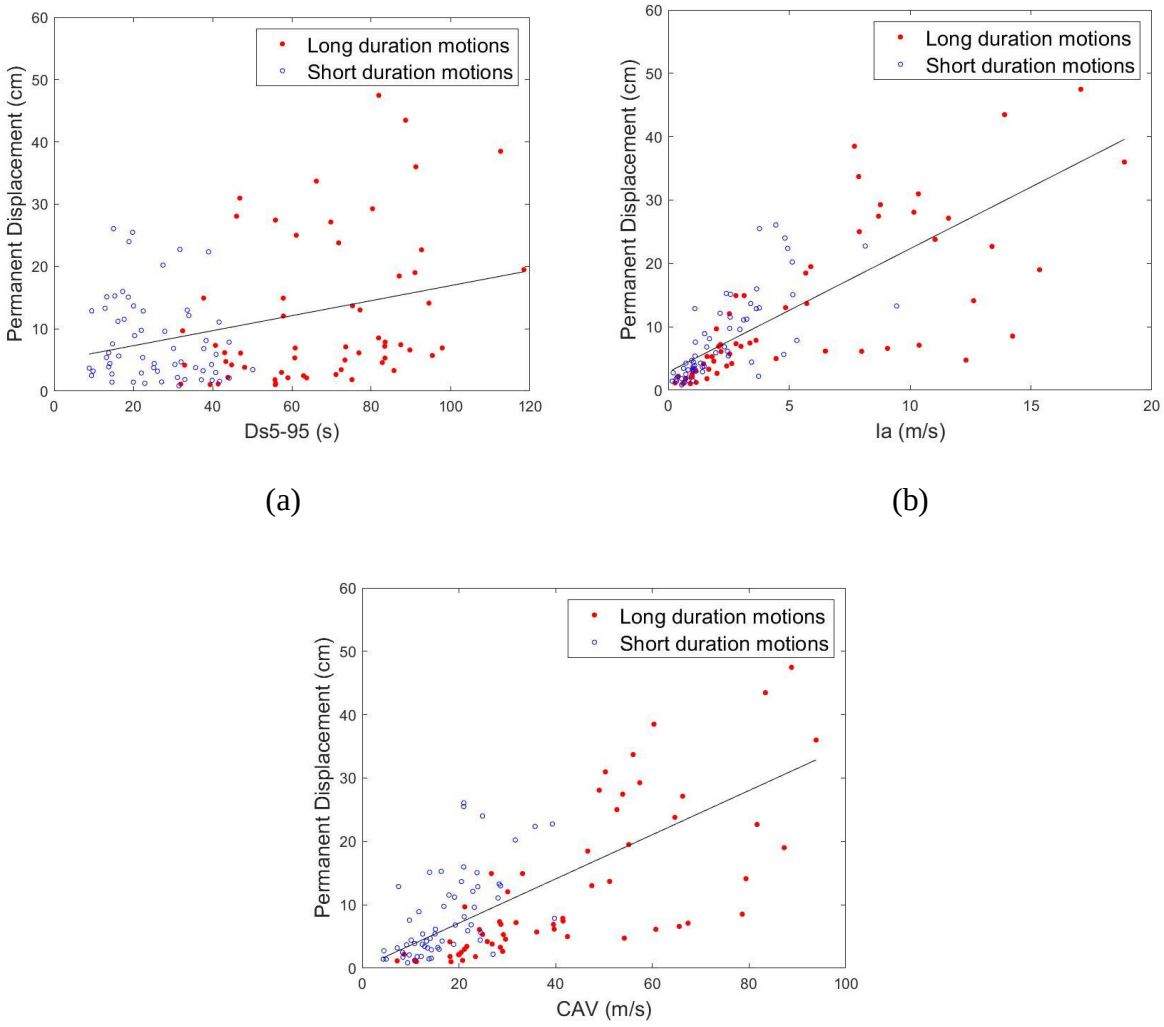

(a) (b)

(c)

Figure 3.8 Permanent displacements vs (a) 5-95% significant duration ($Ds_{5\text{-}95}$), (b) Arias intensity (Ia), and (c) cumulative absolute velocity (CAV) for long and short duration motions.

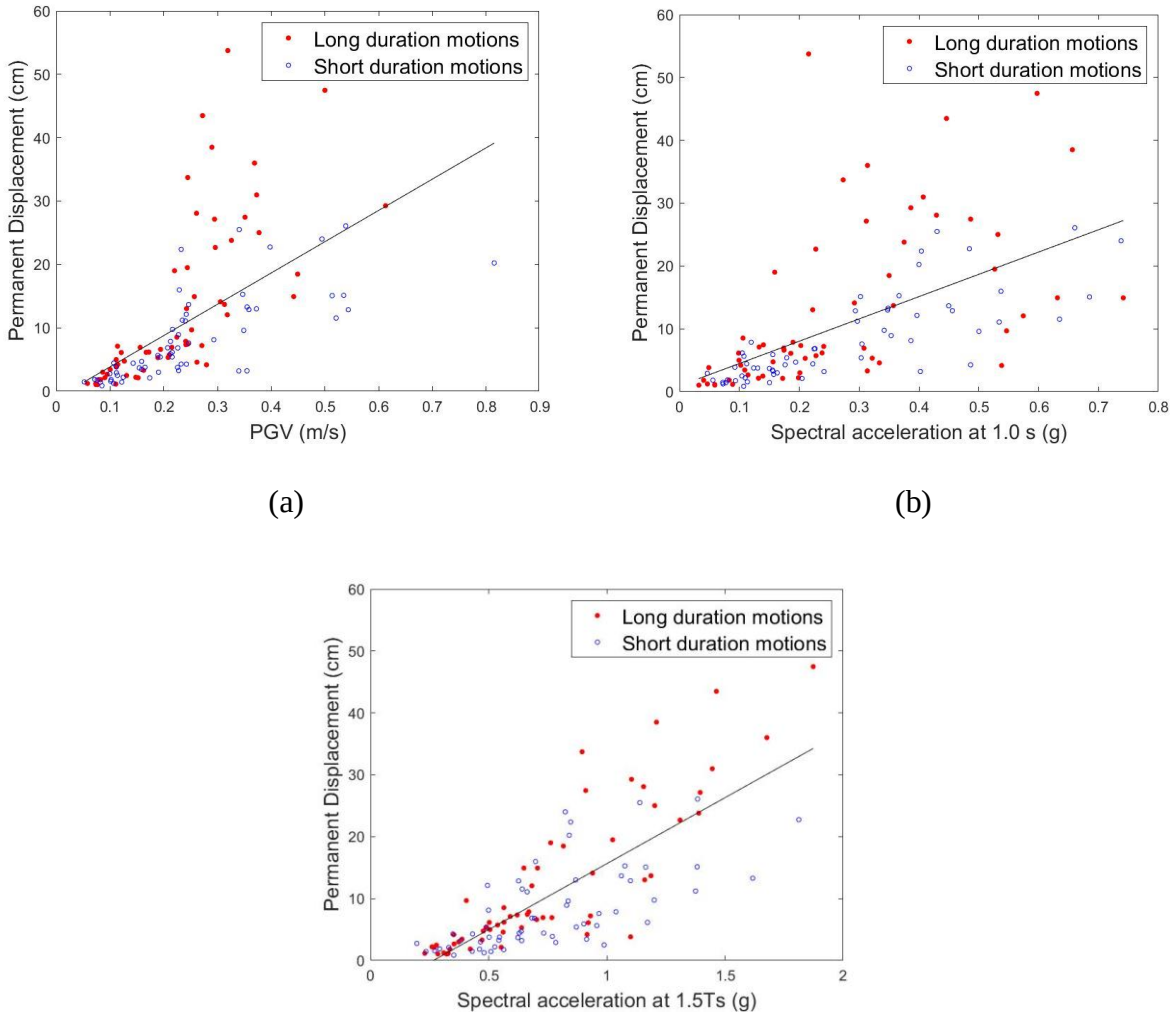

Figure 3.9 Permanent displacements from finite element analyses vs (a) Peak ground velocity (PGV), (b) spectral acceleration at 1.0 s, and (c) spectral acceleration at the degraded site period (1.5Ts) for long and short duration ground motions.

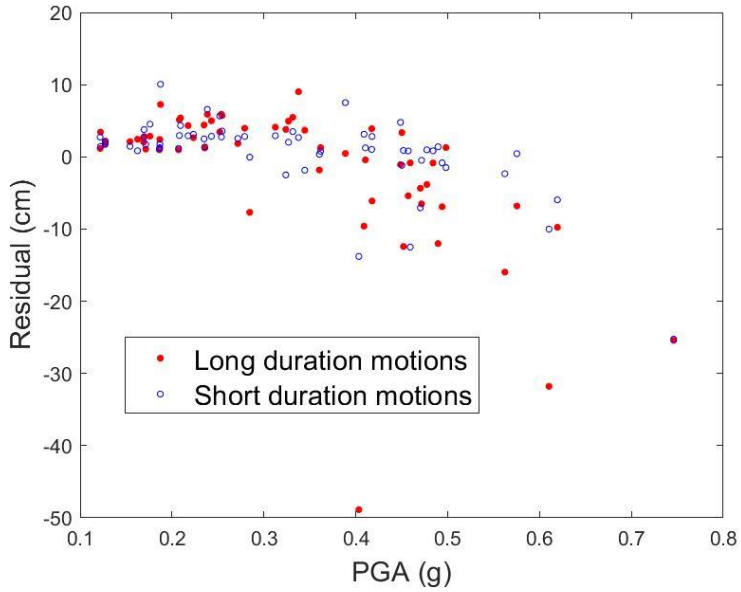

(a)

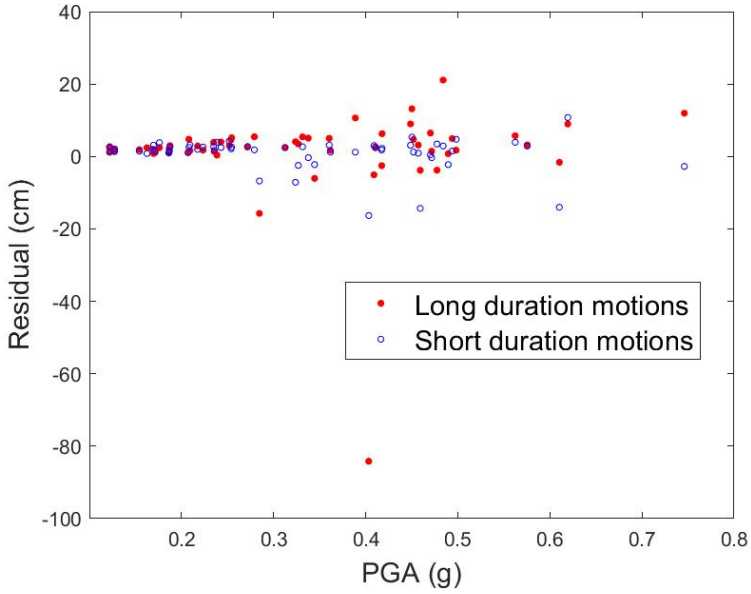

(b)

Figure 3.10 Permanent displacement residual values comparing finite element analysis to the simplified analyses: (a) Rigid block analysis, and (b) Coupled analysis.

3 CHAPTER 4: THE EFFECT OF GROUND MOTION DURATION ON SITE RESPONSE ANALYSIS

Abstract

Site response calculations are required for a variety of engineering analyses to properly characterize site-specific ground motions for the design hazard level. The selection of input motions for site response analyses can be particularly challenging in subduction-zone environments due to the distinct types of earthquakes that contribute to the seismic hazard (shallow crustal and subduction events), each of which has different characteristics. While the effect of long duration ground motions on different structural systems has been investigated in previous studies, the effect of duration on site response analysis has not been quantified. This study aims to investigate the effect of ground motion duration on site response analysis using long duration motions from subduction tectonic settings. The duration of the motion is isolated from other characteristics of the motion by selecting spectrally equivalent ground motions with same amplitude in terms of peak ground acceleration. A long duration suite and an equivalent short duration suite is formed having ground motion pairs of different intensity levels. These suites of motions are used to conduct a one-dimensional fully nonlinear site response analysis at a soft site and at a stiff site at the same study location. Several damage measures and intensity measures including amplification factors, maximum shear strain and spectral displacement are computed to determine whether the ground motion duration has a significant effect. It is observed that long-duration ground motions used as input in nonlinear site response analysis can result in larger damage indices for the estimated ground motion at the ground surface. This finding supports the need to conduct site-specific site response analyses using hazard-consistent ground motions that represent all significant characteristics of the hazard at the location of interest.

4.1 Introduction

The dynamic response of geotechnical systems is a function of not only the amplitude and frequency content of the motion, but also its duration. This is evidenced in simplified assessments of liquefaction triggering where duration and energy effects are explicitly considered (e.g., Green and Terri 2005), and duration-dependent liquefaction-induced lateral spreading empirical models (e.g., Rauch and Martin 2000). Seismic slope displacement analyses have also been found to be affected by the ground motion duration (e.g., chapter 3 of this thesis, Bray et al. 1998). To date, only Kim and Hashash (2013) have examined the effects on long-duration ground motions (from the 2011 M 9.1 Tohoku earthquake) on the dynamic properties of soils and the applicability of 1D site response analysis. Nonetheless, no rigorous assessment has been done yet on the effect of ground motion duration characteristics on site response analysis.

One dimensional (1D) site response analyses (SRA) are commonly used to estimate site-specific ground motions as a function of the properties of the soil profile, the assumed constitutive models to represent dynamic soil behavior, and the input ground motion at the base of the soil profile (Kramer 1996, Kaklamanos et al. 2021). Despite their broad usage in seismic design, site response models are burdened with significant uncertainties. Chapter 2 of this thesis investigated the uncertainty in site response estimates as a function of input motion selection protocols, and found particularly large uncertainties associated to subduction-zone environments where distinct types of earthquakes that contribute to the seismic hazard exist (shallow crustal, intraslab, and interface events). Subduction zones are known for producing longer duration and higher energy events compared to their counterparts from shallow crustal and stable continental tectonic regimes (e.g., Chandramohan et al. 2016, Montalva and Ruz 2017, Rodriguez-Marek et al. 2010). Kim and Hashash (2013) indicated that duration-dependent measures may have an influence on site

response. However, there have not been additional efforts to rigorously quantify the influence of duration on SRA, and further incorporate it in the selection of hazard-consistent ground motions for SRA. A notable exception is the ground motion selection algorithm based on the generalized conditional intensity measure approach (GCIM, Bradley 2010).

Advancing our understanding of the effects of duration on the damaging potential of ground motions and on engineering analyses is crucial to improve seismic hazard assessments in subduction regions in the US, such as the Pacific Northwest and Alaska. Moreover, selecting hazard-consistent ground motions for engineering analysis in regions susceptible to large-magnitude, long-duration earthquake motions is key for resilient design of civil infrastructure in such regions. The objective of this study is to investigate the effects of ground motion duration on nonlinear soil behavior by conducting fully nonlinear seismic site response analysis using long duration ground motions from subduction zones as input.

Spectrally equivalent ground motions with the same amplitude in terms of peak ground acceleration (PGA), but different in significant duration are used in this study. We evaluate two site conditions, one representative of a sedimentary basin, and another one representative of glacial till overlying bedrock. Two study sites are located in Seattle, Washington. Nonlinear site response analyses are conducted using the long- and equivalent short-duration ground motion suites as input. Finally, the results from the site response analyses are compared in terms of several intensity measures, namely response spectral amplification factors, maximum shear strain and spectral displacement.

4.2 Methodology

4.2.1 Equivalent long and short duration suite of motions

To isolate the effect of duration from frequency content and amplitude, ground motion pairs are selected in this study that are similar in spectral shape and have the same in amplitude (in terms of PGA), but different significant duration. These criteria result in a long duration suite and an equivalent short duration suite of motions. A preliminary release of ground motions from the NGA-SUB project (i.e., Mazzoni et al. 2021; last accessed in October 2021) is used in this study. The 5-75% significant duration ($Ds_{5\text{-}75}$) is used to characterize the duration of a ground motion. A $Ds_{5\text{-}75}$ value of 25 s was chosen as the threshold between the short and long duration motions (Chowdhury et al 2022b). The details regarding the creation of the long and short duration datasets, and the selection of equivalent long and short duration ground motions are described in Chowdhury et al. 2022b. Figure 4.1 shows the response spectra of all the ground motions components from short (30 ground motion pairs) and long (30 ground motion pairs) duration suites along with the medians from both suites. The comparison between the median response spectrum of the long duration suite and that corresponding to the equivalent short duration suite shows a good agreement.

4.2.2 Site profiles

Seattle, Washington, is selected as the study site location, because seismic hazards in that region can be dominated by subduction zone earthquakes that can generate long duration ground motions. Seattle is located in a region of active tectonic activity that includes crustal earthquakes and subduction (intraslab and interface) earthquakes associated with the Cascadia subduction zone. A geotechnical profile for one of our study sites is developed so that it is representative of artificial

fill sites in the center of Seattle, although there are significant variations in subsurface conditions throughout the city (Woodhouse and Barosh 2011/2012, Galster and Laprade 1991). This study site consists of artificial fill over a thick layer of deltaic sand and estuarine silt, overlying a dense layer of reworked glacial deposits to a depth of 56.5 m, which represents dense preglacial deposits. The bottom of the soil profile is consistent with the lowest downhole seismometer at the Seattle Liquefaction Array (Shannon and Wilson 2018); suspension logging data at the array were used to develop the assumed V_S profile. The time-averaged shear wave velocity in the top 30 m (V_{S30}) for the profile is 135 m/s, making this a NEHRP (National Earthquake Hazards Reduction Program) class E site. The assumed shear-wave velocity (V_S) and geotechnical profiles are provided in Figure 4.2a.

To evaluate the effect of site conditions on the observed sensitivity of site response analyses to long duration motions, we consider an additional study site in Seattle, but composed of stiffer soil layers, as illustrated in Figure 4.2b. This profile is derived from V_S data from Seattle rock sites in Wong et al. (2011) and consists of 9 m of dry shallow soil (glacial outwash / till). The V_{S30} for the profile is 578 m/s, making this a NEHRP class C site. We denote the former study site as "soft site" and the later site as the "stiff site". For both study sites, the assumed reference rock condition in terms of V_{S30} is equal to 760 m/s (NEHRP site class B/C) which is typical for Western United States (WUS) according to the National Seismic Hazard map. More details on the site profiles can be found on Chowdhury et al (2022a).

4.2.3 Site response analysis

The selected suites of long and short duration motions are used to perform one dimensional (1D), total stress, fully nonlinear site response analyses using the program DEEPSOIL 7.0 (Hashash et al., 2018). For the nonlinear analysis, the dynamic behavior of the soil layers is represented using the General Quadratic/Hyperbolic (GQ/H) constitutive model (Groholski et al. 2016) with non-Masing hysteretic (unload/reload) behavior. The GQ/H model incorporates shear strength corrections at large strains which is important as the nonlinear models neglecting soil strength can provide unrealistic results at large strains (Buccio and Pagliaroli 2020). The selected ground motions in this study have PGA values ranging from 0.1g to 0.75g; at such high PGA, large shear strains are expected. The Darendeli (2001) modulus-reduction and damping curves are used as the target relations for the NL analyses at all layers. The fitting for the non-Masing unload/reload parameters are performed using the MRDF pressure-dependent hyperbolic model procedure with the UIUC reduction factor (Phillips and Hashash, 2009). The frequency-independent damping methodology (Phillips and Hashash, 2009) was used to define the viscous small strain damping. The bedrock (the bottom layer in the profile) is represented as an elastic halfspace. The fundamental period of the soft site and stiff site are found to be 1.2s and 0.06s, respectively, as obtained from the fundamental mode of the transfer function.

4.3 Results and Discussion

After completing SRA, we compare the results from long and short duration suites using several intensity measures. SRA results are most often compared in terms of response spectral amplification factors. Although it is not a cumulative damage index, we investigate if duration has any effect on this measure given its potential implication in earthquake engineering and

engineering seismology applications. Maximum shear strain developed across the soil profile is another widely used measure especially for defining the thresholds for the effectiveness of linear, equivalent-linear and nonlinear site response analysis. The maximum shear strain is considered in this study as it can be a measure of the fatigue in the soil profile due to multiple cycles in an earthquake load. Finally, a more apparent cumulative damage index, the maximum spectral displacement, is evaluated to determine the effects of ground motion duration. The results from the soft and stiff study sites are compared to investigate whether the effects of ground motion duration on site response are consistent across different site conditions.

4.3.1 Comparison of response spectra and amplification factors

Figure 4.3a and 4.3b shows the median and standard deviation of 5% damped acceleration response spectra at the surface of each study site for our long and short duration suite of motions (i.e., 30 pairs of input motions each). The results from the soft site and the stiff site are plotted separately. For the soft site, the median of long and short duration motions merges at short periods (i.e., periods less than 0.07s) and at long periods (i.e., periods greater than 2s). In between (i.e., from 0.07s to 2s period), the median of the long duration suite slightly exceeds that corresponding to the median of the short duration suite. Similarly, at the stiff study site, the median of the long duration suite slightly exceeds the median of the short duration suite at a period range of 0.03s to 0.12s. The long duration suite also shows slightly larger standard deviation than the short duration suite. These observations are expected as differences in ground motion duration cannot be captured by maximum responses used to compute response spectra.

Amplification factors (*AF = response spectrum at surface*/*response spectrum of input motion at bedrock*) are quantified at each site and compared. The median and standard deviation of amplification factors for long and short duration suites of motions are presented in Figure 4.4. The soft site shows greater amplification at long period (low frequency) which is typical for soft sites. Nonetheless, the amplification factors illustrate significant deamplifications at short periods (high frequency). In contrast, amplification over the whole period range is observed for the stiff site. Comparisons between the median from long and short duration suites show the long-duration suite resulting in slightly higher median amplification, while rather similar standard deviations. Larger amplification factors for long-duration motions are more apparent near the site period of each study site (i.e., 1.2s for the soft site and 0.06s for the stiff site). Hence, for further assessment, we focus on the amplification factor value at the site period caused by each ground motion component.

Figure 4.5 illustrates the amplification factor at site period with respect to significant duration (Ds_{5-75}) using the long and short duration suites of motions. Figures 4.5a and 4.5b do not provide a specific trend observed between the amplification factor at site period, AF(Ts) and Ds_{5-75}. Considering that the ground motions have different intensities, the AF(Ts) ratio between the long and short duration motions are calculated and plotted with respect to the PGA (Figure 4.6). On average, larger AF(Ts) ratios are observed for larger values of PGA. We investigated the number of equivalent ground motion pairs for which the long duration motion has created a larger value of AF(Ts) (i.e. the AF(Ts) ratio is greater than 1). For the soft study site, about 70% of the ground motion pairs has resulted in a larger value of AF(Ts) for long duration motion compared to their short duration counterpart. Similarly, for the stiff site, 63% of the ground motion pairs showed similar results. Owing to the fact that the selected ground motion pairs are similar in spectral shape

and have the same in amplitude (PGA), this difference in AF(Ts) can be solely attributed to the duration of the ground motion. The difference in AF(Ts) between the long and short duration motion is found to be as high as 2.25 times.

4.3.2 Comparison of maximum shear strain

The maximum shear strain (γ_{max}) developed across the soft and stiff site profiles are plotted in Figure 4.7. The highest values of maximum shear strain occur in superficial layers of both soil profiles, which is common for many sites that consist of shallow soil deposits over bedrock as shown by Regnier et al. (2013). The soft site (Figure 4.7a) shows a buildup of high strain level (with a median γ_{max} of approximately 1.5% at 5 m depth) within the profile. For the stiff site (Figure 4.7b), the greatest γ_{max} (median of approximately 0.045%) occurs from 0.5 m to 1 m depth. Many researchers have studied the threshold shear strain for the onset of the nonlinear soil behavior. Kaklamanos et al. (2015), using KiK-net vertical seismometer arrays in Japan, recommended using equivalent linear analysis when the maximum shear strains exceed 0.01% and nonlinear analysis after 0.05%. Therefore, the median maximum shear strain of 1.5% at the soft site signifies the presence of high nonlinear soil behavior. It also explains the deamplification of ground motion at short periods for this site profile as observed in Figure 4.4a. In contrast, for the stiff study site, the median of the maximum shear strain is 0.045% and indicates minimal or no nonlinear soil behavior. Comparing the maximum strain from the long duration suite to that from the short duration suite, we observe that the former causes slightly higher maximum strain values in the stiff site. On the contrary, for the soft site, the long duration suite generates slightly lower median maximum strain than the short duration suite.

To further investigate whether the ground motion duration has any effects on maximum strains , the maximum strain is plotted against the corresponding Ds_{5-75} of the input motion in Figure 4.8. The largest value of maximum strain across the soil profile for each ground motion component is considered here. No correlation is observed between maximum strain and Ds_{5-75} for the soft site. Oppositely, for the stiff site, a mild trend of increase in maximum strain can be seen with higher Ds_{5-75} values. Additionally, the effect of intensity level (in terms of PGA) on the maximum strain ratio between the long and short duration motions is explored in Figure 4.9. For both sites, there is a trend of increase in maximum strain ratio with higher PGA value. It is particularly evident for the stiff site after PGA exceeds 0.35 g. At this PGA level, the maximum strain from individual ground motion component was found to exceed 0.1%, that indicates the soil behavior is governed by nonlinearity. Nevertheless, the soft site shows nonlinear soil behavior even for the ground motions with lowest PGA. Therefore, this sharp change in trend between the linear and nonlinear zone is not observed in case of the soft site. For the soft site and stiff site, about 50% and 60% ground motion pairs (respectively) resulted in a larger maximum strain from long duration motion. The maximum strain for long duration motion is found to be as high as 5.7 times at the soft site, and 3.9 times at the stiff site; compared to the maximum strain from short duration motions at each study site.

4.3.3 Comparison of spectral displacement

The spectral displacement represents the peak displacement of elastic single-degree-of freedom oscillators at varying natural frequencies. It can be considered as a cumulative damage index and hence used in this study to evaluate the effect of ground motion duration on site response analysis. The median and standard deviation of 5% damped displacement response spectra at the ground

surface of each study site are plotted in Figure 4.10 for long and short duration suites of input motions. For both study sites, the long duration suite results in a larger median and standard deviation compared to the short duration suite.

Furthermore, the maximum spectral displacement from each ground motion component is plotted with respect to $Ds_{5\text{-}75}$ in Figure 4.11. We can observe a mild trend of increase in spectral displacements with increasing $D_{S5\text{-}75}$. Figure 4.12 shows the spectral displacement ratio between the long and short duration motions against PGA for both study sites. Long duration ground motions caused higher spectral displacements for about 66% (for soft site) and 70% (for stiff site) of the ground motion pairs considered as input to the site response analysis. The long duration motions have caused a spectral displacement as high is 2.6 times that corresponding to the short duration input motion.

4.4 Conclusion

This study focused on investigating the effect of ground motion duration on site response analysis using spectrally equivalent ground motion pairs with same amplitude and different significant duration. Comparisons of different intensity measures: amplification factors, maximum strains and spectral displacements for varying levels of significant duration considered for the input motions in the analysis shows that the duration does not have a strong correlation to these measures. This finding agrees with previous studies that indicated that the duration of a ground motion alone is not a good predictor of the damage potential (Bommer et al. 2009). However, as we simultaneously consider the amplitude in terms of peak ground acceleration, long duration motions seem to result in higher maximum strain and larger spectral displacement compared to their short duration counterparts. About 63-70% of the ground motion pairs has shown larger amplification factor at site period for the long duration motion.

Likewise, a range of 50-60% was found for maximum shear strains, and 66-70% for spectral displacements. Long duration motions have also resulted in amplification factors as high as 2.25 times at the site period than their counterpart from equivalent short duration motions. Hence, in this study we provide evidence that duration can play an important role in site response analysis when evaluated in conjunction with amplitude and frequency content effects. Broader impacts on subsequent analysis will depend on the specific application. For example, the maximum shear strain can be crucial when assessing liquefaction potential and the spectral displacement can be important for long period structures like high rise buildings. Comparing the soft and stiff study sites, it was found that the long duration motions cause larger amplification factors near the site period of each site. The difference in maximum strain between the long and short duration motions is also more prominent for the stiff site after it reaches the threshold of intensity for nonlinear soil behavior. Characterizing the effect of duration on soft sites, where high degree of nonlinear soil behavior is expected, still seems challenging. Future studies can also assess the effect of energy dependent measures such as Arias intensity and cumulative absolute velocity alongside the significant duration.

References

Bommer, J. J., P. J. Stafford, and J. E. Alarcon (2009). Empirical equations for the prediction of the significant, bracketed, and uniform duration of earthquake ground motion. *Bull. Seismol. Soc. Am.*, 99, 3217–3233.

Bradley, B. A. (2010). A generalized conditional intensity measure approach and holistic ground-motion selection. *Earthquake Engineering and Structural Dynamics*, 39, 1321–1342.

Bray, J. D., Rathje, E. M., Augello, A. J., and Merry, S. M. (1998). Simplified seismic design procedure for geosynthetic-lined, solid-waste landfills. *Geosynthetics International*, 5, 203–235.

Buccio, F., and Pagliaroli, A. (2020). Numerical Modelling of Seismic Site Response at Large Strains: A Parametric Study. *American Journal of Civil Engineering*, 8(5), 117-127.

Chandramohan, R., Baker, J. W., and Deierlein, G. G. (2016). Quantifying the influence of ground motion duration on structural collapse capacity using spectrally equivalent records. *Earthquake Spectra*, 32(2), 927–950.

Darendeli, M. B., 2001. Development of a new family of normalized modulus reduction and material damping curves. *Ph.D. Thesis*, University of Texas at Austin, Austin, Texas, 396 pp.

Galster, R. W., and Laprade, W. T. (1991). Geology of Seattle, Washington, United States of America. *Bulletin of Engineering Geology and the Environment*, 28(3), 235–302.

Green, R. A., and Terri, G. A. (2005). Number of equivalent cycles concept for liquefaction evaluations - revisited. *J Geotech Geoenviron Eng*, 131(4), 477–88.

Groholski, D. R., Hashash, Y. M. A., Kim, B., Musgrove, M., Harmon, J., and Stewart, J. P. (2016). Simplified model for small-strain nonlinearity and strength in 1D seismic site response analysis. Journal of Geotechnical and Geoenvironmental Engineering, 142(9).

Hashash, Y. M. A., Musgrove, M. I., Harmon, J. A., Ilhan, O., Groholski, D. R., Phillips, C. A., and Park, D. (2018). *DEEPSOIL 7.0, User Manual*, Univ. of Illinois at Urbana-Champaign, Champaign, Illinois, 169 pp.

Kaklamanos, J., Bradley, B., Moolacattu, A. N., and Picard, B. M. (2021). Physical hypotheses for adjusting coarse profiles and improving 1D site response estimation assessed at 10 KiK-net sites. *Bull. Seismol. Soc. Am*, Vol 110, No. 3, pp. 1338–1358.

Kim, B., and Hashash, Y. M. A. (2013). Site response analysis using downhole array recordings during the March 2011 Tohoku-Oki earthquake and the effect of long-duration ground motions. *Earthquake Spectra*, 29, 37–54.

Kramer, S.L. (1996). *Geotechnical Earthquake Engineering*. Prentice-Hall, New Jersey.

Mazzoni, S., Kishida, T., Contreras, V., Ahdi, S. K., Kwak, D. Y., Bozorgnia, Y., and Stewart J. P. (2021). NGA Subduction Database Preliminary Ground Motion Suite (Public Release), The B. John Garrick Institute for the Risk Sciences. https://www.risksciences.ucla.edu/nhr3/gmdata/preliminary-nga-subduction-records

Woodhouse, D., and Barosh, P. J. (2011/2012). Geotechnical factors in Boston. *Civil Engineering Practice*, 26/27, 237–263.

Montalva, G., and Ruz, F. (2017). Liquefaction Evidence in the Chilean Subduction Zone. Proceedings of the Performance-Based Design in Earthquake Engineering III, Vancouver, Canada, July 16-19.

Phillips, C., and Hashash, Y. M. A. (2009). Damping formulation for nonlinear 1D site response analyses. *Soil Dynamics and Earthquake Engineering*, 29, 1143–1158.

Rauch, A. F., and Martin, J. R. (2000). EPOLLS model for predicting average displacements on lateral spreads. *J. Geotech. Engrg.*, 126, 360–371.

Rodriguez-Marek, A., Bay, J. A., Park, K., Montalva, G. A., Cortez-Flores, A., Wartman, J., and Boroschek, R. (2010). Engineering analysis of ground motion records from the 2001 Mw 8.4 Southern Peru earthquake. *Earthquake Spectra*, *26*(2), 499-524.

Shannon and Wilson (2018). Geotechnical data report, Stanford center liquefaction monitoring array, Seattle, Washington, Report No. 21-1-21441-001, 333 pp.

FIGURES

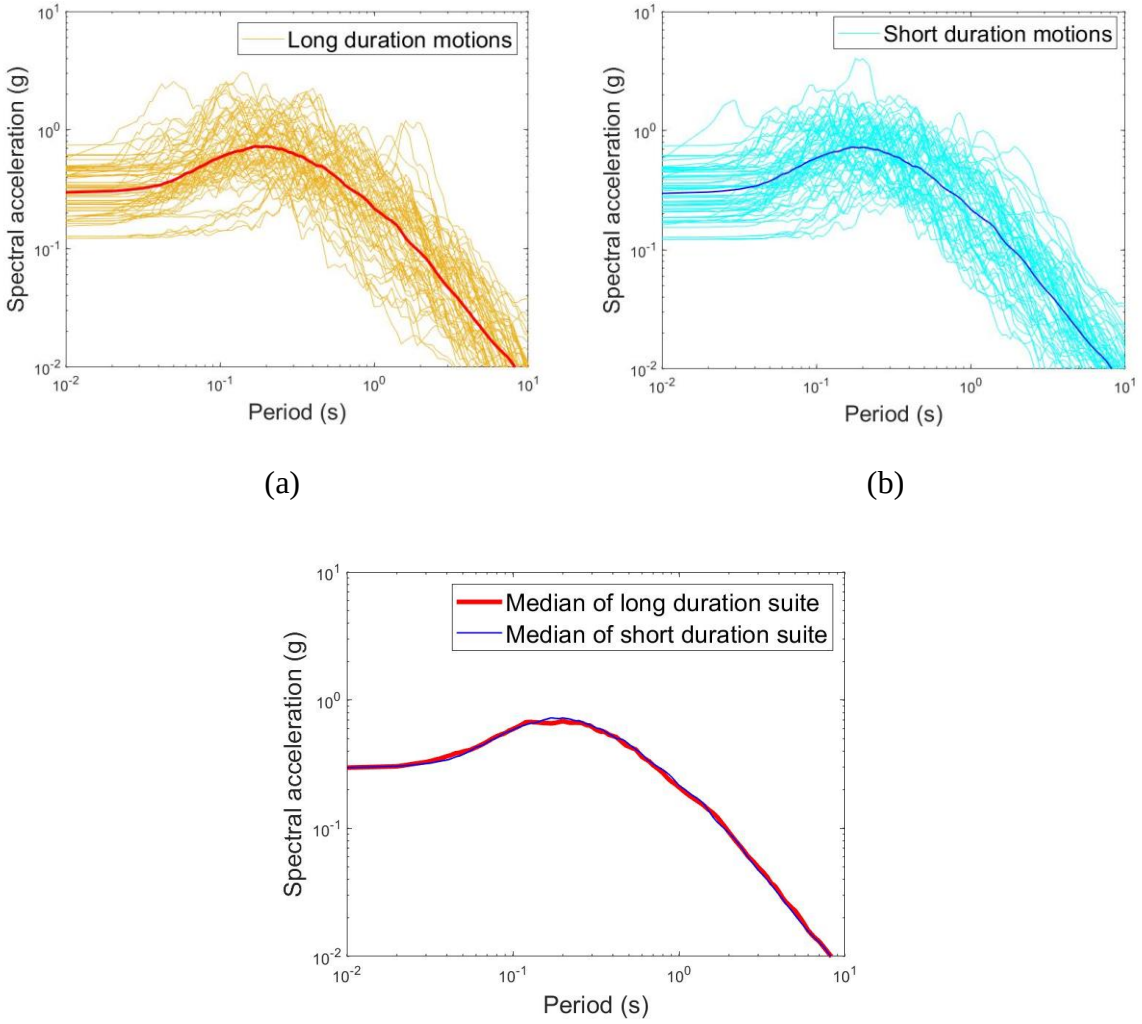

Figure 4.1 Response spectra of all ground motion components from (a) long and (b) short duration suites used in this study, along with (c) a direct comparison between the median response spectra of both suites.

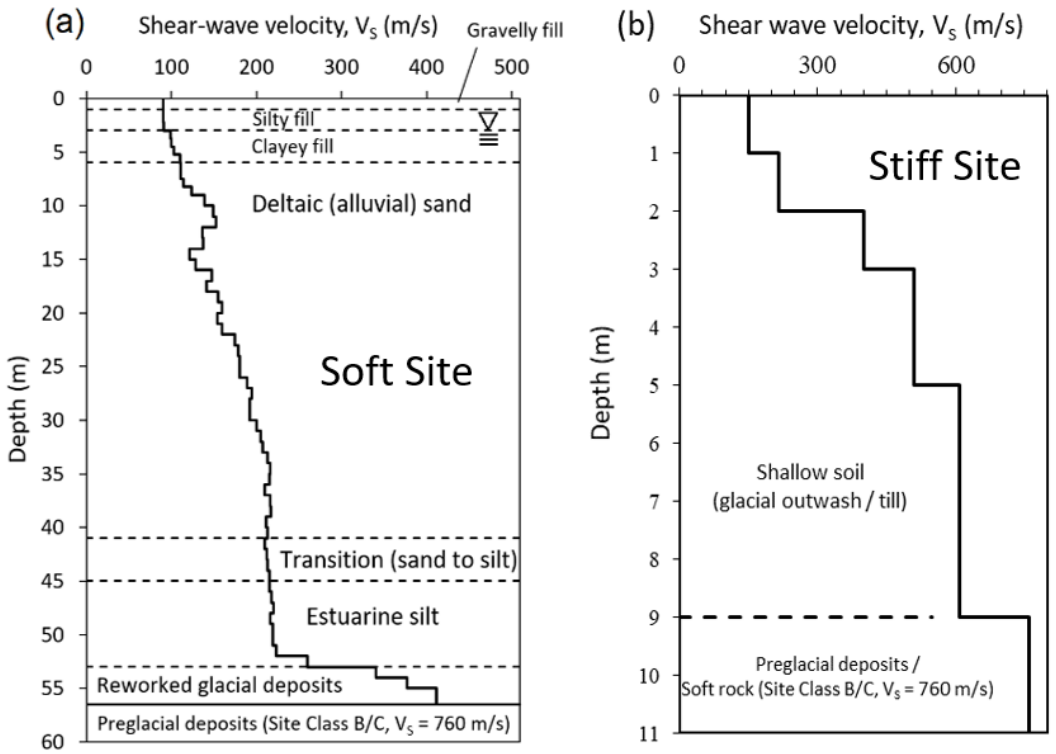

Figure 4.2 Shear-wave velocity and geotechnical profiles associated with two representative site conditions in Seattle for (a) a soft site and (b) a stiff site.

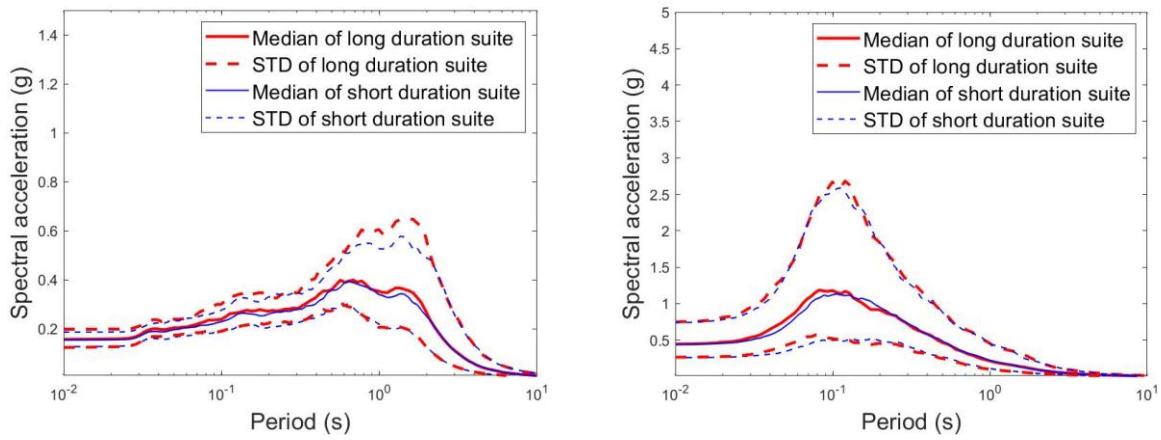

(a) Soft site (b) Stiff site

Figure 4.3 Median and standard deviation of 5% damped acceleration response spectra at ground surface for long and short duration suite of motions: (a) for soft site and (b) stiff site.

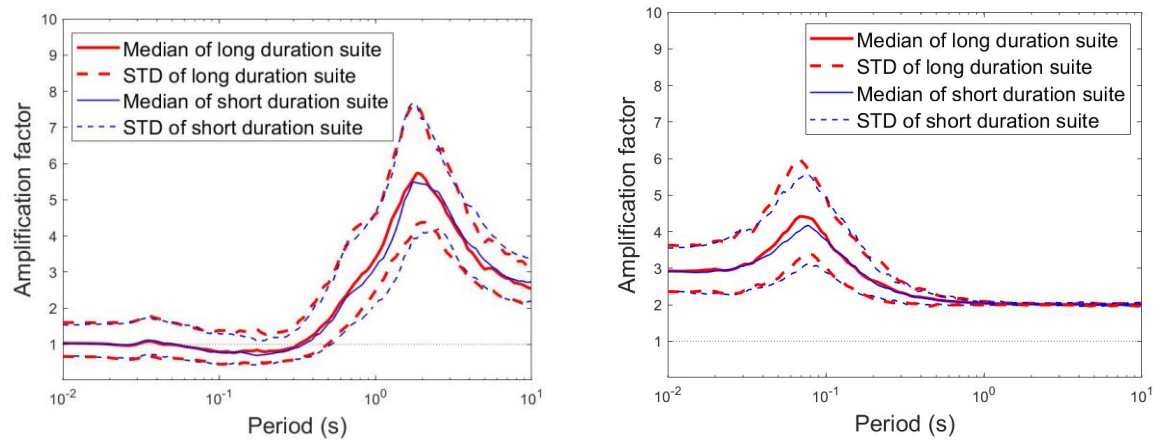

(a) Soft site (b) Stiff site

Figure 4.4 Median and standard deviation of amplification factor for long and short duration suite of motions: (a) for soft site and (b) stiff site.

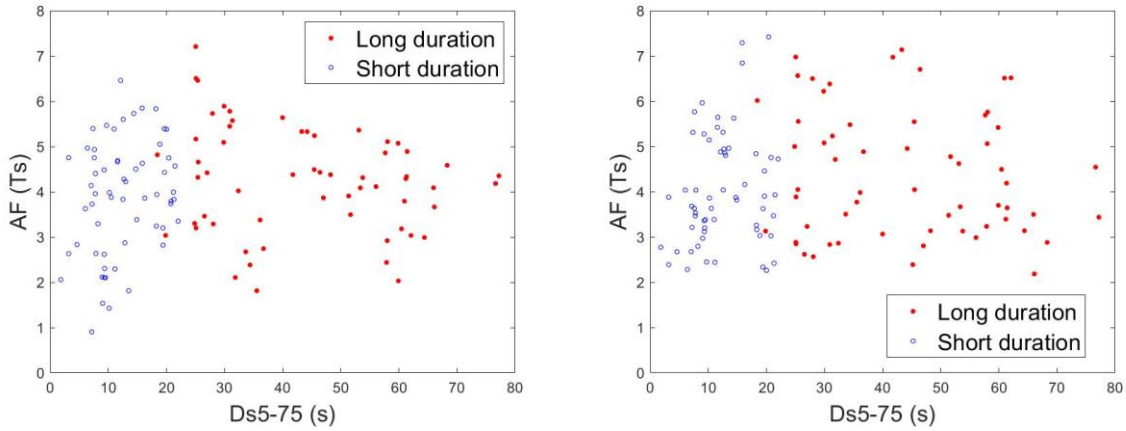

(a) Soft site (b) Stiff site

Figure 4.5 Amplification factor at site period, AF(Ts) with respect to significant duration (Ds5-75) using long and short duration suite (a) for soft site and (b) for stiff site.

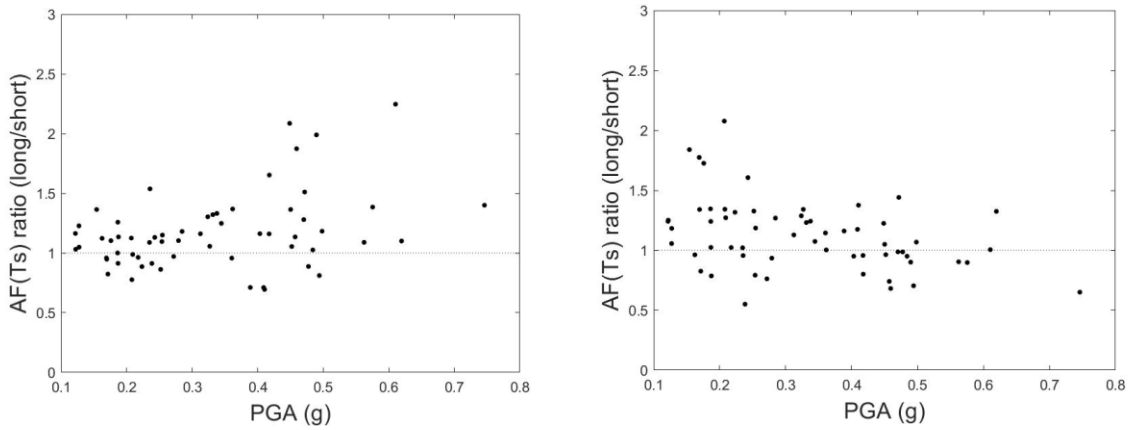

(a) Soft site (b) Stiff site

Figure 4.6 Ratio of amplification factor (AF) at site period (Ts) for long duration motion and equivalent short duration motion, plotted with respect to peak ground acceleration (PGA).

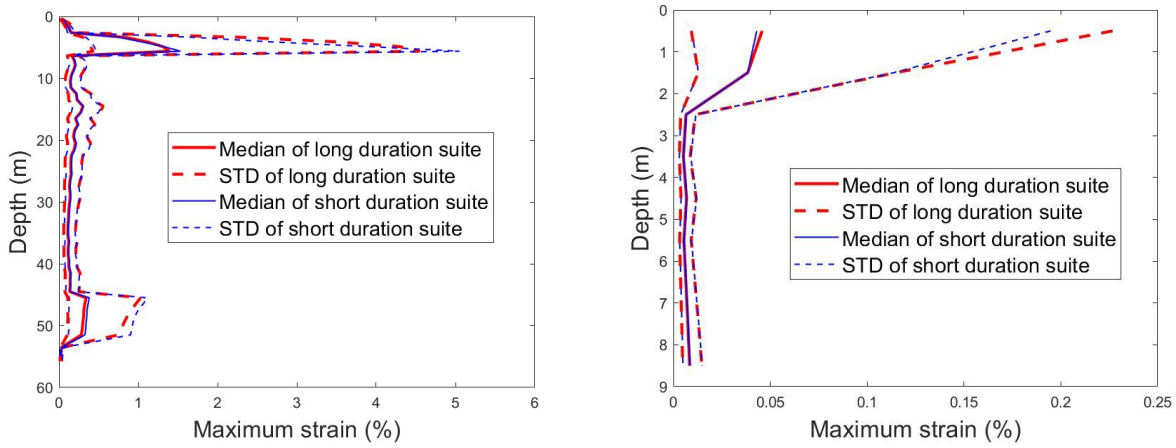

(a) Soft site (b) Stiff site

Figure 4.7 Median and standard deviation of maximum shear strain profiles resulting from site response analysis using long and short duration suites of motions at: (a) the soft study site and (b) the stiff study site.

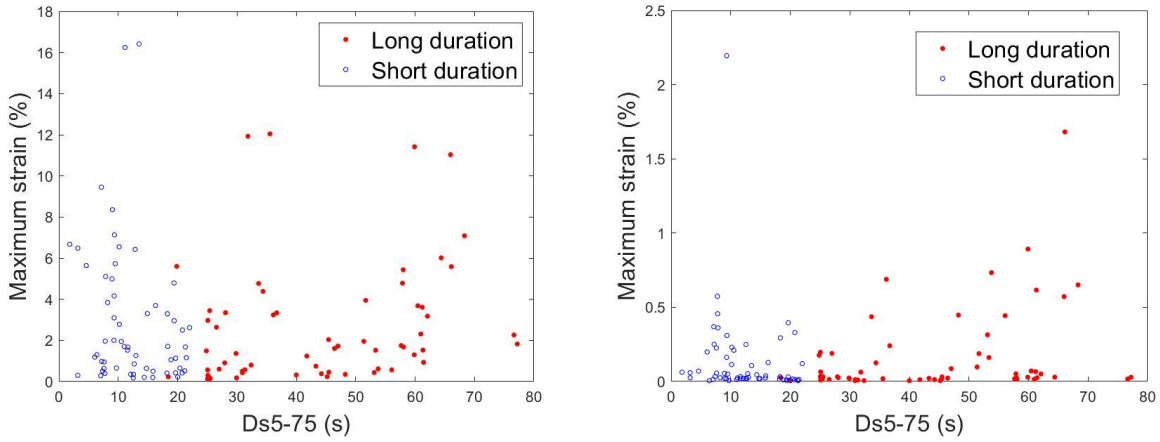

(a) Soft site (b) Stiff site

Figure 4.8 Maximum strain with respect to significant duration ($Ds_{5\text{-}75}$) using long and short duration suite (a) for soft site and (b) for stiff site.

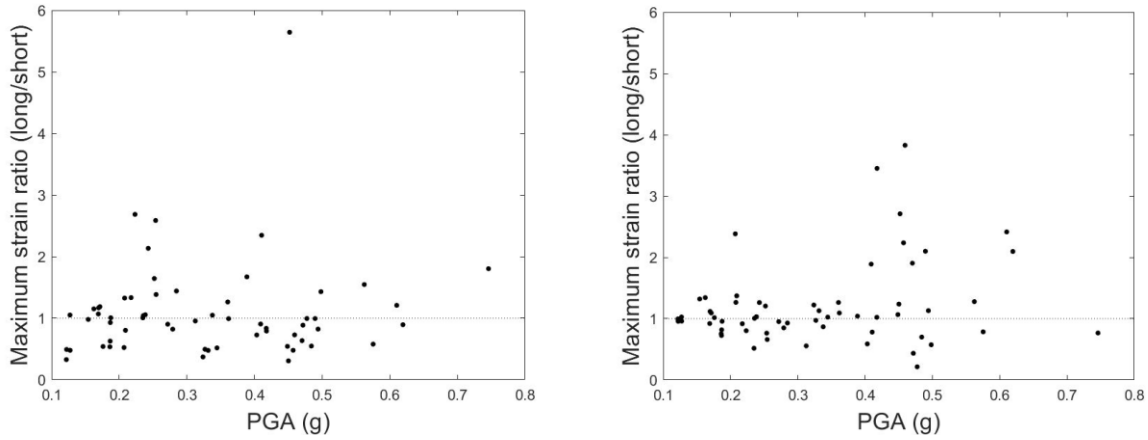

(a) Soft site (b) Stiff site

Figure 4.9 Ratio of maximum strain for long duration motion and equivalent short duration motion, plotted with respect to PGA at the (a) soft study site, and at (b) the stiff study site.

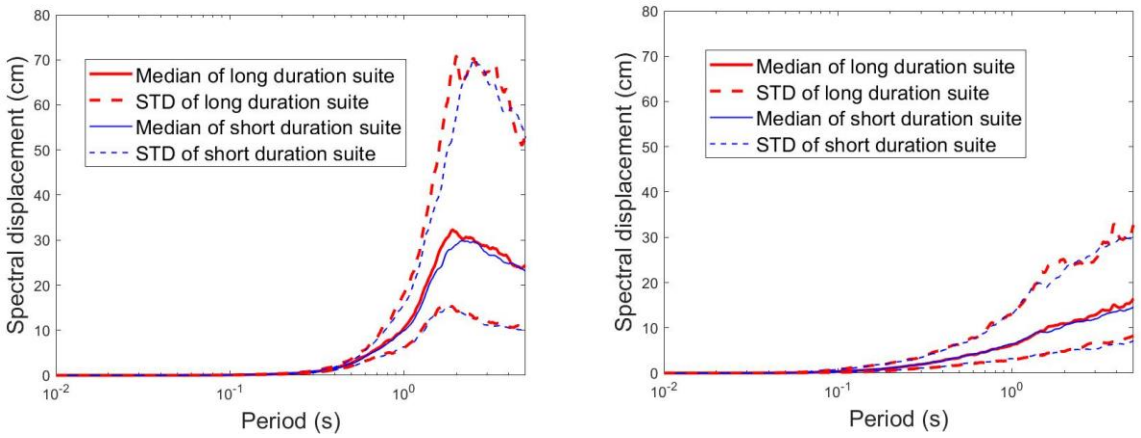

(a) Soft site (b) Stiff site

Figure 4.10 Median and standard deviation of 5% damped displacement response spectra at ground surface for long and short duration suite of motions: (a) for soft site and (b) stiff site.

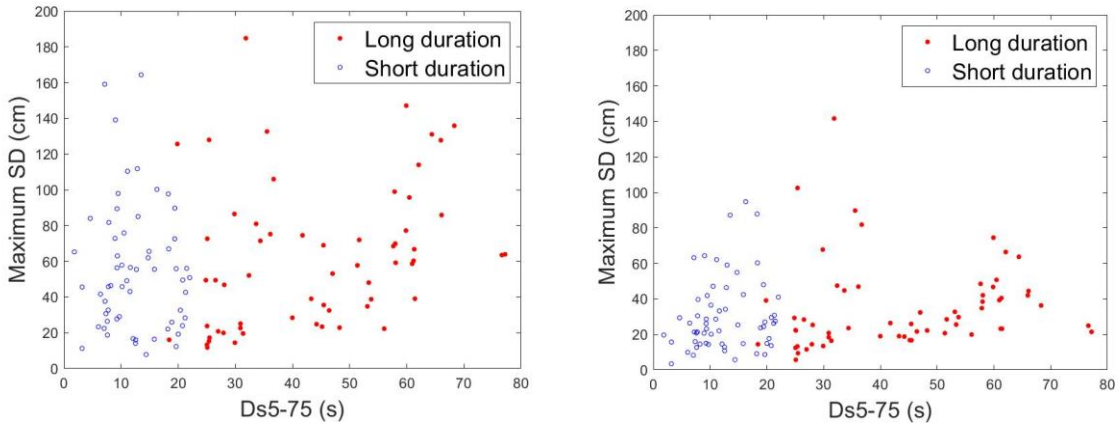

(a) Soft site (b) Stiff site

Figure 4.11 Maximum spectral displacement with respect to significant duration ($Ds_{5\text{-}75}$) using long and short duration suite (a) for soft site and (b) for stiff site.

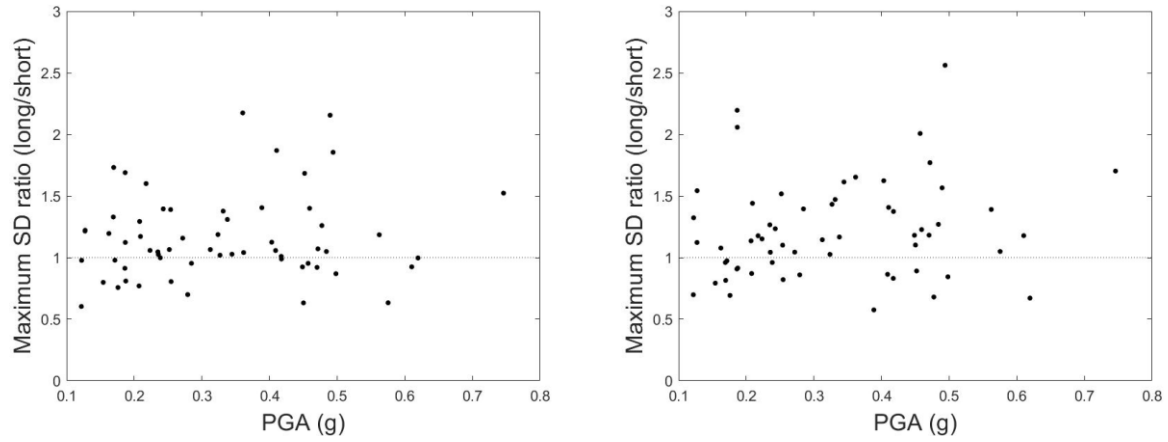

(a) Soft site (b) Stiff site

Figure 4.12 Ratio of maximum spectral displacement for long duration motion and equivalent short duration motion, plotted with respect to PGA for (a) the soft study site, and (b) the stiff study site.

4 CHAPTER 5: CONCLUSION

Summary and Findings

This thesis investigated whether the current practices for hazard consistent ground motion selection provide an unbiased prediction of dynamic responses of soil for geotechnical earthquake engineering applications. Two widely used geotechnical earthquake engineering applications namely site response analysis and seismic slope displacement analysis are investigated. The curation process of ground motion databases and the selection process of ground motions were done using MATLAB. Numerical simulations for site response analysis and seismic slope displacement analysis were done using Deepsoil and Plaxis, respectively.

Chapter 2 investigated the effect of different ground motion selection techniques on the results from site response analyses. The selected study sites (i.e., Seattle and Boston) represented different tectonic and geologic settings, and the selected input motion suites represented variations in the target spectrum definition, spectral period of interest, seismic source scenario, and ground motion database. The following conclusions were obtained from this study:

- The variability in spectral amplification factors for different target spectra definitions reach a peak near the site period and usually decreases beyond that. A similar trend was observed in previous studies (e.g., Kwok et al. 2008, Li and Assimaki 2011, Rathje et al. 2010) for other sources of variability in site response analysis (e.g., Vs profile, MRD curves, model-to-model variability, and suite-to-suite variability of input motions). For sites experiencing significant nonlinearity (e.g., Seattle soft and stiff sites), site period elongation is also observed in this study, i.e., the variability in amplification factor reaches a peak at a degraded site period.

- The selection of the ground-motion database greatly influences the significant duration of the estimated surface motions from site response analysis. Using short-duration ground motions (from shallow crustal events) can result in the underprediction of surface ground-motion IMs (e.g., significant duration, Arias intensity) at locations where the hazard can be dominated by long-duration ground motions, such as subduction zone environments. Therefore, it is crucial to consider all possible seismic source types and use the corresponding databases to select input motions.
- Conditional spectra (CS) is of interest as an alternative target spectrum, partially because it usually predicts a less conservative response spectrum compared to uniform hazard spectrum (UHS). The conditional spectrum is identified as a suitable target spectrum for sites where hazard contributions come from multiple types of seismic sources because it allows the possibility of capturing differences in seismic source types. However, our results indicate that in a low to moderate seismic region like CEUS, the utility of this tool may be limited as CS can exceed UHS. Hence, we need to be cautious about the use of CS for such regions. In cases where the CS exceeds the UHS, the latter is the preferred target spectrum for engineering design.
- Ground motion selection techniques result in higher variability in stiffer sites compared to softer sites. When nonlinearity is significant, the effects of site-response modeling assumptions and parameters may outweigh the effects of input motion selection techniques at short spectral periods. At longer spectral periods for soft sites, nonlinear soil behavior is less prevalent, and predicted surface ground motions are more greatly affected by the input motion selection technique.

Chapter 2 showed that ground motions from subduction events can result in significantly longer duration surface motions from site response analysis compared to crustal motions. However, ground motion duration is not explicitly considered in the current guidelines for ground motion selection (except for the Generalized Conditional Intensity Measure, GCIM approach proposed by Bradley (2010)). Spectral shape can represent the amplitude and frequency characteristics of a ground motion, but correlates poorly with duration. Ground motion duration, however, may impact the geotechnical engineering applications where cumulative effects are important. Therefore, the next two chapters of this thesis focused on investigating the effect of ground motion duration on geotechnical engineering applications.

Chapter 3 investigated the effect of ground motion duration on seismic slope stability analysis. To isolate the effect of duration from frequency content and amplitude, ground motion pairs were selected such that they have similar spectral shapes and the same peak ground acceleration (PGA), but different significant duration. A rigorous finite element analysis was used to more accurately assess the nonlinear soil behavior and strain accumulation due to multiple cycles in a ground motion. The following conclusions were obtained from this study:

- A comparison between the long duration suite of motions and the equivalent short duration suite of motions revealed that the duration of a ground motion affects the permanent displacement of the slope. The long duration suite resulted in up to 75% larger median permanent displacement compared to the median of its counterpart based on the short duration suite of motions. Moreover, a greater number of long duration motions (as high as 30% more) has the potential to cause slope displacements that indicate very high likelihood of landslide occurrence in comparison to the equivalent short duration motions.

- The effect of duration is more prominent at higher intensity levels of ground shaking. As the design level ground motions increase in amplitude, it is crucial to consider the duration of a motion along with other characteristics (amplitude and spectral shape).
- Previously identified efficient ground motion parameters for predicting slope displacement; such as the Arias intensity, peak ground acceleration, spectral acceleration at a period 1.5 times the site period; are found to be good parameters for capturing the effects of long duration motions.
- A comparison with simplified slope displacement methods shows that the simplified coupled analysis can underestimate the displacements from long duration motions, especially at higher intensity levels. It is mainly because the simplified analysis are not able to capture the cyclic degradation of strength and stiffness of soil, which was found to be imperative in determining the true effect of ground motion duration.

Finally, Chapter 4 investigated the effect of ground motion duration on site response analysis. The long and equivalent short duration suites of motions created in Chapter 3 were used in this chapter. One-dimensional, total stress, nonlinear site response analyses were conducted at two sites with different geotechnical conditions. The following conclusions were obtained from this study:

- Comparisons of different intensity measures: amplification factors, maximum shear strains and spectral displacements for varying levels of significant duration considered for the input motions in the analysis showed that duration does not have a strong correlation to these measures. This finding agrees with previous studies that indicated that the duration of a ground motion alone is not a good predictor of the damage potential (Bommer et al. 2009).

- As we simultaneously consider the amplitude in terms of peak ground acceleration, long duration motions resulted in higher maximum strain and larger spectral displacement compared to their short duration counterparts. About 63-70% of the ground motion pairs has shown larger amplification factor at site period for the long duration motion. Likewise, a range of 50-60% was found for maximum shear strains, and 66-70% for spectral displacements. Long duration motions have also resulted in amplification factors as high as 2.25 times at the site period than their counterpart from equivalent short duration motions.
- For both soft and stiff study sites, the long duration suite caused larger median amplification factors near the site period compared to the short duration suite. The difference in maximum shear strain between the long and short duration motions is also more prominent for the stiff site after it reaches the threshold for the onset of nonlinear soil behavior. Characterizing the effect of duration on soft sites, where high degree of nonlinear soil behavior is expected, remains a challenge that requires further investigation.

Essential Contributions

The key contributions of this research work are listed as follow:

- Finding the main sources of uncertainty in ground motion selection that result in higher variability in site response estimates.
- Determining the limitations in current practices for ground motion selection that can cause biased estimates for geotechnical engineering applications.
- Recommending the most suitable target spectra definitions for different seismotectonic and geotechnical settings.

- Showing how soil nonlinear behavior can obscure the variability in site response contributed by the ground motion selection process.
- Providing evidence that duration can play an important role in seismic slope stability analysis and site response analysis when evaluated in conjunction with amplitude and frequency content.
- Emphasizing the importance of considering ground motion duration in the ground motion selection process for geotechnical engineering applications.
- Emphasizing the importance of considering a numerical analysis that can capture the effect of cyclic degradation of strength and stiffness to get unbiased predictions of dynamic soil response for geotechnical engineering applications. It is especially important for design level high intensity ground motions that can trigger nonlinear behavior in soils.

The results of this study advanced our understanding of how input ground motion selection techniques influence the results from geotechnical engineering applications. Moreover, it identified the factors to be considered for hazard consistent ground motion selection for geotechnical engineering applications.

Limitations and Future Work

Several other topics may be worthy of exploring in the future to fill in the limitations of this study, such as:

- The selection of compatible records to hard-rock conditions representative of the bedrock in the CEUS continues to be challenge. Likewise, the paucity of higher intensity ground motions in subduction zones results in difficulties in finding adequate number of design hazard level ground motion selection. Efforts toward expanding and improving ground

motion databases in low-to-moderate seismicity regions and subduction zones remain a priority for our scientific community.

- As this study provided evidence on the importance of considering duration characteristics in ground motion selection, a possible alternative target spectrum can be the GCIM method (Bradley 2010) that can consider any number of ground motion intensity measures (IMs) in ground motion selection. However, implementing the GCIM approach requires access to the corresponding ground motion models (GMMs) for spectral acceleration and non-spectral acceleration IMs and empirical correlation equations between these IMs, all of which are not yet available for subduction zone and stable continental zones. Therefore, developing these GMMs and correlation equations is a much needed future work.
- The computational expense of the finite element method limited us from exploring how other slope characteristics (geometry) or materials (softer to stiffer conditions) may affect our findings in Chapter 3. Future studies can focus on investigating the effect of such characteristics on the observed impact of ground motion duration.
- This study focused on the impact of a duration dependent measure, namely the significant duration on geotechnical engineering applications. Future studies can also assess the effect of energy dependent hybrid measures such as Arias intensity and cumulative absolute velocity alongside the significant duration.

5 APPENDICES

Appendix I

Suite no.	Site	Suite	No. in suite	Record Sequence No.	Scale factor
1	Boston	UHS	1	3982	4.8
1	Boston	UHS	2	4027	3.5
1	Boston	UHS	3	1688	4.7
1	Boston	UHS	4	2749	4
1	Boston	UHS	5	10056	1.9
1	Boston	UHS	6	5711	0.4
1	Boston	UHS	7	8571	0.3
1	Boston	UHS	8	10055	1.7
1	Boston	UHS	9	8567	0.4
1	Boston	UHS	10	8566	0.6
1	Boston	UHS	11	10054	2.2
2	Boston	CS_0.01s	1	8571	0.31
2	Boston	CS_0.01s	2	10056	2.44
2	Boston	CS_0.01s	3	4027	1.46
2	Boston	CS_0.01s	4	5710	0.14
2	Boston	CS_0.01s	5	3982	3.32
2	Boston	CS_0.01s	6	5711	0.3
2	Boston	CS_0.01s	7	10054	2.39
2	Boston	CS_0.01s	8	1684	4.38
2	Boston	CS_0.01s	9	10055	2.14
2	Boston	CS_0.01s	10	10466	4.74
2	Boston	CS_0.01s	11	4039	3.06
3	Boston	CS_1s_near	1	8529	1.1
3	Boston	CS_1s_near	2	10058	1.38
3	Boston	CS_1s_near	3	52	1.15
3	Boston	CS_1s_near	4	8571	0.24
3	Boston	CS_1s_near	5	64	1.04
3	Boston	CS_1s_near	6	10056	1.47
3	Boston	CS_1s_near	7	10057	1.31
3	Boston	CS_1s_near	8	10683	3.5
3	Boston	CS_1s_near	9	10054	1.19
3	Boston	CS_1s_near	10	10517	4.57
3	Boston	CS_1s_near	11	5711	0.79
4	Boston	CS_1s_distant	1	8775	4.08
4	Boston	CS_1s_distant	2	8407	4.36
4	Boston	CS_1s_distant	3	10058	1.38
4	Boston	CS_1s_distant	4	10056	1.47
4	Boston	CS_1s_distant	5	10054	1.19
4	Boston	CS_1s_distant	6	8386	3.43
4	Boston	CS_1s_distant	7	52	1.15
4	Boston	CS_1s_distant	8	8529	1.1
4	Boston	CS_1s_distant	9	64	1.04
4	Boston	CS_1s_distant	10	8566	0.25
4	Boston	CS_1s_distant	11	10477	4.7

Suite no.	Site	Suite	No. in suite	Record Sequence No.	Scale factor
5	Seattle	UHS_Crustal	1	1020	3.8
5	Seattle	UHS_Crustal	2	4845	1.7
5	Seattle	UHS_Crustal	3	8165	1
5	Seattle	UHS_Crustal	4	1521	1.6
5	Seattle	UHS_Crustal	5	810	2
5	Seattle	UHS_Crustal	6	1280	4.5
5	Seattle	UHS_Crustal	7	5791	3.8
5	Seattle	UHS_Crustal	8	496	2.1
5	Seattle	UHS_Crustal	9	748	4.4
5	Seattle	UHS_Crustal	10	1165	2.2
5	Seattle	UHS_Crustal	11	4869	3.4
6	Seattle	UHS_Intraslab	1	6001150	2.96
6	Seattle	UHS_Intraslab	2	6001151	2.13
6	Seattle	UHS_Intraslab	3	6001149	2.21
6	Seattle	UHS_Intraslab	4	6001144	2.96
6	Seattle	UHS_Intraslab	5	7006045	2
6	Seattle	UHS_Intraslab	6	6001245	3.22
6	Seattle	UHS_Intraslab	7	6001155	1.43
6	Seattle	UHS_Intraslab	8	6001153	0.7
6	Seattle	UHS_Intraslab	9	6001154	1.41
6	Seattle	UHS_Intraslab	10	6001243	4.18
6	Seattle	UHS_Intraslab	11	5003311	3.87
7	Seattle	UHS_Interface	1	6001394	3.21
7	Seattle	UHS_Interface	2	6005357	3.51
7	Seattle	UHS_Interface	3	6001373	2.52
7	Seattle	UHS_Interface	4	6001815	1.19
7	Seattle	UHS_Interface	5	4000369	2.49
7	Seattle	UHS_Interface	6	4028568	3.22
7	Seattle	UHS_Interface	7	6001825	1.19
7	Seattle	UHS_Interface	8	3001961	4
7	Seattle	UHS_Interface	9	4000025	0.99
7	Seattle	UHS_Interface	10	4040397	1.59
7	Seattle	UHS_Interface	11	6001799	0.96
8	Seattle	CS_0.01s_Crustal	1	5775	2.48
8	Seattle	CS_0.01s_Crustal	2	4483	1.9
8	Seattle	CS_0.01s_Crustal	3	1520	1.26
8	Seattle	CS_0.01s_Crustal	4	4864	1.93
8	Seattle	CS_0.01s_Crustal	5	1078	2.55
8	Seattle	CS_0.01s_Crustal	6	809	1.76
8	Seattle	CS_0.01s_Crustal	7	1642	2.38
8	Seattle	CS_0.01s_Crustal	8	1111	1.38
8	Seattle	CS_0.01s_Crustal	9	5663	0.9
8	Seattle	CS_0.01s_Crustal	10	741	1.4
8	Seattle	CS_0.01s_Crustal	11	3964	0.88

Suite no.	Site	Suite	No. in suite	Record Sequence No.	Scale factor
9	Seattle	CS_0.01s_Intraslab	1	3000192	4.53
9	Seattle	CS_0.01s_Intraslab	2	5003989	2.12
9	Seattle	CS_0.01s_Intraslab	3	4032463	2.46
9	Seattle	CS_0.01s_Intraslab	4	4040459	1.21
9	Seattle	CS_0.01s_Intraslab	5	2000054	3.38
9	Seattle	CS_0.01s_Intraslab	6	6001147	1.53
9	Seattle	CS_0.01s_Intraslab	7	4007389	1.07
9	Seattle	CS_0.01s_Intraslab	8	4022568	3.48
9	Seattle	CS_0.01s_Intraslab	9	5003311	4.01
9	Seattle	CS_0.01s_Intraslab	10	5000049	3.92
9	Seattle	CS_0.01s_Intraslab	11	4007347	4.18
10	Seattle	CS_0.01s_Interface	1	6001805	3.3
10	Seattle	CS_0.01s_Interface	2	6001385	1.16
10	Seattle	CS_0.01s_Interface	3	4040376	3.27
10	Seattle	CS_0.01s_Interface	4	4028567	2.57
10	Seattle	CS_0.01s_Interface	5	6001819	1.88
10	Seattle	CS_0.01s_Interface	6	6001374	1.4
10	Seattle	CS_0.01s_Interface	7	3001998	1.69
10	Seattle	CS_0.01s_Interface	8	3001971	2.7
10	Seattle	CS_0.01s_Interface	9	4040396	1.57
10	Seattle	CS_0.01s_Interface	10	4000369	2.39
10	Seattle	CS_0.01s_Interface	11	4000192	1.32
11	Seattle	CS_1s_Crustal	1	787	0.78
11	Seattle	CS_1s_Crustal	2	4148	2.39
11	Seattle	CS_1s_Crustal	3	1549	0.72
11	Seattle	CS_1s_Crustal	4	4869	2.63
11	Seattle	CS_1s_Crustal	5	3964	2.27
11	Seattle	CS_1s_Crustal	6	8158	1.27
11	Seattle	CS_1s_Crustal	7	3475	1.15
11	Seattle	CS_1s_Crustal	8	3269	2.87
11	Seattle	CS_1s_Crustal	9	4229	1.8
11	Seattle	CS_1s_Crustal	10	1488	1.92
11	Seattle	CS_1s_Crustal	11	1787	1.14
12	Seattle	CS_1s_Intraslab	1	6000989	3.42
12	Seattle	CS_1s_Intraslab	2	4007389	3.25
12	Seattle	CS_1s_Intraslab	3	6001243	4
12	Seattle	CS_1s_Intraslab	4	7006045	2.65
12	Seattle	CS_1s_Intraslab	5	2000055	3.69
12	Seattle	CS_1s_Intraslab	6	3001283	3.27
12	Seattle	CS_1s_Intraslab	7	2000065	3.36
12	Seattle	CS_1s_Intraslab	8	2000904	1.3
12	Seattle	CS_1s_Intraslab	9	7006078	1.19
12	Seattle	CS_1s_Intraslab	10	2000903	1.23
12	Seattle	CS_1s_Intraslab	11	5000133	2.99

Suite no.	Site	Suite	No. in suite	Record Sequence No.	Scale factor
13	Seattle	CS_1s_Interface	1	6002262	0.62
13	Seattle	CS_1s_Interface	2	4028563	2.46
13	Seattle	CS_1s_Interface	3	4001181	2.7
13	Seattle	CS_1s_Interface	4	6001804	1.12
13	Seattle	CS_1s_Interface	5	6001805	0.68
13	Seattle	CS_1s_Interface	6	7004777	3.43
13	Seattle	CS_1s_Interface	7	6001383	2.14
13	Seattle	CS_1s_Interface	8	4000106	1.3
13	Seattle	CS_1s_Interface	9	6001800	0.7
13	Seattle	CS_1s_Interface	10	6001018	0.85
13	Seattle	CS_1s_Interface	11	4001060	0.86
14	Seattle	GCIM_0.01s_Crustal	1	924	17.69
14	Seattle	GCIM_0.01s_Crustal	2	1035	3.95
14	Seattle	GCIM_0.01s_Crustal	3	2650	5.16
14	Seattle	GCIM_0.01s_Crustal	4	765	1.5
14	Seattle	GCIM_0.01s_Crustal	5	73	4.59
14	Seattle	GCIM_0.01s_Crustal	6	3202	12.64
14	Seattle	GCIM_0.01s_Crustal	7	562	4.35
14	Seattle	GCIM_0.01s_Crustal	8	455	8.05
14	Seattle	GCIM_0.01s_Crustal	9	2658	1.08
14	Seattle	GCIM_0.01s_Crustal	10	2626	3.64
14	Seattle	GCIM_0.01s_Crustal	11	545	8.9
15	Seattle	GCIM_1s_Crustal	1	1773	5.74
15	Seattle	GCIM_1s_Crustal	2	339	1.33
15	Seattle	GCIM_1s_Crustal	3	147	1.8
15	Seattle	GCIM_1s_Crustal	4	160	1.005
15	Seattle	GCIM_1s_Crustal	5	1293	3.01
15	Seattle	GCIM_1s_Crustal	6	59	21.84
15	Seattle	GCIM_1s_Crustal	7	391	3.25
15	Seattle	GCIM_1s_Crustal	8	1833	18.31
15	Seattle	GCIM_1s_Crustal	9	410	2.92
15	Seattle	GCIM_1s_Crustal	10	1079	5.88
15	Seattle	GCIM_1s_Crustal	11	920	3.18

Appendix II

Ground motion No.	Com-ponent No.	Long duration		Short duration		
		Filename	Ds_{5-75} (s)	Filename	Ds_{5-75} (s)	Scale factor
1	1	NGAsubRSN3001965_VILEN00E.AT2	32.39	NGAsubRSN4028581_HKD102-NS.AT2	21.31	1.56
	2	NGAsubRSN3001965_VILEN90E.AT2	30.91	NGAsubRSN3001962_SUCHS00E.AT2	6.41	1.18
2	1	NGAsubRSN4000025_4C0-EW.AT2	68.32	NGAsubRSN7004778_ILA066--N.AT2	9.37	3.44
	2	NGAsubRSN4000025_4C0-NS.AT2	61.32	NGAsubRSN6001807_MELP-T.AT2	18.34	0.80
3	1	NGAsubRSN4000106_8B2-EW.AT2	61.20	NGAsubRSN2000893_89781360.AT2	1.84	1.37
	2	NGAsubRSN4000106_8B2-NS.AT2	61.43	NGAsubRSN4028609_HKD131-NS.AT2	19.66	3.35
4	1	NGAsubRSN4000113_904-EW.AT2	46.43	NGAsubRSN6001145_COSTA--L.AT2	9.28	1.30
	2	NGAsubRSN4000113_904-NS.AT2	45.43	NGAsubRSN6001145_COSTA--T.AT2	11.57	1.35
5	1	NGAsubRSN4000192_D2E-EW.AT2	53.36	NGAsubRSN6001150_IDIEM--T.AT2	10.20	2.47
	2	NGAsubRSN4000192_D2E-NS.AT2	47.02	NGAsubRSN2000904_1725360.AT2	4.62	2.01
6	1	NGAsubRSN4000224_E06-EW.AT2	64.40	NGAsubRSN7006078_KAU082--E.AT2	11.15	1.46
	2	NGAsubRSN4000224_E06-NS.AT2	57.88	NGAsubRSN7006078_KAU082--N.AT2	9.50	1.70
7	1	NGAsubRSN4000369_FKSH16W2.AT2	77.21	NGAsubRSN2000905_1746360.AT2	8.22	2.54
	2	NGAsubRSN4000369_FKSH16S2.AT2	76.65	NGAsubRSN1002947_8021360.AT2	11.01	3.38
8	1	NGAsubRSN4000463_IWTH23W2.AT2	48.24	NGAsubRSN4007347_IWTH17S2.AT2	19.66	2.75
	2	NGAsubRSN4000463_IWTH23S2.AT2	53.12	NGAsubRSN4030862_IWT008EW.AT2	12.57	3.63
9	1	NGAsubRSN4000518_MYGH04W2.AT2	56.07	NGAsubRSN5003311_20140120_025252_MRZ_20_N90W.AT2	6.05	2.66
	2	NGAsubRSN4000518_MYGH04S2.AT2	53.78	NGAsubRSN4022568_IWTH17EW2.AT2	7.77	2.99
10	1	NGAsubRSN4000789_FKS005EW.AT2	65.97	NGAsubRSN4028568_HKD088-EW.AT2	10.52	2.72
	2	NGAsubRSN4000789_FKS005NS.AT2	66.10	NGAsubRSN7006045_KAU042--N.AT2	9.31	3.19
11	1	NGAsubRSN4001181_TCG007EW.AT2	43.29	NGAsubRSN6001148_LOA--T.AT2	20.39	1.65
	2	NGAsubRSN4001181_TCG007NS.AT2	41.76	NGAsubRSN4028609_HKD131-EW.AT2	21.48	2.57
12	1	NGAsubRSN4040369_GN4-EW.AT2	60.96	NGAsubRSN4028569_HKD089-EW.AT2	12.69	0.82
	2	NGAsubRSN4040369_GN4-NS.AT2	57.66	NGAsubRSN4028569_HKD089-NS.AT2	12.98	1.14

Ground motion No.	Com-ponent No.	Long duration		Short duration		
		Filename	Ds_{5-75} (s)	Filename	Ds_{5-75} (s)	Scale factor
13	1	NGAsubRSN4040370_GN5-EW.AT2	58.00	NGAsubRSN4022988_TKCH01NS2.AT2	14.91	1.85
	2	NGAsubRSN4040370_GN5-NS.AT2	58.06	NGAsubRSN4028567_HKD087-EW.AT2	11.64	0.97
14	1	NGAsubRSN4040371_GS1-EW.AT2	59.92	NGAsubRSN7006501_KAU043--E.AT2	7.16	3.41
	2	NGAsubRSN4040371_GS1-NS.AT2	60.46	NGAsubRSN2000905_1746090.AT2	9.32	3.78
15	1	NGAsubRSN4040373_GS3-EW.AT2	62.09	NGAsubRSN4032552_51562-EW.AT2	12.85	0.85
	2	NGAsubRSN4040373_GS3-NS.AT2	59.87	NGAsubRSN6001141_TAC1-SN.AT2	15.86	2.64
16	1	NGAsubRSN6000319_GO01HNE.AT2	29.93	NGAsubRSN6001147_CUYA--L.AT2	12.54	0.55
	2	NGAsubRSN6000319_GO01HNN.AT2	25.10	NGAsubRSN1002922_ARTYHNN.AT2	3.19	1.19
17	1	NGAsubRSN6001374_MNMCXHLE.AT2	27.93	NGAsubRSN7004777_ILA065--N.AT2	7.62	1.53
	2	NGAsubRSN6001374_MNMCXHLN.AT2	27.00	NGAsubRSN6005360_C11OHNN.AT2	20.77	0.70
18	1	NGAsubRSN6001803_SLUC360.AT2	29.85	NGAsubRSN4022990_TKCH03EW2.AT2	14.75	1.32
	2	NGAsubRSN6001803_SLUC090.AT2	25.41	NGAsubRSN4028592_HKD113-NS.AT2	18.28	2.12
19	1	NGAsubRSN6001809_CONC-L.AT2	31.85	NGAsubRSN4022988_TKCH01EW2.AT2	13.52	2.99
	2	NGAsubRSN6001809_CONC-T.AT2	35.56	NGAsubRSN7006533_KAU082--E.AT2	9.03	1.53
20	1	NGAsubRSN6001815_CURI-NS.AT2	36.13	NGAsubRSN4032630_S-2490WEST.AT2	7.88	2.71
	2	NGAsubRSN6001815_CURI-EW.AT2	36.71	NGAsubRSN4022835_HDKH05EW2.AT2	16.28	3.94
21	1	NGAsubRSN6001816_HUAL-L.AT2	34.39	NGAsubRSN6001802_SNJM090.AT2	22.02	0.81
	2	NGAsubRSN6001816_HUAL-T.AT2	33.65	NGAsubRSN7004779_ILA068--E.AT2	10.15	3.71
22	1	NGAsubRSN6001825_TAL-L.AT2	51.37	NGAsubRSN6001151_PLAZA--T.AT2	7.80	1.73
	2	NGAsubRSN6001825_TAL-T.AT2	51.69	NGAsubRSN2000890_89486090.AT2	8.95	3.06
23	1	NGAsubRSN6002202_T09AHNE.AT2	24.85	NGAsubRSN6001154_PISAG--L.AT2	7.60	1.35
	2	NGAsubRSN6002202_T09AHNN.AT2	25.07	NGAsubRSN6001154_PISAG--T.AT2	7.21	1.29

Ground motion No.	Com-ponent No.	Long duration		Short duration		
		Filename	Ds_{5-75} (s)	Filename	Ds_{5-75} (s)	Scale factor
24	1	NGAsubRSN6002253_MT05HNE.AT2	39.99	NGAsubRSN3001962_SUCHN90W.AT2	9.71	1.47
	2	NGAsubRSN6002253_MT05HNN.AT2	45.19	NGAsubRSN4028612_HKD134-NS.AT2	20.02	1.13
25	1	NGAsubRSN6002259_VA03HNE.AT2	45.48	NGAsubRSN5000326_20030821_121249_MANS_N14E.AT2	7.37	1.57
	2	NGAsubRSN6002259_VA03HNN.AT2	44.22	NGAsubRSN4007388_MYGH02S2.AT2	18.20	2.32
26	1	NGAsubRSN6002262_GO04HNN.AT2	28.07	NGAsubRSN2000904_1725090.AT2	3.20	0.96
	2	NGAsubRSN6002262_GO04HNE.AT2	26.54	NGAsubRSN6001802_SNJM360.AT2	20.80	0.51
27	1	NGAsubRSN6005357_C01OHNE.AT2	30.90	NGAsubRSN4028592_HKD113-EW.AT2	21.21	0.74
	2	NGAsubRSN6005357_C01OHNN.AT2	31.36	NGAsubRSN6001808_OLMU-X.AT2	18.89	0.71
28	1	NGAsubRSN6005358_C09OHNE.AT2	25.39	NGAsubRSN4028568_HKD088-NS.AT2	12.11	1.15
	2	NGAsubRSN6005358_C09OHNN.AT2	25.05	NGAsubRSN4030862_IWT008NS.AT2	14.39	2.52
29	1	NGAsubRSN3000185_2747-EW.AT2	25.10	NGAsubRSN6001818_MAT-L.AT2	19.42	0.55
	2	NGAsubRSN3000185_2747-NS.AT2	19.86	NGAsubRSN4028581_HKD102-EW.AT2	19.40	2.32
30	1	NGAsubRSN6001144_CERRO-EW.AT2	18.44	NGAsubRSN6001142_TAC2-EW.AT2	15.83	1.42
	2	NGAsubRSN6001144_CERRO-NS.AT2	25.49	NGAsubRSN2000900_1580090.AT2	7.06	2.42